

# Two-loop electroweak next-to-leading logarithmic corrections to massless fermionic processes

A. DENNER<sup>1†</sup>, B. JANTZEN<sup>1‡</sup>, AND S. POZZORINI<sup>2§</sup>

<sup>1</sup> *Paul Scherrer Institut  
CH-5232 Villigen PSI, Switzerland*

<sup>2</sup> *Max-Planck-Institut für Physik, Föhringer Ring 6  
D-80805 München, Germany*

## Abstract:

We consider two-loop leading and next-to-leading logarithmic virtual corrections to arbitrary processes with external massless fermions in the electroweak Standard Model at energies well above the electroweak scale. Using the sector-decomposition method and alternatively the strategy of regions we calculate the mass singularities that arise as logarithms of  $Q^2/M_W^2$ , where  $Q$  is the energy scale of the considered process, and  $1/\epsilon$  poles in  $D = 4 - 2\epsilon$  dimensions, to one- and two-loop next-to-leading logarithmic accuracy. The derivations are performed within the complete electroweak theory with spontaneous symmetry breaking. Our results indicate a close analogy between the form of two-loop electroweak logarithmic corrections and the singular structure of scattering amplitudes in massless QCD. We find agreement with the resummation prescriptions that have been proposed in the literature based on a symmetric  $SU(2) \times U(1)$  theory matched with QED at the electroweak scale and provide new next-to-leading contributions proportional to  $\ln(M_Z^2/M_W^2)$ .

August 2006

---

<sup>†</sup>Ansgar.Denner@psi.ch

<sup>‡</sup>physics@bernd-jantzen.de

<sup>§</sup>pozzorin@mppmu.mpg.de

# 1 Introduction

The electroweak radiative corrections to high-energy processes are characterized by the presence of logarithms of the type  $\ln(Q^2/M^2)$ , which involve the ratio of the typical scattering energy  $Q$  over the gauge-boson mass scale  $M = M_W \sim M_Z$  [1]. These logarithmic corrections affect every reaction that involves electroweakly interacting particles and has a characteristic scale  $Q \gg M$ . They start to be sizable at energies of the order of a few hundred GeV and their impact increases with energy. At the LHC [2] and future lepton colliders [3–5], where scattering energies of the order of 1 TeV will be reached, logarithmic electroweak effects can amount to tens of per cent at one loop and several per cent at two loops. Thus, this class of corrections will be very important for the interpretation of precision measurements at future high-energy colliders.

For sufficiently high  $Q$ , terms of  $\mathcal{O}(M^2/Q^2)$  become negligible and, at  $l$  loops, the electroweak corrections assume the form of a tower of logarithms,

$$\alpha^l \ln^j \left( \frac{Q^2}{M^2} \right), \quad \text{with} \quad 0 \leq j \leq 2l, \quad (1.1)$$

where the leading logarithms (LLs), also known as Sudakov logarithms [6], have power  $j = 2l$ , and the subleading terms with  $j = 2l - 1, 2l - 2, \dots$  are denoted as next-to-leading logarithms (NLLs), next-to-next-to-leading logarithms (NNLLs), and so on. The complete asymptotic limit includes all logarithmic contributions ( $j > 0$ ) as well as terms that are not logarithmically enhanced at high energy ( $j = 0$ ).<sup>1</sup>

Electroweak logarithmic corrections have a twofold origin. On the one hand they can appear as terms of the form  $\ln(Q^2/\mu_R^2)$  resulting from the renormalization of ultraviolet (UV) singularities at the renormalization scale  $\mu_R \sim M$ . These logarithms can easily be controlled through the running of the coupling constants. The other source of electroweak logarithms are mass singularities, i.e. logarithms of the form  $\ln(Q^2/M^2)$  that are formally singular in the limit where the gauge-boson masses tend to zero. As is well known, in gauge theories, mass singularities result from the interactions of the initial- and final-state particles with soft and/or collinear gauge bosons. This permits, in principle, to treat mass singularities in a process-independent way and to derive universal properties of mass-singular logarithmic corrections.

At one loop, it was proven that the electroweak LLs and NLLs are universal, and a general formula was derived that expresses the logarithmic corrections to arbitrary processes in terms of the electroweak quantum numbers of the initial- and final-state particles [7,8]. In recent years, the impact of one-loop electroweak corrections was studied in detail for various specific processes at high-energy colliders [9–15]. At the LHC, in general, large negative corrections are observed that appear at transverse momenta  $p_T$  around 100 GeV and grow with  $p_T$ . Depending on the process, the size of these corrections can reach up to 10–40% at  $p_T \sim 500$ –1000 GeV. In Refs. [12,14], the predictions based on NLL and NNLL high-energy approximations were compared with exact one-loop calculations.

---

<sup>1</sup> In the literature, such terms are sometimes denoted as “constants” since they do not involve logarithms that grow with energy. However, in general they are functions of the ratios of kinematical invariants, which depend on the scattering angles. At one loop such terms are formally classified as NNLLs.

In both cases it turned out that in the high- $p_T$  region, where the corrections are large, the NNLL predictions deviate from the exact calculation by much less than 1%, i.e. the numerical effect of  $\mathcal{O}(M^2/Q^2)$  contributions is negligible. Also the NLL approximation provides a correct description of the bulk of the corrections and their energy dependence. However, it was found that the actual precision of the NLL approximation, better than 1% for  $pp \rightarrow \text{jet} + Z/\gamma$  [14] and about 5% for  $pp \rightarrow W\gamma$  [12], depends relatively strongly on the process. As it was shown for  $pp \rightarrow \text{jet} + Z/\gamma$ , also the two-loop electroweak logarithms can have an impact at the several per-cent level on high- $p_T$  measurements at the LHC [14].

In the recent years, the properties of electroweak logarithmic corrections beyond one loop have been studied with two complementary approaches.<sup>2</sup> On the one hand, evolution equations, which are well known in QED and QCD, have been applied to the electroweak theory in order to obtain the higher-order terms through a resummation of the one-loop logarithms<sup>3</sup> [17–23]. On the other hand, explicit diagrammatic calculations based on the electroweak Feynman rules have been performed [24–31].

Fadin *et al.* [17] have resummed the electroweak LL corrections to arbitrary matrix elements by means of the infrared evolution equation (IREE), and this approach has been extended by Melles to the NLL terms for arbitrary processes [18–21]. In Refs. [22, 23] Kühn *et al.* have resummed the logarithmic corrections to neutral-current massless 4-fermion processes up to the NNLL level. These resummations [17–23] are based on the IREE [17], which describes the all-order LL dependence of matrix elements with respect to the cut-off parameter  $\mu_\perp$ . This cut-off fixes the minimal transverse momentum for the gauge bosons that couple to the initial- and final-state particles and acts as a regulator of mass singularities. The IREE, which was originally derived within symmetric gauge theories (QED and QCD), has been applied to the spontaneously broken electroweak theory under the assumption that this latter can be split into two regimes with exact gauge symmetry. In practice, in the regime  $Q \geq \mu_\perp \geq M$  the masses of the electroweak gauge bosons, which result from the breaking of gauge symmetry, are supposed to be negligible and exact  $SU(2) \times U(1)$  symmetry is assumed. Instead, in the regime  $M \geq \mu_\perp$  the weak gauge bosons are supposed to be frozen owing to their masses such that only photons contribute to the evolution, and this is characterized by exact  $U(1)_{\text{em}}$  symmetry.

As a result, the resummed electroweak corrections factorize into two parts corresponding to these two regimes: (i) a symmetric-electroweak part that can be computed within a symmetric  $SU(2) \times U(1)$  gauge theory using the same cut-off parameter  $M$  to regularize the mass singularities that result from all gauge bosons, i.e. assuming that the photon is as heavy as the weak gauge bosons, and (ii) an electromagnetic part that originates from the mass gap between photons and massive gauge bosons and can be computed within QED. The electromagnetic part contains divergences that are due to massless photons and depend on the scheme adopted for their regularization. These divergences cancel when the contributions of virtual and real photons are combined, and then the

---

<sup>2</sup>For recent developments in the exact numerical calculation of complete two-loop integrals see, for instance, Ref. [16].

<sup>3</sup>In order to resum the LLs and NLLs it is sufficient to determine the kernel of the evolution equations to one-loop accuracy. However, starting from the NNLLs also the two-loop contributions to the  $\beta$ -function and to the anomalous dimensions are needed.

electromagnetic contribution depends on the cuts imposed on real photons. Instead the symmetric-electroweak part involves logarithms of the form  $\ln(Q^2/M^2)$  which are formally mass singular but numerically finite since  $M$  does not vanish. These logarithms are present in all physical observables that are exclusive with respect to real radiation of Z and W bosons. Moreover, the electroweak logarithms remain present even in inclusive observables due to a lack of cancellation between virtual and real contributions from electroweak gauge bosons. This is due to the fact that the conditions of the Bloch–Nordsieck theorem are not fulfilled since fermions and gauge bosons carry non-abelian weak-isospin charges [32].

The resummations [17–23] rely on the assumption that all relevant implications of electroweak symmetry breaking are correctly taken into account by simply splitting the evolution equation into two regimes with exact gauge symmetry. In particular, the following assumptions are explicitly or implicitly made. (i) In the massless limit  $M/Q \rightarrow 0$ , all couplings with mass dimension, which originate from symmetry breaking, are neglected. (ii) The weak-boson masses are introduced in the corresponding propagators as regulators of soft and collinear singularities from W and Z bosons without spontaneous symmetry breaking. Since these masses are of the same order, one uses  $M_W = M_Z$  as an approximation. (iii) The regimes above and below the electroweak scale are treated as an unmixed  $SU(2) \times U(1)$  theory and QED, respectively, and mixing effects in the gauge sector, i.e. the interaction of photons with W bosons, are neglected.

It is important to understand to which extent the above assumptions are legitimate and whether the resulting resummation prescriptions are correct. This can be achieved by explicit diagrammatic two-loop calculations based on the electroweak Lagrangian, where all effects related to spontaneous symmetry breaking are consistently taken into account. At the LL level, these checks have already been completed. A calculation of the massless fermionic singlet form factor [24, 25] and then a Coulomb-gauge calculation for arbitrary processes [26] have supported the exponentiation of the electroweak LLs predicted by the IREE. Also the angular-dependent subset of the NLL corrections for arbitrary processes [27] has been shown to be consistent with the exponentiation anticipated in Refs. [21–23]. At present the complete set of electroweak NLLs is known only for the so-called fermionic form factor, which corresponds to the gluon–fermion–antifermion vertex [28]. This calculation has confirmed that the IREE approach provides a correct description of the terms that do not depend on the difference between the masses of the Z and the W bosons and has provided first insights into the behaviour of the NLL terms of the type  $\alpha^2 \ln(M_Z^2/M_W^2) \ln^3(Q^2/M^2)$ . The complete tower of two-loop logarithms for the fermionic form factor has been computed in Refs. [29, 30] adopting an unmixed  $SU(2) \times U(1)$  theory with  $M_Z = M_W$  as approximation. Within this framework it was found that the soft–collinear singularities resulting from massless photons factorize as suggested by the IREE and that, in absence of mixing, symmetry breaking is negligible up to the NNLL level and its first non-trivial effects appear through a Higgs-mass dependence of the NNNLL terms. Using QCD resummation techniques, the NNNLL two-loop results for the fermionic form-factor have been extended to the amplitude for neutral-current four-fermion scattering [30, 31]. Here terms of the type  $\ln(M_Z^2/M_W^2)$  were included through an expansion in  $s_w^2 = 1 - M_W^2/M_Z^2$  up to the first order in  $s_w^2$ .

In this paper we develop a formalism to derive virtual electroweak two-loop LL and NLL corrections for arbitrary processes and apply it to the case of massless  $n$ -fermion reactions. The calculation is performed diagrammatically using the electroweak Feynman rules in the 't Hooft–Feynman gauge. The mass-singular logarithms are extracted from the relevant Feynman diagrams by means of a soft–collinear approximation for the interaction of initial- and final-state fermions with gauge bosons. Using Ward identities we prove that the LL and NLL mass singularities for generic  $n$ -fermion amplitudes factorize from the corresponding Born amplitudes. All relevant loop integrals are evaluated in the high-energy region  $Q \gg M$  to NLL accuracy using an automatized algorithm based on the sector-decomposition technique [33] and alternatively the method of expansion by regions combined with Mellin–Barnes representations [34]. We do not assume  $M_Z = M_W$  and we include all relevant contributions depending on the difference  $M_Z - M_W$ . In addition to the logarithms of the type (1.1), which arise from massive virtual particles, we include also mass singularities from massless virtual photons. The latter are regularized dimensionally and arise as  $1/\epsilon$  poles in  $D = 4 - 2\epsilon$  dimensions. In our result the photonic singularities are factorized in a gauge-invariant electromagnetic term. The remaining part of the corrections, which is also gauge invariant and does not depend on the scheme adopted to regularize photonic singularities, contains only finite  $\log(Q^2/M^2)$  terms. The divergences contained in the electromagnetic term cancel if real-photon emission is included.

The paper is organized as follows. Section 2 contains definitions and conventions used in the calculation. In Sect. 3 we identify the diagrams that produce ultraviolet and mass singularities, split them into factorizable and non-factorizable parts and discuss our method to treat these contributions. Using collinear Ward identities, we prove in Sect. 4 that all non-factorizable contributions cancel. Explicit expressions for the factorizable contributions and for the counterterms needed for the renormalization are provided in Sects. 5 and 6, respectively. The complete one- and two-loop results are presented in Sect. 7 and discussed in Sect. 8. Our conclusions are contained in Sect. 9, and various appendices are devoted to technical aspects of the calculation.

## 2 Definitions and conventions

We consider a generic  $n \rightarrow 0$  process involving an even number  $n$  of polarized fermionic particles,

$$\varphi_1(p_1) \dots \varphi_n(p_n) \rightarrow 0. \quad (2.1)$$

The symbols  $\varphi_i$  represent  $n/2$  antifermions and  $n/2$  fermions:  $\varphi_i = \bar{f}_{\sigma_i}^{\kappa_i}$  for  $i = 1, \dots, n/2$  and  $\varphi_i = f_{\sigma_i}^{\kappa_i}$  for  $i = n/2 + 1, \dots, n$ . These particles are massless chiral eigenstates with  $p_k^2 = m_k^2 = 0$  and chirality  $\kappa_i = R$  or  $L$ . In practice every fermion or antifermion can be a lepton or a light quark. The indices  $\sigma_i$  characterize the lepton/quark nature, the isospin and the generation of the fermions,  $f_{\sigma_i} = \nu_e, e, u, d, \dots$

The matrix element for the process (2.1) reads

$$\mathcal{M}^{\varphi_1 \dots \varphi_n} = \left[ \prod_{i=1}^{n/2} \bar{v}(p_i, \kappa_i) \right] G^{\varphi_1 \dots \varphi_n}(p_1, \dots, p_n) \left[ \prod_{j=n/2+1}^n u(p_j, \kappa_j) \right], \quad (2.2)$$

where  $G^{\varphi_1 \dots \varphi_n}$  is the corresponding truncated Green function. The spinors for chiral fermions and antifermions fulfil

$$\omega_\rho u(p, \kappa) = \delta_{\kappa\rho} u(p, \kappa), \quad \bar{v}(p, \kappa) \bar{\omega}_\rho = \delta_{\kappa\rho} \bar{v}(p, \kappa) \quad (2.3)$$

for  $\rho, \kappa = \text{R, L}$ , and

$$\omega_{\text{R}} = \bar{\omega}_{\text{L}} = \frac{1}{2}(1 + \gamma^5), \quad \omega_{\text{L}} = \bar{\omega}_{\text{R}} = \frac{1}{2}(1 - \gamma^5). \quad (2.4)$$

The matrix elements (2.2) are often abbreviated as  $\mathcal{M} \equiv \mathcal{M}^{\varphi_1 \dots \varphi_n}$ .

The amplitudes for physical scattering processes, i.e.  $2 \rightarrow n - 2$  reactions, are easily obtained from our results for  $n \rightarrow 0$  reactions using crossing symmetry.

## 2.1 Perturbative and asymptotic expansions

For the perturbative expansion of the matrix elements in  $\alpha = e^2/(4\pi)$ , where  $e$  is the electromagnetic coupling constant, we write

$$\mathcal{M} = \sum_{l=0}^{\infty} \mathcal{M}_l, \quad (2.5)$$

with

$$\mathcal{M}_l = \left( \frac{\alpha_\epsilon}{4\pi} \right)^l \tilde{\mathcal{M}}_l, \quad (2.6)$$

and

$$\alpha_\epsilon = \left( \frac{4\pi\mu_{\text{D}}^2}{e^{\gamma_{\text{E}}} Q^2} \right)^\epsilon \alpha. \quad (2.7)$$

Note that, for convenience, in  $D = 4 - 2\epsilon$  dimensions we include in the definition of  $\alpha_\epsilon$  a normalization factor depending on  $\epsilon$ , the scale  $\mu_{\text{D}}$  of dimensional regularization, the characteristic energy  $Q$  of the scattering process and Euler's constant  $\gamma_{\text{E}}$ . For  $\mu_{\text{D}}^2 = Q^2 e^{\gamma_{\text{E}}}/(4\pi)$  we have  $\alpha_\epsilon = \alpha$ .

The electroweak corrections are evaluated in the region where all kinematical invariants,  $r_{jk} = (p_j + p_k)^2$ , are much larger than the squared masses of the heavy particles that enter the loops,

$$|r_{jk}| \sim Q^2 \gg M_{\text{W}}^2 \sim M_{\text{Z}}^2 \sim m_{\text{t}}^2 \sim M_{\text{H}}^2. \quad (2.8)$$

This means that we consider a situation with essentially two different scales, one fixed by  $Q$ , which can be identified with (the square root of the absolute value of) one of the kinematical invariants,  $Q = \sqrt{|r_{jk}|}$ , and one fixed by the heavy masses of the Standard Model. In this region, the electroweak corrections are dominated by mass-singular logarithms,

$$L = \ln \left( \frac{Q^2}{M_{\text{W}}^2} \right), \quad (2.9)$$

and logarithms of UV origin. Mass singularities that originate from soft and collinear massless photons and UV singularities are regularized dimensionally and give rise to  $1/\epsilon$  poles in  $D = 4 - 2\epsilon$  dimensions. Therefore, the  $l$ -loop contributions to the polarized matrix elements can be written as an expansion in  $L$  and  $\epsilon$ ,

$$\mathcal{M}_l = \sum_{m=0}^{2l} \sum_{n=-m}^{\infty} \mathcal{M}_{l,m,n} \epsilon^n L^{m+n}. \quad (2.10)$$

The logarithmic terms in (2.10) are classified according to their degree of singularity, defined as the total power  $m$  of logarithms  $L$  and  $1/\epsilon$  poles. The maximal degree of singularity at  $l$ -loop level is  $m = 2l$  and the corresponding terms are denoted as leading logarithms (LLs). The terms with  $m = 2l - 1, 2l - 2, \dots$  represent the next-to-leading logarithms (NLLs), next-to-next-to-leading logarithms (NNLLs), and so on.

In this paper we systematically neglect mass-suppressed corrections of order  $M_W^2/Q^2$  and we calculate the one- and two-loop corrections to NLL accuracy, i.e. including LLs and NLLs. For this approximation we use the symbol  $\stackrel{\text{NLL}}{=}$ . The two-loop corrections are expanded in  $\epsilon$  up to the finite terms, i.e. contributions of order  $\epsilon^0 L^4$  and  $\epsilon^0 L^3$ . Instead, the one-loop corrections are expanded up to order  $\epsilon^2$ , i.e. including terms of order  $\epsilon^2 L^4$  and  $\epsilon^2 L^3$ . These higher-order terms in the  $\epsilon$ -expansion must be taken into account when expressing two-loop mass singularities in terms of one-loop ones.

Since the loop corrections depend on various masses,  $M_W \sim M_Z \sim m_t \sim M_H$ , and different invariants  $r_{jk}$ , the coefficients  $\mathcal{M}_{l,m,n}$  in (2.10) depend on mass ratios and ratios of invariants.<sup>4</sup> Actually, as we will see in the final result, they depend only on logarithms of these ratios,

$$l_i = \ln \left( \frac{M_i^2}{M_W^2} \right), \quad l_{jk} = \ln \left( \frac{-r_{jk}}{Q^2} \right). \quad (2.11)$$

The logarithms of  $-r_{jk}$  are extracted in the region  $r_{jk} < 0$ , where the corrections are real. The imaginary parts that arise in the physical region can be obtained via analytic continuation replacing  $r_{jk}$  by  $r_{jk} + i0$ .

## 2.2 Symmetry breaking and mixing

In the electroweak Standard Model, the physical gauge bosons result from the gauge bosons  $W^1, W^2, W^3$  and  $B$  associated with the SU(2) and U(1) gauge groups via the unitary transformation

$$W_\mu^\pm = \frac{1}{\sqrt{2}} (W_\mu^1 \mp iW_\mu^2), \quad Z_\mu = c_w W_\mu^3 + s_w B_\mu, \quad A_\mu = -s_w W_\mu^3 + c_w B_\mu, \quad (2.12)$$

where  $c_w = \cos \theta_w$ ,  $s_w = \sin \theta_w$ , and  $\theta_w$  is the weak mixing angle. The generators associated with the physical gauge bosons are related to the weak isospin generators  $T^i$  and the weak hypercharge  $Y$  through

$$eI^{W^\pm} = \frac{g_2}{\sqrt{2}} (T^1 \pm iT^2), \quad eI^Z = g_2 c_w T^3 - g_1 s_w \frac{Y}{2}, \quad eI^A = -g_2 s_w T^3 - g_1 c_w \frac{Y}{2}, \quad (2.13)$$

---

<sup>4</sup> This dependence only appears at the next-to-leading level, i.e. for  $m = 2l - 1$ .

where  $g_1$  and  $g_2$  are the coupling constants associated with the U(1) and SU(2) groups, respectively. The electromagnetic charge operator is defined as

$$Q = -I^A, \quad (2.14)$$

and the generator associated with the Z boson can be expressed as

$$eI^Z = \frac{g_2}{c_w} T^3 - e \frac{s_w}{c_w} Q. \quad (2.15)$$

The SU(2)  $\times$  U(1) Casimir operator is given by

$$\sum_{V=A,Z,W^\pm} I^{\bar{V}} I^V = \frac{g_1^2}{e^2} \left( \frac{Y}{2} \right)^2 + \frac{g_2^2}{e^2} C, \quad (2.16)$$

where  $\bar{V}$  denotes the complex conjugate of  $V$ , and  $C = \sum_{i=1}^3 (T^i)^2$  is the Casimir operator of the SU(2) group with eigenvalues 3/4 and 0 for left- and right-handed fermions, respectively. The generators (2.13) obey the commutation relations

$$e [I^{V_1}, I^{V_2}] = i g_2 \sum_{V_3=A,Z,W^\pm} \varepsilon^{V_1 V_2 V_3} I^{\bar{V}_3}, \quad (2.17)$$

with

$$\varepsilon^{V_1 V_2 V_3} = i \times \begin{cases} (-1)^{p+1} c_w & \text{if } V_1 V_2 V_3 = \pi(ZW^+W^-), \\ (-1)^p s_w & \text{if } V_1 V_2 V_3 = \pi(AW^+W^-), \\ 0 & \text{otherwise,} \end{cases} \quad (2.18)$$

and  $(-1)^p$  represents the sign of the permutation  $\pi$ .

The SU(2)  $\times$  U(1) symmetry is spontaneously broken by a scalar Higgs doublet which acquires a vacuum expectation value  $v$ . We parametrize the Higgs doublet in terms of the four degrees of freedom  $\Phi_i = H, \chi, \phi^+, \phi^-$ , where  $\phi^- = (\phi^+)^+$ . In this representation the gauge-group generators are  $4 \times 4$  matrices with components  $I_{\Phi_i \Phi_j}^V$ . The gauge-boson masses and the mixing parameters are fixed by the condition that the gauge-boson mass matrix is diagonal,

$$M_{V\bar{V}'}^2 = \frac{1}{2} e^2 v^2 \{I^V, I^{\bar{V}'}\}_{HH} = \delta_{V\bar{V}'} M_V^2, \quad (2.19)$$

for  $V, V' = A, Z, W^\pm$ . The curly brackets in (2.19) denote an anticommutator. The mass eigenvalues are given by

$$M_{W^\pm} = \frac{1}{2} g_2 v, \quad M_Z = \frac{1}{2 c_w} g_2 v, \quad M_A = 0. \quad (2.20)$$

The weak mixing angle  $\theta_w$  is related to the gauge-boson masses via

$$c_w = \frac{M_W}{M_Z}. \quad (2.21)$$



The vanishing mass of the photon is connected to the fact that the electric charge of the vacuum expectation value is zero. This provides the relation

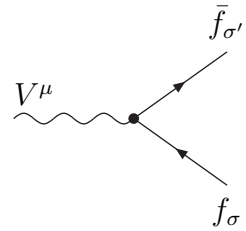
$$c_w g_1 Y_\Phi = s_w g_2, \quad (2.22)$$

between the weak mixing angle, the coupling constants  $g_1$ ,  $g_2$  and the hypercharge  $Y_\Phi$  of the Higgs doublet. Identifying  $e = c_w g_1$ , the Gell-Mann–Nishijima relation for general  $Y_\Phi$  reads  $Q = Y/2 + Y_\Phi T^3$ . In the calculation we keep  $Y_\Phi$  as a free parameter, which determines the degree of mixing in the gauge sector. In this way our analysis applies to the Standard Model case,  $Y_\Phi = 1$ , as well as to the case  $Y_\Phi = 0$  corresponding to an unmixed theory with

$$s_w = 0, \quad c_w = 1, \quad Z_\mu = W_\mu^3, \quad A_\mu = B_\mu, \quad M_W = M_Z. \quad (2.23)$$

### 2.3 Gauge interactions of massless fermions

For the Feynman rules and various group-theoretical quantities we adopt the formalism of Ref. [8] (see Apps. A and B therein). The Feynman rules for the vector-boson–fermion–antifermion vertices read



The diagram shows a wavy line representing a vector boson  $V^\mu$  entering a vertex from the left. From this vertex, two fermionic lines emerge: one pointing upwards and to the right, labeled  $\bar{f}_{\sigma'}$ , and another pointing downwards and to the right, labeled  $f_\sigma$ .

$$= ie\gamma^\mu \sum_{\kappa=R,L} \omega_\kappa I_{f_{\sigma'}^\kappa f_\sigma^\kappa}^V, \quad (2.24)$$

where  $V = A, Z, W^\pm$ , and  $I_{f_{\sigma'}^\kappa f_\sigma^\kappa}^V$  are the generators that describe  $SU(2) \times U(1)$  transformations of fermions in the fundamental ( $\kappa = L$ ) or trivial ( $\kappa = R$ ) representation. For antifermions we have

$$I_{\bar{f}_{\sigma'}^\kappa f_\sigma^\kappa}^V = -I_{f_{\sigma'}^\kappa f_\sigma^\kappa}^V. \quad (2.25)$$

The chiral projectors  $\omega_\kappa$  that are associated with the gauge couplings (2.24) can easily be shifted along the fermionic lines using anticommutation relations<sup>5</sup> until they can be eliminated using (2.3). As an example, for the coupling of a vector boson  $V$  to an incoming fermion  $\varphi_i = f_{\sigma_i}^{\kappa_i}$  one obtains

$$\frac{i(\not{p}_i + \not{q})}{(p_i + q)^2} ie\gamma^\mu I_{\varphi_i' \varphi_i}^V u(p_i, \kappa_i) \quad \text{with} \quad I_{\varphi_i' \varphi_i}^V = I_{f_{\sigma_i'}^{\kappa_i} f_{\sigma_i}^{\kappa_i}}^V, \quad (2.26)$$

where the gauge coupling  $I_{\varphi_i' \varphi_i}^V$  depends on the chirality  $\kappa_i$  of the fermion. Similarly, for the coupling of a vector boson to an incoming antifermion  $\varphi_i = \bar{f}_{\sigma_i}^{\kappa_i}$  one obtains

$$\bar{v}(p_i, \kappa_i) ie\gamma^\mu I_{\varphi_i' \varphi_i}^V \frac{i(\not{p}_i + \not{q})}{(p_i + q)^2} \quad \text{with} \quad I_{\varphi_i' \varphi_i}^V = I_{\bar{f}_{\sigma_i'}^{\kappa_i} \bar{f}_{\sigma_i}^{\kappa_i}}^V = -I_{f_{\sigma_i'}^{\kappa_i} f_{\sigma_i}^{\kappa_i}}^V, \quad (2.27)$$

<sup>5</sup> In our calculation we use  $\{\gamma^\mu, \gamma^5\} = 0$  in  $D = 4 - 2\epsilon$  dimensions.

where the minus sign of the propagator is absorbed in the coupling of the antifermion.

In our results, the matrix elements (2.2) are often multiplied by various matrices resulting from the couplings of gauge bosons to the external fermions. For such expressions we introduce the shorthands

$$\begin{aligned}\mathcal{M}I_k^{V_1} &= \sum_{\varphi'_k} \mathcal{M}^{\varphi_1 \dots \varphi'_k \dots \varphi_n} I_{\varphi'_k \varphi_k}^{V_1}, \\ \mathcal{M}I_k^{V_1} I_k^{V_2} &= \sum_{\varphi'_k, \varphi''_k} \mathcal{M}^{\varphi_1 \dots \varphi'_k \dots \varphi_n} I_{\varphi'_k \varphi_k}^{V_1} I_{\varphi''_k \varphi_k}^{V_2},\end{aligned}\tag{2.28}$$

etc. The gauge couplings in (2.28) satisfy the commutation relations

$$e \left[ I_k^{V_1}, I_{k'}^{V_2} \right] = ig_2 \delta_{kk'} \sum_{V_3=A,Z,W^\pm} \varepsilon^{V_1 V_2 V_3} I_k^{\bar{V}_3},\tag{2.29}$$

and the  $\varepsilon$ -tensor is defined in (2.18).

Global gauge invariance implies the charge-conservation relation

$$\mathcal{M} \sum_{k=1}^n I_k^V = 0,\tag{2.30}$$

which is fulfilled up to mass-suppressed terms in the high-energy limit.

### 3 Treatment of ultraviolet and mass singularities

Large logarithms and  $1/\epsilon$  poles originate from UV and from mass singularities. In this section we present the technique that we use to extract these singularities from one- and two-loop Feynman diagrams. In Sect. 3.1 we identify the diagrams that are responsible for mass singularities within the 't Hooft–Feynman gauge and classify their contributions into factorizable and non-factorizable ones. In Sect. 3.2 we introduce an approximation that describes the exchange of virtual gauge bosons in the soft and collinear limit. Our treatment of UV singularities is discussed in Sect. 3.3.

#### 3.1 Mass singularities

In gauge theories, as is well known, mass singularities appear in loop diagrams involving virtual gauge bosons that couple to the on-shell external legs.<sup>6</sup> These singularities originate from the integration over the loop momenta in the regions where the momenta of the virtual gauge bosons become soft and/or collinear to the external momenta.

---

<sup>6</sup> In principle it is possible to adopt particular gauge fixings in order to isolate mass singularities in a smaller subset of diagrams. In the Coulomb gauge, for instance, collinear singularities appear only in external-leg self-energy corrections [26]. However, we prefer to use the 't Hooft–Feynman gauge for our analysis of mass singularities. Thus, we must consider the most general set of Feynman diagrams which gives rise to mass singularities.

### 3.1.1 Mass-singular diagrams at one loop

At one loop, the mass singularities of the  $n$ -fermion amplitude originate from diagrams of the type


(3.1)

where an electroweak gauge boson,  $V = A, Z, W^\pm$ , couples to one of the external fermions,  $i = 1, \dots, n$ , and to any other line of the diagram. These diagrams can be classified into three types:

- (i) The diagrams where the virtual gauge boson  $V$  couples to the external leg  $i$  and to another external leg  $j$  with  $j \neq i$ ,


(3.2)

These diagrams produce single- and double-logarithmic mass singularities that originate from the regions where the gauge-boson momentum becomes soft and/or collinear to the momentum of the external leg  $i$  or  $j$ .

- (ii) The external-leg self-energy insertions


(3.3)

These diagrams constitute a subset of the general mass-singular diagrams depicted in (3.1). However, they have to be omitted in our calculation since we express  $S$ -matrix elements in terms of truncated Green functions and on-shell renormalized fields.

- (iii) The diagrams where the virtual gauge boson  $V$  couples to the external line  $i$  and to an internal line, i.e. an internal propagator of the tree subdiagram that is represented as the grey blob in (3.1). These diagrams produce only single-logarithmic mass singularities that originate from the region where the momenta of the gauge boson and the external fermion  $i$  become collinear.

### 3.1.2 Factorizable and non-factorizable contributions at one loop

The diagrams of type (i) involve an  $n$ -fermion tree subdiagram. It is thus possible to extract from the diagrams (3.2) mass-singular contributions that factorize from the

$n$ -fermion Born matrix element. Such contributions are called factorizable and are defined as<sup>7</sup>

$$\begin{aligned}
\begin{array}{c} i \\ \diagup \\ \textcircled{F} \\ \diagdown \\ j \end{array} &= -ie^2 \mu_D^{4-D} \sum_{\varphi'_i, \varphi'_j} I_{\varphi'_i \varphi_i}^V I_{\varphi'_j \varphi_j}^{\bar{V}} \int \frac{d^D q}{(2\pi)^D} \frac{1}{(q^2 - M_V^2)(p_i + q)^2(p_j - q)^2} \\
&\times \bar{v}(p_j, \kappa_j) \gamma^\mu (\not{p}_j - \not{q}) G^{\varphi_1 \dots \varphi'_i \dots \varphi'_j \dots \varphi_n}(p_1, \dots, p_i, \dots, p_j, \dots, p_n) (\not{p}_i + \not{q}) \gamma_\mu u(p_i, \kappa_i). \tag{3.4}
\end{aligned}$$

Here  $G^{\varphi_1 \dots \varphi'_i \dots \varphi'_j \dots \varphi_n}$  denotes the truncated Green function corresponding to the  $n$ -fermion tree subdiagram. By definition, in the factorizable contributions (F) we include only those parts of the above diagrams that are obtained by performing the loop integration with the momentum  $q$  of the gauge boson  $V$  set to zero in the tree subdiagram. This prescription is indicated by the label F in the tree subdiagram. In (3.4) the spinors of the external fermions  $k = 1, \dots, n$  with  $k \neq i, j$  are implicitly understood.

By construction, the factorizable terms (3.4) contain all one-loop soft singularities, since the soft singularities originate only from the diagrams of type (3.2) in the region where the gauge-boson momentum tends to zero. Actually, as we will show, the factorizable contributions (3.4) contain all one-loop mass singularities, i.e. not only all soft singularities but also all collinear singularities.

The combination of all factorizable one-loop contributions is obtained by summing over all gauge bosons  $V = A, Z, W^\pm$  and external legs  $i, j$  in (3.4),

$$\mathcal{M}_1^F = \frac{1}{2} \sum_{i=1}^n \sum_{\substack{j=1 \\ j \neq i}}^n \sum_{V=A, Z, W^\pm} \left[ \begin{array}{c} i \\ \diagup \\ \textcircled{F} \\ \diagdown \\ j \end{array} \right]_{q^\mu \rightarrow xp_i^\mu, xp_j^\mu}. \tag{3.5}$$

Note that the symmetry factor  $1/2$  avoids double counting of the pairs of external legs  $i, j$ . The limit  $q^\mu \rightarrow xp_i^\mu, xp_j^\mu$  in (3.5) indicates that the above diagrams are evaluated in the approximation where the four-momentum  $q^\mu$  of the gauge boson  $V$  is soft and/or collinear to one of the momenta of the external legs  $i$  and  $j$ . This approximation, which is defined in Sect. 3.2, permits to extract all mass singularities, which result from soft and/or collinear regions.<sup>8</sup> As we will see, these terms can be expressed as products of  $n$ -fermion Born matrix elements and one-loop integrals. The factorizable one-loop terms (3.5) are computed in Sect. 5.1.

<sup>7</sup>Here we consider the case where the particles  $i$  and  $j$  are a fermion and an antifermion, respectively. The generalization to other combinations of particles or antiparticles is obvious.

<sup>8</sup>Here we adopt a different approach as compared to Ref. [7]. There the diagrams of type (3.5) were evaluated using the eikonal approximation, which extracts only soft singularities, and the collinear singularities were treated separately.

The remaining one-loop mass singularities are obtained by subtracting the factorizable contributions (3.4) and the external self-energy contributions (3.3) from the diagrams (3.1),

$$\mathcal{M}_1^{\text{NF}} = \sum_{i=1}^n \sum_{V=A,Z,W^\pm} \left[ \begin{array}{c} \text{Diagram 1} - \text{Diagram 2} \\ - \sum_{\substack{j=1 \\ j \neq i}}^n \text{Diagram 3} \end{array} \right]_{q^\mu \rightarrow xp_i^\mu} \quad (3.6)$$

These contributions are called non-factorizable (NF). We note that these NF terms are free of soft singularities since all soft singularities are contained in the factorizable parts and are subtracted in (3.6). We also observe that, in contrast to (3.5), the sum over pairs of external legs  $i, j$  appearing in front of the factorizable contributions that are subtracted in (3.6) is not multiplied by a symmetry factor  $1/2$ . This is due to the fact that in the subtraction terms in (3.6) we include only the contribution of the collinear region  $q^\mu \rightarrow xp_i^\mu$ , whereas in (3.5) every diagram contains the mass singularities resulting from the two regions  $q^\mu \rightarrow xp_i^\mu$  and  $q^\mu \rightarrow xp_j^\mu$ .

In Sect. 4 we will prove that the non-factorizable one-loop terms (3.6) vanish.

### 3.1.3 Mass-singular diagrams at two loops

The diagrams that give rise to NLL mass singularities at two loops, i.e. terms with triple and quartic logarithmic singularities, can be obtained from the one-loop diagrams of type (3.2), which produce double logarithms in the soft-collinear region, by inserting

- a second soft and/or collinear gauge boson that couples to an external line or to the virtual gauge boson in (3.2) providing an additional single or double logarithm,
- or a self-energy subdiagram in the propagator of the virtual gauge boson in (3.2), which provides an additional single logarithm.

There are five types of such diagrams:

$$(3.7)$$

Here the NLL mass singularities originate from the regions where the gauge boson  $V_1$ , which couples to two external legs or to an external leg and another virtual gauge boson, is soft and collinear and the gauge bosons  $V_2$  and  $V_3$ , in the first four diagrams in (3.7), are soft and/or collinear.

### 3.1.4 Factorizable and non-factorizable contributions at two loops

The two-loop mass singularities resulting from the diagrams (3.7) are split into factorizable and non-factorizable contributions. The factorizable contributions result from the diagrams that contain  $n$ -fermion tree subdiagrams,

$$\begin{aligned}
 \mathcal{M}_2^F = & \sum_{i=1}^n \sum_{\substack{j=1 \\ j \neq i}}^n \sum_{V_m=A,Z,W^\pm} \left\{ \frac{1}{2} \left[ \text{Diagram 1} + \text{Diagram 2} \right] \right. \\
 & + \text{Diagram 3} + \text{Diagram 4} + \text{Diagram 5} + \frac{1}{2} \text{Diagram 6} \\
 & \left. + \sum_{\substack{k=1 \\ k \neq i,j}}^n \left[ \text{Diagram 7} + \frac{1}{6} \text{Diagram 8} \right] + \frac{1}{8} \sum_{\substack{k=1 \\ k \neq i,j}}^n \sum_{\substack{l=1 \\ l \neq i,j,k}}^n \text{Diagram 9} \right\} \Bigg|_{q^\mu \rightarrow xp^\mu} \quad (3.8)
 \end{aligned}$$

As in the one-loop case, these factorizable contributions are defined as those parts of the diagrams (3.8) that are obtained by performing the loop integrations with the momenta of the gauge bosons  $V_1, V_2, V_3$  set to zero in the tree subdiagrams. This prescription is indicated by the label F in the tree subdiagrams in (3.8).

By construction, the factorizable terms (3.8) contain all two-loop soft-soft singularities, i.e. the singularities that originate from the region where all gauge bosons  $V_1, V_2, V_3$  are soft. Actually, as we will show, the factorizable contributions (3.8) contain all two-loop NLL mass singularities, i.e. not only all soft singularities but also all collinear singularities.

The symmetry factors  $1/2$ ,  $1/6$  and  $1/8$  in (3.8) avoid double counting in the sums over combinations of external legs  $i, j, k, l$ . The limit  $q^\mu \rightarrow xp^\mu$  in (3.8) indicates that the above diagrams are evaluated in the approximation where each of the four-momenta  $q^\mu$  of the various gauge bosons is collinear to one of the momenta  $p^\mu$  of the external legs and/or soft. Where relevant, also the contributions of hard regions are taken into account (see Sect. 3.2). The factorizable two-loop terms (3.8) are computed in Sect. 5.2.

The remaining two-loop NLL mass singularities, which we call non-factorizable (NF), are obtained by subtracting from the diagrams of type (3.7) the factorizable terms (3.8) and external self-energy diagrams. There are four sets of non-factorizable contributions that are associated with the first four diagrams in (3.7), whereas the last diagram in (3.7) does not produce non-factorizable NLL terms. This is due to the fact that all NLL mass singularities resulting from the last diagram in (3.7) originate from the region where the momenta of the gauge bosons  $V_1, V_2$  are soft and are thus included in the factorizable part of this diagram.

The non-factorizable terms associated with the first diagram in (3.7) read

$$\mathcal{M}_2^{\text{NF},A} = \sum_{i=1}^n \sum_{\substack{j=1 \\ j \neq i}}^n \sum_{V_m=A,Z,W^\pm} \left[ \begin{array}{c} \text{Diagram 1} - \text{Diagram 2} - \text{Diagram 3} \\ \text{Diagram 4} \end{array} \right]_{\substack{q_2^\mu \rightarrow xp_i^\mu \\ q_1^\mu \rightarrow 0}} \quad (3.9)$$

The diagrams in (3.9) are:

- Diagram 1: A vertex with three external legs labeled  $i$ ,  $j$ , and  $k$ . Two internal wavy lines are labeled  $V_1$  and  $V_2$ .
- Diagram 2: A vertex with a cross (F) and three external legs labeled  $i$ ,  $j$ , and  $k$ . Two internal wavy lines are labeled  $V_1$  and  $V_2$ .
- Diagram 3: A vertex with a cross (F) and three external legs labeled  $i$ ,  $j$ , and  $k$ . Two internal wavy lines are labeled  $V_1$  and  $V_2$ .
- Diagram 4: A vertex with a cross (F) and three external legs labeled  $i$ ,  $j$ , and  $k$ . Two internal wavy lines are labeled  $V_1$  and  $V_2$ .

The non-factorizable contributions associated with the second diagram in (3.7) are

$$\mathcal{M}_2^{\text{NF},B} = \sum_{i=1}^n \sum_{\substack{j=1 \\ j \neq i}}^n \sum_{V_m=A,Z,W^\pm} \left[ \begin{array}{c} \text{Diagram 1} - \text{Diagram 2} - \text{Diagram 3} \\ \text{Diagram 4} \end{array} \right]_{\substack{q_2^\mu \rightarrow xp_i^\mu \\ q_1^\mu \rightarrow 0}} \quad (3.10)$$

The diagrams in (3.10) are:

- Diagram 1: A vertex with three external legs labeled  $i$ ,  $j$ , and  $k$ . Two internal wavy lines are labeled  $V_1$  and  $V_2$ .
- Diagram 2: A vertex with a cross (F) and three external legs labeled  $i$ ,  $j$ , and  $k$ . Two internal wavy lines are labeled  $V_1$  and  $V_2$ .
- Diagram 3: A vertex with a cross (F) and three external legs labeled  $i$ ,  $j$ , and  $k$ . Two internal wavy lines are labeled  $V_1$  and  $V_2$ .
- Diagram 4: A vertex with a cross (F) and three external legs labeled  $i$ ,  $j$ , and  $k$ . Two internal wavy lines are labeled  $V_1$  and  $V_2$ .

The non-factorizable contributions associated with the third diagram in (3.7) are

$$\mathcal{M}_2^{\text{NF},C} = \frac{1}{2} \sum_{i=1}^n \sum_{\substack{j=1 \\ j \neq i}}^n \sum_{\substack{k=1 \\ k \neq i,j}}^n \sum_{V_m=A,Z,W^\pm} \left[ \begin{array}{c} \text{Diagram 1} - \text{Diagram 2} - \text{Diagram 3} \\ \text{Diagram 4} - \sum_{\substack{l=1 \\ l \neq i,j,k}}^n \text{Diagram 5} \end{array} \right]_{\substack{q_2^\mu \rightarrow xp_i^\mu \\ q_1^\mu \rightarrow 0}} \quad (3.11)$$

The diagrams in (3.11) are:

- Diagram 1: A vertex with three external legs labeled  $i$ ,  $j$ , and  $k$ . Two internal wavy lines are labeled  $V_1$  and  $V_2$ .
- Diagram 2: A vertex with three external legs labeled  $i$ ,  $j$ , and  $k$ . Two internal wavy lines are labeled  $V_1$  and  $V_2$ .
- Diagram 3: A vertex with a cross (F) and three external legs labeled  $i$ ,  $j$ , and  $k$ . Two internal wavy lines are labeled  $V_1$  and  $V_2$ .
- Diagram 4: A vertex with a cross (F) and three external legs labeled  $i$ ,  $j$ , and  $k$ . Two internal wavy lines are labeled  $V_1$  and  $V_2$ .
- Diagram 5: A vertex with a cross (F) and three external legs labeled  $i$ ,  $j$ , and  $k$ . Two internal wavy lines are labeled  $V_1$  and  $V_2$ .

Here the first subtraction term represents an external-leg self-energy insertion and the symmetry factor  $1/2$  is introduced in order to avoid double counting of the terms resulting from the permutation of the external legs  $j$  and  $k$ . The non-factorizable contributions associated with the fourth diagram in (3.7) read

$$\mathcal{M}_2^{\text{NF},D} = \sum_{i=1}^n \sum_{\substack{j=1 \\ j \neq i}}^n \sum_{V_m=A,Z,W^\pm} \left[ \begin{array}{c} \text{Diagram 1} - \text{Diagram 2} - \text{Diagram 3} \end{array} \right]$$

The diagrams in (3.12) are:

- Diagram 1: A vertex with three external legs labeled  $i$ ,  $j$ , and  $k$ . Three internal wavy lines are labeled  $V_1$ ,  $V_2$ , and  $V_3$ .
- Diagram 2: A vertex with a cross (F) and three external legs labeled  $i$ ,  $j$ , and  $k$ . Three internal wavy lines are labeled  $V_1$ ,  $V_2$ , and  $V_3$ .
- Diagram 3: A vertex with a cross (F) and three external legs labeled  $i$ ,  $j$ , and  $k$ . Three internal wavy lines are labeled  $V_1$ ,  $V_2$ , and  $V_3$ .

$$- \sum_{\substack{k=1 \\ k \neq i, j}}^n \left[ \text{Diagram} \right]_{\substack{q_2^\mu \rightarrow xp_i^\mu \\ q_1^\mu \rightarrow 0}}. \quad (3.12)$$

As indicated by the limits  $q_2^\mu \rightarrow xp_i^\mu$ ,  $q_1^\mu \rightarrow 0$  in (3.9)–(3.12), we extract the NLL mass singularities that appear in the above combinations of diagrams in the regions where the momentum  $q_1^\mu$  of the gauge boson  $V_1$  is soft and the momentum  $q_2^\mu$  of the gauge boson  $V_2$  is collinear to the external momentum  $p_i^\mu$ . The terms (3.9)–(3.12) are free of singularities in the soft limit  $x \rightarrow 0$  since all soft–soft singularities are included in the factorizable parts that are subtracted.

The subtraction of the factorizable terms must be performed without double-counting of diagrams and regions, i.e. the terms that are subtracted in (3.9)–(3.12) must correspond exactly to the ones that are included in (3.8). This correspondence is not obvious at first sight, since certain diagrams appear a different number of times or with different symmetry factors in (3.8) and (3.9)–(3.12). This is due to the fact that in (3.9)–(3.12) the contributions of certain diagrams are split into various terms that result from different singular regions, whereas in (3.8) every diagram includes the contributions of all singular regions. For instance, let us consider the last diagram in (3.9). This diagram appears only once in (3.8) but is subtracted four times in (3.9)–(3.12). These four subtraction terms can be rewritten as

$$\sum_{i=1}^n \sum_{\substack{j=1 \\ j \neq i}}^n \sum_{\substack{k=1 \\ k \neq i, j}}^n \sum_{V_m=A, Z, W^\pm} \left\{ \left[ \text{Diagram} \right]_{\substack{q_a^\mu \rightarrow 0 \\ q_b^\mu \rightarrow xp_i^\mu}} + \left[ \text{Diagram} \right]_{\substack{q_a^\mu \rightarrow xp_i^\mu \\ q_b^\mu \rightarrow 0}} + \left[ \text{Diagram} \right]_{\substack{q_a^\mu \rightarrow 0 \\ q_b^\mu \rightarrow xp_k^\mu}} \right\}, \quad (3.13)$$

where the last term in (3.13) corresponds to the two terms that are multiplied with a symmetry factor  $1/2$  in (3.11). As can easily be seen in (3.13), these three contributions are associated with the three non-overlapping singular regions of the diagram that give rise to NLL terms,<sup>9</sup> and their sum corresponds to the complete contribution included in (3.8). Similarly, one can verify that all other subtraction terms in (3.9)–(3.12) correspond exactly to the factorizable contributions included in (3.8).

In Sect. 4 we will prove that the non-factorizable contributions (3.9)–(3.12) cancel.

### 3.2 Soft–collinear approximation for virtual gauge-boson exchange

As discussed in the previous section, mass singularities appear when the external fermions emit virtual gauge bosons in the soft and collinear regions. Here we introduce a

<sup>9</sup>The region  $q_a^\mu \rightarrow xp_j^\mu$ ,  $q_b^\mu \rightarrow 0$  does not give rise to NLL mass singularities.



soft-collinear approximation that describes the gauge-boson-fermion-antifermion vertices in these regions. This approximation permits to derive the soft and collinear singularities of generic  $n$ -fermion amplitudes in a process-independent way.

Let us first consider an  $n$ -fermion diagram involving the exchange of a virtual gauge boson  $V = A, Z, W^\pm$  between the external leg  $i$  and some other (external or internal) line,<sup>10</sup>

$$\begin{array}{c} \text{---} \end{array} \text{---} i = \sum_{\varphi'_i} G_\mu^{\bar{V}\varphi'_i}(-q, p_i + q) \frac{i(\not{p}_i + \not{q})}{(p_i + q)^2} i e \gamma^\mu I_{\varphi'_i \varphi_i}^V u(p_i, \kappa_i). \quad (3.14)$$

Here  $G_\mu^{\bar{V}\varphi'_i}(-q, p_i + q)$  represents the truncated Green function corresponding to the internal part of the diagram, which is depicted as a grey blob. The contraction with the spinors of the external fermions  $j = 1, \dots, n$  with  $j \neq i$  is implicitly understood. The loop momentum of the gauge boson is denoted as  $q$  and the propagator that connects the gauge boson lines  $V^\mu$  and  $\bar{V}^\mu$  has been omitted. Commuting the Dirac matrices associated with the fermion propagator and the gauge-boson-fermion vertex and using the massless Dirac equation we have

$$i(\not{p}_i + \not{q})i e \gamma^\mu u(p_i, \kappa_i) = -e [2(p_i + q)^\mu - \gamma^\mu \not{q}] u(p_i, \kappa_i). \quad (3.15)$$

In the collinear limit  $q^\mu \rightarrow x p_i^\mu$  the  $\not{q} u(p_i, \kappa_i)$  term vanishes owing to the Dirac equation. Thus, we obtain

$$\lim_{q^\mu \rightarrow x p_i^\mu} \begin{array}{c} \text{---} \end{array} \text{---} i = G_\mu^{\bar{V}i}(-q, p_i + q) u(p_i, \kappa_i) \frac{-2e I_i^V (p_i + q)^\mu}{(p_i + q)^2}, \quad (3.16)$$

where we have introduced the shorthand  $G_\mu^{\bar{V}i}(-q, p_i + q) I_i^V = \sum_{\varphi'_i} G_\mu^{\bar{V}\varphi'_i}(-q, p_i + q) I_{\varphi'_i \varphi_i}^V$ . The approximation (3.16) is applicable also to the case where the gauge boson  $V$  becomes collinear to another leg  $j \neq i$ . In this case, the term  $\gamma^\mu \not{q}$  on the right-hand side of (3.15) is contracted with another soft-collinear factor  $(p_j - q)_\mu$  resulting from the coupling of the gauge boson  $V$  to the leg  $j$  and

$$\lim_{q^\mu \rightarrow x p_j^\mu} (p_j - q)_\mu \gamma^\mu \not{q} = (1 - x) x \not{p}_j^2 = 0. \quad (3.17)$$

Similarly, (3.16) applies also to the case where the gauge boson  $V$  splits into two gauge bosons,  $V'$  and  $V''$ , with  $V'$  being collinear to an external leg  $j \neq i$  and  $V''$  soft. Here, the combination of the soft-collinear factor associated with the external leg  $j$ , the triple gauge-boson vertex and the term  $\gamma^\mu \not{q}$  on the right-hand side of (3.15) yields

$$\lim_{q^\mu \rightarrow x p_j^\mu} (p_j - q)^{\mu'} [-2g_{\mu\mu'} q_{\mu''} + g_{\mu'\mu''} q_\mu + g_{\mu\mu''} q_{\mu'}] \gamma^\mu \not{q} = 0. \quad (3.18)$$

<sup>10</sup>For the moment, we consider the case where the external particle  $i$  is a fermion. The generalization to antifermions is discussed below.

For the multiple emission of collinear gauge bosons  $V_1 \dots V_n$  by an external fermion  $i$  we obtain

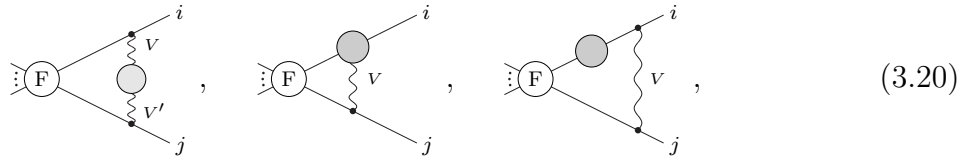
$$\begin{aligned}
\lim_{q_k^\mu \rightarrow x_k p_i^\mu} \text{diagram} &= G_{\mu_1 \dots \mu_n}^{\bar{V}_1 \dots \bar{V}_n} \hat{z}(-q_1, \dots, -q_n, p_i + \tilde{q}_n) u(p_i, \kappa_i) \\
&\times \frac{-2eI_i^{V_n}(p_i + \tilde{q}_n)^{\mu_n}}{(p_i + \tilde{q}_n)^2} \dots \frac{-2eI_i^{V_1}(p_i + q_1)^{\mu_1}}{(p_i + q_1)^2},
\end{aligned} \tag{3.19}$$

where  $\tilde{q}_j = q_1 + \dots + q_j$ . This approximation is also applicable to all cases where one of the gauge bosons  $V_1, \dots, V_n$  becomes collinear to one of the other external legs  $j \neq i$  and all remaining gauge bosons are soft. Therefore (3.19) provides a correct description of the gauge-boson-fermion couplings in all regions that are relevant for our NLL analysis.

Also for the case where the external line  $i$  represents an antifermion, the emission of collinear gauge bosons produces factors  $-2eI_i^{V_k}(p_i + \tilde{q}_k)^{\mu_k}$  and, apart from the obvious replacement of the spinor  $u(p_i, \kappa_i)$  by  $\bar{v}(p_i, \kappa_i)$ , we obtain exactly the same formula as in (3.19).

The soft-collinear approximation (3.19) permits to replace the Dirac matrices associated with each gauge-boson emission by simple four-vector factors  $-2(p_i + \tilde{q}_k)^{\mu_k}$ . In the soft limit,  $q_j^\mu \rightarrow 0$ , these factors correspond to the well-known factors  $-2p_i^{\mu_k}$  that are used to derive soft singularities in the eikonal approximation. The soft-collinear approximation (3.19) can be regarded as an extension of the eikonal approximation that permits to describe the emission of gauge bosons in the soft and the collinear regions. When applied to the one- and two-loop factorizable contributions (3.5) and (3.8), this approximation permits to factorize the mass singularities from the  $n$ -fermion Born amplitude explicitly.

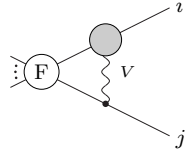
We note that the soft-collinear approximation is not applicable in the case where NLL two-loop contributions arise as a combination of logarithmic singularities originating from soft-collinear and UV regions. In particular, for the two-loop factorizable terms of the type



where a soft-collinear singularity resulting from the exchange of the gauge bosons  $V$  (and  $V'$ ) appears in combination with an UV singularity resulting from hard particles in one-loop subdiagrams, the approximation (3.19) can be applied only to the vertices that occur outside the UV-divergent one-loop subdiagrams whereas for the vertices and propagators inside the one-loop subdiagrams we have to apply the usual Feynman rules.

In the case of the last two diagrams in (3.20) this approximation is not sufficient to eliminate the chain of Dirac matrices along the external fermionic leg  $i$ . However, this chain of Dirac matrices can be contracted with the spinor of the external fermion by

means of a simple projector. Let us illustrate how this is achieved for the second diagram in (3.20),



$$= -2eI_{\varphi'_j\varphi_j}^{\bar{V}}G^{\varphi'_i}(p_i)X^{V\varphi_i\bar{\varphi}'_i}(p_i,p_j)u(p_i,\kappa_i) \quad (3.21)$$

with

$$X^{V\varphi_i\bar{\varphi}'_i}(p_i,p_j) = \mu_D^{4-D} \int \frac{d^Dq}{(2\pi)^D} \frac{(p_j - q)^\mu (\not{p}_i + \not{q}) i\Gamma_\mu^{V\varphi_i\bar{\varphi}'_i}(q,p_i)}{(q^2 - M_V^2)(p_i + q)^2(p_j - q)^2}. \quad (3.22)$$

Here the factor  $(p_j - q)^\mu$  comes from the soft-collinear vertex along the leg  $j$ , and  $i\Gamma_\mu^{V\varphi_i\bar{\varphi}'_i}$  represents the one-loop vertex. The truncated Green function  $G^{\varphi'_i}(p_i)$  in (3.21) represents the internal part of the diagram, where the momentum  $q$  of the gauge boson  $V$  is set to zero according to the definition of the factorizable part. The contraction with the spinors of the external fermions  $j = 1, \dots, n$  with  $j \neq i$  is implicitly understood. If one contracts this Green function with the spinor of the fermion  $i$  one simply obtains the on-shell Born matrix element,

$$G^{\varphi'_i}(p_i)u(p_i,\kappa_i) = \mathcal{M}_0^{\varphi_1\dots\varphi'_i\dots\varphi'_j\dots\varphi_n}. \quad (3.23)$$

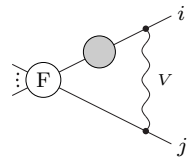
The chain of Dirac matrices occurring in (3.22) can be projected on the Dirac spinor using<sup>11</sup>

$$X^{V\varphi_i\bar{\varphi}'_i}(p_i,p_j)u(p_i,\kappa_i) = \frac{1}{2p_i p_j} \text{Tr} \left[ X^{V\varphi_i\bar{\varphi}'_i}(p_i,p_j)\omega_{\kappa_i}\not{p}_i\not{p}_j \right] u(p_i,\kappa_i), \quad (3.24)$$

so that one obtains

$$G^{\varphi'_i}(p_i)X^{V\varphi_i\bar{\varphi}'_i}(p_i,p_j)u(p_i,\kappa_i) = \frac{1}{2p_i p_j} \text{Tr} \left[ X^{V\varphi_i\bar{\varphi}'_i}(p_i,p_j)\omega_{\kappa_i}\not{p}_i\not{p}_j \right] \mathcal{M}_0^{\varphi_1\dots\varphi'_i\dots\varphi'_j\dots\varphi_n}. \quad (3.25)$$

The same trace projector can be applied to the last diagram in (3.20),



$$= 2e^2 I_{\varphi'_i\varphi_i}^V I_{\varphi'_j\varphi_j}^{\bar{V}} G^{\varphi'_i}(p_i)X^{\varphi'_i\bar{\varphi}'_i}(p_i,p_j)u(p_i,\kappa_i), \quad (3.26)$$

<sup>11</sup>This identity can easily be verified by means of the general decomposition

$$X^{V\varphi_i\bar{\varphi}'_i}(p_i,p_j)\omega_\kappa = \sum_{k=0}^N \sum_{l_1=i,j} \dots \sum_{l_{2k}=i,j} A_{l_1\dots l_{2k}}(p_i,p_j)\not{p}_{l_1}\dots\not{p}_{l_{2k}}\omega_\kappa,$$

the Dirac equation,  $\not{p}_i u(p_i,\kappa_i) = 0$ , the anticommutation relation  $\{\not{p}_i,\not{p}_j\} = 2p_i p_j$ , the identities  $\not{p}_i^2 = \not{p}_j^2 = 0$ , and the fact that, for massless fermions, the subamplitude  $X^{V\varphi_i\bar{\varphi}'_i}(p_i,p_j)$  contains only Dirac chains with even numbers  $2k$  of Dirac matrices.

where

$$X^{\varphi'_i \bar{\varphi}'_i}(p_i, p_j) = \mu_D^{4-D} \int \frac{d^D q}{(2\pi)^D} \frac{(p_j - q)^\mu (\not{p}_i + \not{q}) i \Sigma^{\varphi'_i \bar{\varphi}'_i}(p_i + q) (\not{p}_i + \not{q}) \gamma_\mu}{(q^2 - M_V^2) [(p_i + q)^2]^2 (p_j - q)^2}, \quad (3.27)$$

and  $i \Sigma^{\varphi'_i \bar{\varphi}'_i}$  represents the fermionic self-energy. Again we can project (3.27) on the Dirac spinor using

$$G_{\pm}^{\varphi'_i}(p_i) X^{\varphi'_i \bar{\varphi}'_i}(p_i, p_j) u(p_i, \kappa_i) = \frac{1}{2p_i p_j} \text{Tr} \left[ X^{\varphi'_i \bar{\varphi}'_i}(p_i, p_j) \omega_{\kappa_i} \not{p}_i \not{p}_j \right] \mathcal{M}_0^{\varphi_1 \dots \varphi'_i \dots \varphi'_j \dots \varphi_n}. \quad (3.28)$$

### 3.3 Ultraviolet singularities

Let us first discuss our treatment of UV singularities at one loop. The UV singularities appearing in the bare loop amplitudes are cancelled by corresponding singularities provided by the counterterms. These cancellations give rise to logarithmic contributions of the form

$$\left( \frac{\mu_D^2}{Q^2} \right)^\epsilon \left[ \frac{1}{\epsilon} \left( \frac{Q^2}{\mu_{\text{loop}}^2} \right)^\epsilon - \frac{1}{\epsilon} \left( \frac{Q^2}{\mu_R^2} \right)^\epsilon \right] = \ln \left( \frac{\mu_R^2}{\mu_{\text{loop}}^2} \right) + \mathcal{O}(\epsilon), \quad (3.29)$$

where the first and the second term between the brackets result from bare loop diagrams and counterterms, respectively. Here  $\mu_D$  is the scale of dimensional regularization and we have factorized the term  $(\mu_D^2/Q^2)^\epsilon$  that we always absorb in  $\alpha_\epsilon$  [see (2.7)]. The renormalization scale is denoted as  $\mu_R$ , and  $\mu_{\text{loop}}$  represents the characteristic scale of the UV-singular loop diagram. This latter is related to the momenta of the lines that enter the loop.

At one loop, since in the high-energy limit all combinations of external momenta are hard, the characteristic scale of UV-divergent diagrams that contribute to truncated  $n$ -fermion Green functions is always of the order  $\mu_{\text{loop}}^2 \sim Q^2$ . This permits us to isolate all logarithms that result from UV singularities, i.e. terms of the type (3.29), in the counterterms. To this end, in our calculation we perform a minimal subtraction of all UV poles that appear in the bare loop diagrams and in the counterterms. The combination of these subtracted terms corresponds to

$$\left( \frac{\mu_D^2}{Q^2} \right)^\epsilon \left\{ \frac{1}{\epsilon} \left[ \left( \frac{Q^2}{\mu_{\text{loop}}^2} \right)^\epsilon - 1 \right] - \frac{1}{\epsilon} \left[ \left( \frac{Q^2}{\mu_R^2} \right)^\epsilon - 1 \right] \right\} \quad (3.30)$$

and is obviously equivalent to (3.29). As a result of the minimal subtraction the logarithmic contributions  $\epsilon^{-1} [(Q^2/\mu_{\text{loop}}^2)^\epsilon - 1]$  originating from bare loop diagrams that are characterized by a hard scale  $\mu_{\text{loop}}^2 \sim Q^2$  vanish.

Thus, at one loop we can restrict ourselves to the calculation of the mass-singular bare diagrams and the counterterms. The minimal subtraction of the UV singularities appearing in these two types of contributions permits us to ignore any other bare diagram that produces UV singularities.

At two loops, pure UV singularities produce only NNLL contributions since every UV-singular loop produces only a single-logarithmic term. The only NLL two-loop terms resulting from UV singularities are combinations of one-loop UV logarithms with one-loop double logarithms resulting from soft-collinear gauge bosons. These terms originate

from one-loop insertions in the one-loop diagrams (3.2). Here, as in the one-loop case, we perform a minimal subtraction of the UV singularity, such that the logarithms associated with one-loop subdivergences from hard subdiagrams with  $\mu_{\text{loop}}^2 \sim Q^2$  are completely isolated in the counterterms. As a consequence, the UV contributions associated with one-loop insertions in the internal part of the one-loop diagram (3.2) become irrelevant. In particular the UV logarithmic contributions resulting from the two-loop ladder diagrams of type

$$(3.31)$$

in the region where  $V_1$  is soft and  $V_2$  is hard vanish. Minimal subtraction of the UV singularities permits us to use the soft-collinear approximation for all gauge bosons  $V_1, V_2$  in the above diagrams despite of the fact that this approximation is not appropriate to describe the hard region and can in principle produce fake logarithms of UV origin. Instead, the diagrams of the type (3.20), which result from the insertion of one-loop subdiagrams in the lines that are not hard ( $\mu_{\text{loop}}^2 \ll Q^2$ ) in (3.2), give rise to non-negligible NLL contributions of UV type. These UV contributions are correctly taken into account in our calculation as explained in Sect. 3.2.

#### 4 Collinear Ward identities and cancellation of non-factorizable terms

In this section we prove that the non-factorizable subset of mass singularities, i.e. the one-loop terms (3.6) and the two-loop terms (3.9)–(3.12), vanish. The proof is based on the collinear Ward identities that have been derived in Ref. [7].

Let us start with the non-factorizable one-loop terms (3.6). This contribution can be written as

$$\begin{aligned} \mathcal{M}_1^{\text{NF}} = & \sum_{i=1}^n \sum_{V=A,Z,W^\pm} \sum_{\varphi'_i} \mu_D^{4-D} \int \frac{d^D q}{(2\pi)^D} \frac{1}{(q^2 - M_V^2)(p_i - q)^2} \lim_{q^\mu \rightarrow x p_i^\mu} 2(p_i - q)^\mu \\ & \times \left\{ G_\mu^{[V\varphi'_i]}(q, p_i - q) u(p_i, \kappa_i) + \sum_{\substack{j=1 \\ j \neq i}}^n \sum_{\varphi'_j} \frac{2(p_j + q)_\mu}{(p_j + q)^2} \mathcal{M}_0^{\varphi_1 \dots \varphi'_i \dots \varphi'_j \dots \varphi_n} e I_{\varphi'_j \varphi_j}^V \right\} i e I_{\varphi'_i \varphi_i}^{\bar{V}}, \end{aligned} \quad (4.1)$$

where we have factorized the two propagators that appear in all three diagrams in (3.6). Here  $u(p_i, \kappa_i)$  is the spinor of the external fermion  $i$  and we have introduced the abbreviation

$$G_\mu^{[V\varphi'_i]}(q, p_i - q) = \text{diagram 1} - \text{diagram 2} \quad (4.2)$$

for the tree subdiagrams that are associated with the first two terms on the right-hand side of (3.6). In (4.2) the contraction with the spinors of the external fermions  $j = 1, \dots, n$

with  $j \neq i$  is implicitly understood, and the incoming momenta associated with the lines  $V_\mu$  and  $i$  are  $q$  and  $p_i - q$ , respectively.

The combination of tree subdiagrams (4.2) fulfils the collinear Ward identities [7]

$$\lim_{q^\mu \rightarrow xp_i^\mu} q^\mu G_\mu^{[V\varphi_i]}(q, p_i - q)u(p_i, \kappa_i) = \sum_{\varphi'_i} \mathcal{M}_0^{\varphi_1 \dots \varphi'_i \dots \varphi_n} eI_{\varphi'_i \varphi_i}^V. \quad (4.3)$$

Using the charge-conservation relation (2.30) and

$$\lim_{q^\mu \rightarrow xp_i^\mu} \frac{2q^\mu (p_j + q)_\mu}{(p_j + q)^2} = 1 \quad \text{for } j \neq i, \quad (4.4)$$

we can rewrite the identities (4.3) as

$$\lim_{q^\mu \rightarrow xp_i^\mu} q^\mu \left\{ G_\mu^{[V\varphi_i]}(q, p_i - q)u(p_i, \kappa_i) + \sum_{\substack{j=1 \\ j \neq i}}^n \sum_{\varphi'_j} \frac{2(p_j + q)_\mu}{(p_j + q)^2} \mathcal{M}_0^{\varphi_1 \dots \varphi'_j \dots \varphi_n} eI_{\varphi'_j \varphi_j}^V \right\} = 0, \quad (4.5)$$

where the expression between the curly brackets is identical to the one that appears on the right-hand side of (4.1). These collinear Ward identities can be represented diagrammatically as

$$\lim_{q^\mu \rightarrow xp_i^\mu} q^\mu \times \left[ \begin{array}{c} \text{Diagram 1: } \text{---} \bullet \text{---} i \text{ with } V_\mu \text{ wavy line} \\ \text{Diagram 2: } \text{---} \bullet \text{---} i \text{ with } V_\mu \text{ wavy line} \\ \text{Diagram 3: } \text{---} \textcircled{F} \text{---} i \text{ with } V_\mu \text{ wavy line and } j \text{ line} \end{array} \right] = 0, \quad (4.6)$$

where the contraction with all fermionic spinors, including  $u(p_i, \kappa_i)$ , is implicitly understood.

The cancellation of the non-factorizable terms (4.1) is simply due to the fact that in the collinear limit  $q^\mu \rightarrow xp_i^\mu$  the four-vector  $(p_i - q)^\mu$  on the right-hand side of (4.1) becomes proportional to the gauge-boson momentum  $q^\mu$  and its contraction with the expression between the curly brackets vanishes as a result of the collinear Ward identities (4.5).

Let us now consider the two-loop non-factorizable terms (3.9)–(3.12). The contribution (3.9) yields

$$\begin{aligned} \mathcal{M}_2^{\text{NF},A} &= \sum_{i=1}^n \sum_{\substack{j=1 \\ j \neq i}}^n \sum_{V_m=A,Z,W^\pm} \sum_{\varphi'_i, \varphi''_i, \varphi'_j} \mu_D^{2(4-D)} \int \frac{d^D q_1}{(2\pi)^D} \int \frac{d^D q_2}{(2\pi)^D} \frac{8e^3 (p_i - q_1)(p_j + q_1)}{(q_1^2 - M_{V_1}^2)(q_2^2 - M_{V_2}^2)} \\ &\times \frac{1}{(p_i - q_1)^2 (p_j + q_1)^2 (p_i - q_1 - q_2)^2} \lim_{q_1^\mu \rightarrow 0} \lim_{q_2^\mu \rightarrow xp_i^\mu} (p_i - q_1 - q_2)^\mu \\ &\times \left\{ G_\mu^{[\bar{V}_2 \varphi''_i]}(q_2, p_i - q_1 - q_2)u(p_i, \kappa_i) \right. \\ &+ \frac{2(p_j + q_1 + q_2)_\mu}{(p_j + q_1 + q_2)^2} \sum_{\varphi'_j} \mathcal{M}_0^{\varphi_1 \dots \varphi''_i \dots \varphi'_j \dots \varphi_n} eI_{\varphi'_j \varphi_j}^{\bar{V}_2} \\ &\left. + \sum_{\substack{k=1 \\ k \neq i,j}}^n \frac{2(p_k + q_2)_\mu}{(p_k + q_2)^2} \sum_{\varphi'_k} \mathcal{M}_0^{\varphi_1 \dots \varphi''_i \dots \varphi'_j \dots \varphi'_k \dots \varphi_n} eI_{\varphi'_k \varphi_k}^{\bar{V}_2} \right\} I_{\varphi'_i \varphi_i}^{V_2} I_{\varphi'_j \varphi_j}^{\bar{V}_1} I_{\varphi_i \varphi_i}^{V_1} = 0. \quad (4.7) \end{aligned}$$

This cancellation can easily be verified by means of the collinear Ward identities (4.5) by observing that in the soft-collinear limit  $q_1^\mu \rightarrow 0$ ,  $q_2^\mu \rightarrow xp_i^\mu$  the four-vector  $(p_i - q_1 - q_2)^\mu$  tends to  $(1/x - 1)q_2^\mu$  and the expression within the curly brackets in (4.7) becomes equivalent to the one in (4.5). Similarly, for the contributions (3.10) and (3.11) we obtain

$$\begin{aligned}
\mathcal{M}_2^{\text{NF},B} &= \sum_{i=1}^n \sum_{\substack{j=1 \\ j \neq i}}^n \sum_{V_m=A,Z,W^\pm} \sum_{\varphi'_i, \varphi'_j} \mu_D^{2(4-D)} \int \frac{d^D q_1}{(2\pi)^D} \int \frac{d^D q_2}{(2\pi)^D} \frac{8e^3(p_i - q_1 - q_2)(p_j + q_1)}{(q_1^2 - M_{V_1}^2)(q_2^2 - M_{V_2}^2)} \\
&\quad \times \frac{1}{(p_i - q_2)^2(p_j + q_1)^2(p_i - q_1 - q_2)^2} \lim_{q_1^\mu \rightarrow 0} \lim_{q_2^\mu \rightarrow xp_i^\mu} (p_i - q_2)^\mu \\
&\quad \times \left\{ G_\mu^{[\bar{V}_2 \varphi'_i]}(q_2, p_i - q_1 - q_2) u(p_i, \kappa_i) \right. \\
&\quad + \frac{2(p_j + q_1 + q_2)_\mu}{(p_j + q_1 + q_2)^2} \sum_{\varphi'_j} \mathcal{M}_0^{\varphi_1 \dots \varphi'_i \dots \varphi'_j \dots \varphi_n} e^{I_{\varphi'_j \varphi'_j} \bar{V}_2} \\
&\quad \left. + \sum_{\substack{k=1 \\ k \neq i,j}}^n \frac{2(p_k + q_2)_\mu}{(p_k + q_2)^2} \sum_{\varphi'_k} \mathcal{M}_0^{\varphi_1 \dots \varphi'_i \dots \varphi'_j \dots \varphi'_k \dots \varphi_n} e^{I_{\varphi'_k \varphi'_k} \bar{V}_2} \right\} I_{\varphi'_j \varphi_j}^{\bar{V}_1} I_{\varphi'_i \varphi_i}^{V_1} I_{\varphi'_i \varphi_i}^{V_2} = 0, \quad (4.8)
\end{aligned}$$

and

$$\begin{aligned}
\mathcal{M}_2^{\text{NF},C} &= \frac{1}{2} \sum_{i=1}^n \sum_{\substack{j=1 \\ j \neq i}}^n \sum_{\substack{k=1 \\ k \neq i,j}}^n \sum_{V_m=A,Z,W^\pm} \sum_{\varphi'_i, \varphi'_j, \varphi'_k} \mu_D^{2(4-D)} \int \frac{d^D q_1}{(2\pi)^D} \int \frac{d^D q_2}{(2\pi)^D} \frac{1}{(q_1^2 - M_{V_1}^2)} \\
&\quad \times \frac{8e^3(p_k - q_1)(p_j + q_1)}{(q_2^2 - M_{V_2}^2)(p_i - q_2)^2(p_j + q_1)^2(p_k - q_1)^2} \lim_{q_1^\mu \rightarrow 0} \lim_{q_2^\mu \rightarrow xp_i^\mu} (p_i - q_2)^\mu \\
&\quad \times \left\{ G_\mu^{[\bar{V}_2 \varphi'_i]}(q_2, p_i - q_2) u(p_i, \kappa_i) \right. \\
&\quad + \frac{2(p_j + q_1 + q_2)_\mu}{(p_j + q_1 + q_2)^2} \sum_{\varphi'_j} \mathcal{M}_0^{\varphi_1 \dots \varphi'_i \dots \varphi'_j \dots \varphi'_k \dots \varphi_n} e^{I_{\varphi'_j \varphi'_j} \bar{V}_2} \\
&\quad + \frac{2(p_k - q_1 + q_2)_\mu}{(p_k - q_1 + q_2)^2} \sum_{\varphi'_k} \mathcal{M}_0^{\varphi_1 \dots \varphi'_i \dots \varphi'_j \dots \varphi'_k \dots \varphi_n} e^{I_{\varphi'_k \varphi'_k} \bar{V}_2} \\
&\quad \left. + \sum_{\substack{l=1 \\ l \neq i,j,k}}^n \frac{2(p_l + q_2)_\mu}{(p_l + q_2)^2} \sum_{\varphi'_l} \mathcal{M}_0^{\varphi_1 \dots \varphi'_i \dots \varphi'_j \dots \varphi'_k \dots \varphi'_l \dots \varphi_n} e^{I_{\varphi'_l \varphi'_l} \bar{V}_2} \right\} I_{\varphi'_j \varphi_j}^{\bar{V}_1} I_{\varphi'_k \varphi_k}^{V_1} I_{\varphi'_i \varphi_i}^{V_2} = 0. \quad (4.9)
\end{aligned}$$

Finally, for the contribution (3.12) we have

$$\begin{aligned}
\mathcal{M}_2^{\text{NF},D} &= \sum_{i=1}^n \sum_{\substack{j=1 \\ j \neq i}}^n \sum_{V_m=A,Z,W^\pm} \sum_{\varphi'_i, \varphi'_j} \mu_D^{2(4-D)} \int \frac{d^D q_1}{(2\pi)^D} \int \frac{d^D q_2}{(2\pi)^D} \frac{4ie^2 g_2 \varepsilon^{V_1 V_2 V_3}}{(q_1^2 - M_{V_1}^2)(q_2^2 - M_{V_2}^2)} \\
&\quad \times \frac{1}{(q_3^2 - M_{V_3}^2)(p_i - q_2)^2(p_j - q_1)^2} \lim_{q_1^\mu \rightarrow 0} \lim_{q_2^\mu \rightarrow xp_i^\mu} (p_i - q_2)^{\mu_2} (p_j - q_1)^{\mu_1} \\
&\quad \times \left[ g_{\mu_1 \mu_2} (q_1 - q_2)^{\mu_3} + g_{\mu_2}^{\mu_3} (q_2 + q_3)_{\mu_1} - g_{\mu_1}^{\mu_3} (q_3 + q_1)_{\mu_2} \right]
\end{aligned}$$

$$\begin{aligned}
& \times \left\{ G_{\mu_3}^{[\bar{V}_3 \varphi'_i]}(q_3, p_i - q_2) u(p_i, \kappa_i) + \frac{2(p_j + q_2)_{\mu_3}}{(p_j + q_2)^2} \sum_{\varphi'_j} \mathcal{M}_0^{\varphi_1 \dots \varphi'_i \dots \varphi'_j \dots \varphi_n} e I_{\varphi'_j \varphi'_j}^{\bar{V}_3} \right. \\
& \left. + \sum_{\substack{k=1 \\ k \neq i, j}}^n \frac{2(p_k + q_3)_{\mu_3}}{(p_k + q_3)^2} \sum_{\varphi'_k} \mathcal{M}_0^{\varphi_1 \dots \varphi'_i \dots \varphi'_j \dots \varphi'_k \dots \varphi_n} e I_{\varphi'_k \varphi_k}^{\bar{V}_3} \right\} I_{\varphi'_j \varphi_j}^{\bar{V}_1} I_{\varphi'_i \varphi_i}^{\bar{V}_2}, \quad (4.10)
\end{aligned}$$

where  $q_3 = q_1 + q_2$ . In the soft-collinear limit we observe that

$$\begin{aligned}
& \lim_{q_1^\mu \rightarrow 0} \lim_{q_2^\mu \rightarrow x p_i^\mu} (p_i - q_2)^{\mu_2} (p_j - q_1)^{\mu_1} \left[ g_{\mu_1 \mu_2}(q_1 - q_2)^{\mu_3} + g_{\mu_2}^{\mu_3}(q_2 + q_3)_{\mu_1} - g_{\mu_1}^{\mu_3}(q_3 + q_1)_{\mu_2} \right] = \\
& = (1 - x)(p_i p_j) q_3^{\mu_3}, \quad (4.11)
\end{aligned}$$

and again the contraction of this four-vector with the expression between the curly brackets in (4.10) cancels as a result of the collinear Ward identities (4.5).

## 5 Factorizable contributions

In this section, we present explicit results for the one- and two-loop factorizable contributions defined in Sects. 3.1.2 and 3.1.4. These are evaluated within the 't Hooft–Feynman gauge, where the masses of the Faddeev–Popov ghosts  $u^A, u^Z, u^{W^\pm}$  and would-be Goldstone bosons  $\chi, \phi^\pm$  read  $M_{u^A} = M_A = 0$ ,  $M_\chi = M_{u^Z} = M_Z$ , and  $M_{\phi^\pm} = M_{u^W} = M_W$ . Using the soft-collinear approximation introduced in Sect. 3.2, we express the factorizable contributions resulting from individual diagrams as products of the  $n$ -fermion Born amplitude with matrix-valued gauge couplings and loop integrals. The definitions of these loop integrals are provided in App. A. The integrals are computed in NLL accuracy, and the result is expanded in  $\epsilon$  up to  $\mathcal{O}(\epsilon^2)$  at one loop and  $\mathcal{O}(\epsilon^0)$  at two loops. The UV poles are eliminated by means of a minimal subtraction as explained in Sect. 3.3 such that the presented results are UV finite. All loop integrals have been solved and cross-checked using two independent methods: an automatized algorithm based on the sector-decomposition technique [33] and the method of expansion by regions combined with Mellin–Barnes representations [34].

### 5.1 One-loop diagrams

The one-loop factorizable contributions originate only from one type of diagram,<sup>12</sup>

$$\tilde{\mathcal{M}}_1^{ij} = \text{diagram} = -\mathcal{M}_0 \sum_{V_1=A, Z, W^\pm} I_i^{\bar{V}_1} I_j^{V_1} D_0(M_{V_1}; r_{ij}). \quad (5.1)$$

The corresponding loop integral  $D_0$  is defined in (A.6) and to NLL accuracy yields

$$\begin{aligned}
D_0(M_W; r_{ij}) & \stackrel{\text{NLL}}{=} -L^2 - \frac{2}{3}L^3\epsilon - \frac{1}{4}L^4\epsilon^2 + 2(2 - l_{ij}) \left( L + \frac{1}{2}L^2\epsilon + \frac{1}{6}L^3\epsilon^2 \right), \\
D_0(M_Z; r_{ij}) & \stackrel{\text{NLL}}{=} D_0(M_W; r_{ij}) + l_Z (2L + 2L^2\epsilon + L^3\epsilon^2), \\
D_0(0; r_{ij}) & \stackrel{\text{NLL}}{=} -2\epsilon^{-2} - 2(2 - l_{ij})\epsilon^{-1}, \quad (5.2)
\end{aligned}$$

<sup>12</sup>The  $l$ -loop diagrams depicted in this section are understood without factors  $(\alpha_\epsilon/4\pi)^l$ .



where the UV singularities

$$D_0^{\text{UV}}(M_W; r_{ij}) \stackrel{\text{NLL}}{=} D_0^{\text{UV}}(M_Z; r_{ij}) \stackrel{\text{NLL}}{=} D_0^{\text{UV}}(0; r_{ij}) \stackrel{\text{NLL}}{=} 4\epsilon^{-1} \quad (5.3)$$

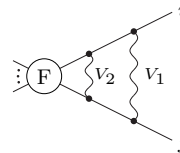
have been subtracted.

## 5.2 Two-loop diagrams

The two-loop NLL factorizable terms (3.8) involve fourteen different types of diagrams. The diagrams 1–3, 12, and 14 in this section give rise to LLs and NLLs, whereas all other diagrams yield only NLLs. The loop integrals associated with the various diagrams are denoted with symbols of the type  $D_h(m_1, \dots, m_j; r_{kl}, \dots)$  and depend on various kinematical invariants  $r_{kl}$  and masses  $m_i$ . The symbols  $m_i$  are always used to denote generic mass parameters, which can assume the values  $m_i = M_W, M_Z, m_t, M_H$  or  $m_i = 0$ . Instead we use the symbols  $M_i$  to denote non-zero masses, i.e.  $M_i = M_W, M_Z, m_t, M_H$ . The integrals are often singular when certain mass parameters tend to zero, and the cases where such parameters are zero or non-zero need to be treated separately. For every integral we first evaluate  $D_h(M_W, \dots, M_W; r_{kl}, \dots)$ , i.e. the case where all mass parameters are equal to  $M_W$ . The dependence of the integral on the various masses is then described by subtracted functions of the type

$$\Delta D_h(m_1, \dots, m_j; r_{kl}, \dots) = D_h(m_1, \dots, m_j; r_{kl}, \dots) - D_h(M_W, \dots, M_W; r_{kl}, \dots). \quad (5.4)$$

*Diagram 1*

$$\tilde{\mathcal{M}}_2^{1,ij} = \text{Diagram} = \mathcal{M}_0 \sum_{V_1, V_2=A, Z, W^\pm} I_i^{\bar{V}_2} I_i^{\bar{V}_1} I_j^{V_2} I_j^{V_1} D_1(M_{V_1}, M_{V_2}; r_{ij}), \quad (5.5)$$


where the loop integral  $D_1$  is defined in (A.6) and yields

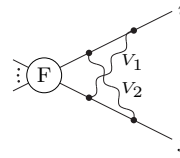
$$\begin{aligned} D_1(M_W, M_W; r_{ij}) &\stackrel{\text{NLL}}{=} \frac{1}{6} L^4 - \frac{2}{3} (2 - l_{ij}) L^3, \\ \Delta D_1(M_1, M_2; r_{ij}) &\stackrel{\text{NLL}}{=} -\frac{2}{3} l_1 L^3, \\ \Delta D_1(0, M_2; r_{ij}) &\stackrel{\text{NLL}}{=} 2L^2 \epsilon^{-2} + \frac{8}{3} L^3 \epsilon^{-1} + \frac{11}{6} L^4 - (2 - l_{ij}) (4L \epsilon^{-2} + 4L^2 \epsilon^{-1} + 2L^3) \\ &\quad - l_2 (4L \epsilon^{-2} + 8L^2 \epsilon^{-1} + 8L^3), \\ \Delta D_1(M_1, 0; r_{ij}) &\stackrel{\text{NLL}}{=} -\frac{2}{3} l_1 L^3, \\ \Delta D_1(0, 0; r_{ij}) &\stackrel{\text{NLL}}{=} \epsilon^{-4} - \frac{1}{6} L^4 + (2 - l_{ij}) \left( 2\epsilon^{-3} + \frac{2}{3} L^3 \right). \end{aligned} \quad (5.6)$$

Here the UV singularities

$$\begin{aligned} D_1^{\text{UV}}(M_1, m_2; r_{ij}) &\stackrel{\text{NLL}}{=} -4L^2 \epsilon^{-1} - \frac{8}{3} L^3, \\ D_1^{\text{UV}}(0, m_2; r_{ij}) &\stackrel{\text{NLL}}{=} -8\epsilon^{-3} \end{aligned} \quad (5.7)$$

have been subtracted.

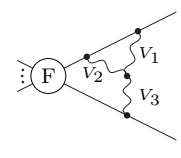
Diagram 2

$$\tilde{\mathcal{M}}_2^{2,ij} = \text{Diagram} = \mathcal{M}_0 \sum_{V_1, V_2=A, Z, W^\pm} I_i^{\bar{V}_2} I_i^{\bar{V}_1} I_j^{V_1} I_j^{V_2} D_2(M_{V_1}, M_{V_2}; r_{ij}), \quad (5.8)$$


where the loop integral  $D_2$  is defined in (A.6). This integral is free of UV singularities and yields

$$\begin{aligned} D_2(M_W, M_W; r_{ij}) &\stackrel{\text{NLL}}{=} \frac{1}{3}L^4 - \frac{4}{3}(2 - l_{ij})L^3, \\ \Delta D_2(M_1, M_2; r_{ij}) &\stackrel{\text{NLL}}{=} -\frac{2}{3}(l_1 + l_2)L^3, \\ \Delta D_2(0, M_2; r_{ij}) &\stackrel{\text{NLL}}{=} -\frac{2}{3}L^3\epsilon^{-1} - \frac{7}{6}L^4 + (2 - l_{ij} + l_2) \left( 2L^2\epsilon^{-1} + \frac{10}{3}L^3 \right), \\ \Delta D_2(M_1, 0; r_{ij}) &\stackrel{\text{NLL}}{=} -\frac{2}{3}L^3\epsilon^{-1} - \frac{7}{6}L^4 + (2 - l_{ij} + l_1) \left( 2L^2\epsilon^{-1} + \frac{10}{3}L^3 \right), \\ \Delta D_2(0, 0; r_{ij}) &\stackrel{\text{NLL}}{=} \epsilon^{-4} - \frac{1}{3}L^4 + (2 - l_{ij}) \left( 2\epsilon^{-3} + \frac{4}{3}L^3 \right). \end{aligned} \quad (5.9)$$

Diagram 3

$$\begin{aligned} \tilde{\mathcal{M}}_2^{3,ij} &= \text{Diagram} = \\ &= -i \frac{g_2}{e} \mathcal{M}_0 \sum_{V_1, V_2, V_3=A, Z, W^\pm} \epsilon^{V_1 V_2 V_3} I_i^{\bar{V}_2} I_i^{\bar{V}_1} I_j^{\bar{V}_3} D_3(M_{V_1}, M_{V_2}, M_{V_3}; r_{ij}), \end{aligned} \quad (5.10)$$


where the  $\epsilon$ -tensor is defined in (2.18). The loop integral  $D_3$  is defined in (A.6) and yields

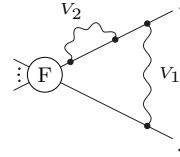
$$\begin{aligned} D_3(M_W, M_W, M_W; r_{ij}) &\stackrel{\text{NLL}}{=} \frac{1}{6}L^4 - \left( 3 - \frac{2l_{ij}}{3} \right) L^3, \\ \Delta D_3(M_1, M_2, M_3; r_{ij}) &\stackrel{\text{NLL}}{=} -\frac{1}{3}(l_1 + l_3)L^3, \\ \Delta D_3(0, M_2, M_3; r_{ij}) &\stackrel{\text{NLL}}{=} -\frac{1}{3}L^3\epsilon^{-1} - \frac{7}{12}L^4 + (2 - l_{ij} + l_3) \left( L^2\epsilon^{-1} + \frac{5}{3}L^3 \right), \\ \Delta D_3(M_1, 0, M_3; r_{ij}) &\stackrel{\text{NLL}}{=} -\frac{1}{3}(l_1 + l_3)L^3, \\ \Delta D_3(M_1, M_2, 0; r_{ij}) &\stackrel{\text{NLL}}{=} -\frac{1}{3}L^3\epsilon^{-1} - \frac{7}{12}L^4 - 6L\epsilon^{-2} - (2 + l_{ij} - l_1)L^2\epsilon^{-1} \\ &\quad + \left( \frac{11}{3} - \frac{5l_{ij}}{3} + \frac{5l_1}{3} \right) L^3, \end{aligned} \quad (5.11)$$

where the UV singularities

$$\begin{aligned} D_3^{\text{UV}}(m_1, m_2, M_3; r_{ij}) &\stackrel{\text{NLL}}{=} -3L^2\epsilon^{-1} - 2L^3, \\ D_3^{\text{UV}}(m_1, m_2, 0; r_{ij}) &\stackrel{\text{NLL}}{=} -6\epsilon^{-3} \end{aligned} \quad (5.12)$$

have been subtracted.

*Diagram 4*

$$\tilde{\mathcal{M}}_2^{4,ij} = \text{Diagram} = -\mathcal{M}_0 \sum_{V_1, V_2=A, Z, W^\pm} I_i^{V_2} I_i^{\bar{V}_2} I_i^{V_1} I_j^{\bar{V}_1} D_4(M_{V_1}, M_{V_2}; r_{ij}), \quad (5.13)$$


where the loop integral  $D_4$  is defined in (A.6) and yields

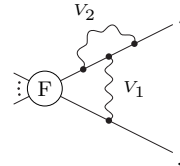
$$\begin{aligned} D_4(M_W, M_W; r_{ij}) &\stackrel{\text{NLL}}{=} \frac{1}{3}L^3, \\ \Delta D_4(M_1, M_2; r_{ij}) &\stackrel{\text{NLL}}{=} 0, \\ \Delta D_4(0, M_2; r_{ij}) &\stackrel{\text{NLL}}{=} 2L\epsilon^{-2} + 2L^2\epsilon^{-1} + L^3, \\ \Delta D_4(M_1, 0; r_{ij}) &\stackrel{\text{NLL}}{=} 0, \\ \Delta D_4(0, 0; r_{ij}) &\stackrel{\text{NLL}}{=} -\epsilon^{-3} - \frac{1}{3}L^3. \end{aligned} \quad (5.14)$$

Here the UV singularities

$$\begin{aligned} D_4^{\text{UV}}(M_1, m_2; r_{ij}) &\stackrel{\text{NLL}}{=} L^2\epsilon^{-1} + \frac{2}{3}L^3, \\ D_4^{\text{UV}}(0, m_2; r_{ij}) &\stackrel{\text{NLL}}{=} 2\epsilon^{-3} \end{aligned} \quad (5.15)$$

have been subtracted.

*Diagram 5*

$$\tilde{\mathcal{M}}_2^{5,ij} = \text{Diagram} = -\mathcal{M}_0 \sum_{V_1, V_2=A, Z, W^\pm} I_i^{V_2} I_i^{V_1} I_i^{\bar{V}_2} I_j^{\bar{V}_1} D_5(M_{V_1}, M_{V_2}; r_{ij}), \quad (5.16)$$


where the loop integral  $D_5$  is defined in (A.6) and yields

$$\begin{aligned} D_5(M_W, M_W; r_{ij}) &\stackrel{\text{NLL}}{=} -\frac{1}{3}L^3, \\ \Delta D_5(M_1, M_2; r_{ij}) &\stackrel{\text{NLL}}{=} 0, \\ \Delta D_5(0, M_2; r_{ij}) &\stackrel{\text{NLL}}{=} -2L\epsilon^{-2} - 2L^2\epsilon^{-1} - L^3, \\ \Delta D_5(M_1, 0; r_{ij}) &\stackrel{\text{NLL}}{=} 0, \\ \Delta D_5(0, 0; r_{ij}) &\stackrel{\text{NLL}}{=} \epsilon^{-3} + \frac{1}{3}L^3. \end{aligned} \quad (5.17)$$

Here the UV singularities

$$\begin{aligned} D_5^{\text{UV}}(M_1, m_2; r_{ij}) &\stackrel{\text{NLL}}{=} -L^2\epsilon^{-1} - \frac{2}{3}L^3, \\ D_5^{\text{UV}}(0, m_2; r_{ij}) &\stackrel{\text{NLL}}{=} -2\epsilon^{-3} \end{aligned} \quad (5.18)$$

have been subtracted.

Diagrams 6

$$\begin{aligned}
\tilde{\mathcal{M}}_2^{6,ij} &= \text{Diagram 1} + \text{Diagram 2} = \\
&= \frac{1}{2} \frac{g_2^2}{e^2} \mathcal{M}_0 \sum_{V_1, V_2, V_3, V_4=A, Z, W^\pm} I_i^{\bar{V}_1} I_j^{\bar{V}_4} \varepsilon^{V_1 \bar{V}_2 \bar{V}_3} \varepsilon^{V_4 V_2 V_3} D_6(M_{V_1}, M_{V_2}, M_{V_3}, M_{V_4}; r_{ij}),
\end{aligned} \tag{5.19}$$

where the loop integral  $D_6$  is defined in (A.6) and yields

$$\begin{aligned}
D_6(M_W, M_W, M_W, M_W; r_{ij}) &\stackrel{\text{NLL}}{=} \frac{20}{9} L^3, \\
\Delta D_6(M_1, M_2, M_3, M_4; r_{ij}) &\stackrel{\text{NLL}}{=} 0, \\
\Delta D_6(0, M_2, M_3, M_4; r_{ij}) &\stackrel{\text{NLL}}{=} \frac{M_2^2 + M_3^2}{2M_4^2} \left[ -16L\epsilon^{-2} - 8L^2\epsilon^{-1} + \frac{16}{3}L^3 \right], \\
\Delta D_6(M_1, 0, M_3, M_4; r_{ij}) &\stackrel{\text{NLL}}{=} 0, \\
\Delta D_6(M_1, M_2, 0, M_4; r_{ij}) &\stackrel{\text{NLL}}{=} 0, \\
\Delta D_6(M_1, M_2, M_3, 0; r_{ij}) &\stackrel{\text{NLL}}{=} \frac{M_2^2 + M_3^2}{2M_1^2} \left[ -16L\epsilon^{-2} - 8L^2\epsilon^{-1} + \frac{16}{3}L^3 \right], \\
\Delta D_6(0, M_2, M_3, 0; r_{ij}) &\stackrel{\text{NLL}}{=} \frac{20}{3}L\epsilon^{-2} + \frac{10}{3}L^2\epsilon^{-1} - \frac{20}{9}L^3.
\end{aligned} \tag{5.20}$$

Here the UV singularities

$$\begin{aligned}
D_6^{\text{UV}}(M_1, m_2, m_3, M_4; r_{ij}) &\stackrel{\text{NLL}}{=} \frac{10}{3}L^2\epsilon^{-1} + \frac{20}{9}L^3, \\
D_6^{\text{UV}}(0, m_2, m_3, M_4; r_{ij}) &\stackrel{\text{NLL}}{=} \frac{10}{3}L^2\epsilon^{-1} + \frac{20}{9}L^3 \\
&\quad + \frac{m_2^2 + m_3^2}{2M_4^2} \left[ -16\epsilon^{-3} + 8L^2\epsilon^{-1} + \frac{16}{3}L^3 \right], \\
D_6^{\text{UV}}(M_1, m_2, m_3, 0; r_{ij}) &\stackrel{\text{NLL}}{=} \frac{10}{3}L^2\epsilon^{-1} + \frac{20}{9}L^3 \\
&\quad + \frac{m_2^2 + m_3^2}{2M_1^2} \left[ -16\epsilon^{-3} + 8L^2\epsilon^{-1} + \frac{16}{3}L^3 \right], \\
D_6^{\text{UV}}(0, m_2, m_3, 0; r_{ij}) &\stackrel{\text{NLL}}{=} \frac{20}{3}\epsilon^{-3}
\end{aligned} \tag{5.21}$$

have been subtracted. We observe that the loop integrals associated with  $A$ - $Z$  mixing-energy subdiagrams give rise to the contributions

$$\Delta D_6(0, M_W, M_W, M_Z; r_{ij}) = \frac{M_W^2}{M_Z^2} \left[ -16L\epsilon^{-2} - 8L^2\epsilon^{-1} + \frac{16}{3}L^3 \right], \tag{5.22}$$

which depend linearly on the ratio  $M_W^2/M_Z^2$ .

Diagram 7

$$\begin{aligned}
\tilde{\mathcal{M}}_2^{7,ij} &= \text{Diagram 7} = -\frac{g_2^2}{e^2} \mathcal{M}_0 \sum_{V_1, V_2, V_3=A, Z, W^\pm} I_i^{\bar{V}_1} I_j^{\bar{V}_3} \sum_{V=A, Z, W^\pm} \varepsilon^{V_1 V_2 \bar{V}} \varepsilon^{V_3 V_2 V} \\
&\times (D-1) D_7(M_{V_1}, M_{V_2}, M_{V_3}; r_{ij}), \tag{5.23}
\end{aligned}$$

where  $D = 4 - 2\epsilon$ . The loop integral  $D_7$  is defined in (A.6) and yields

$$\begin{aligned}
D_7(M_W, M_W, M_W; r_{ij}) &\stackrel{\text{NLL}}{=} 0, \\
\Delta D_7(M_1, M_2, M_3; r_{ij}) &\stackrel{\text{NLL}}{=} 0, \\
\Delta D_7(0, M_2, M_3; r_{ij}) &\stackrel{\text{NLL}}{=} \frac{M_2^2}{M_3^2} \left[ -2L\epsilon^{-2} - L^2\epsilon^{-1} + \frac{2}{3}L^3 \right], \\
\Delta D_7(M_1, 0, M_3; r_{ij}) &\stackrel{\text{NLL}}{=} 0, \\
\Delta D_7(M_1, M_2, 0; r_{ij}) &\stackrel{\text{NLL}}{=} \frac{M_2^2}{M_1^2} \left[ -2L\epsilon^{-2} - L^2\epsilon^{-1} + \frac{2}{3}L^3 \right], \\
\Delta D_7(0, M_2, 0; r_{ij}) &\stackrel{\text{NLL}}{=} 0, \tag{5.24}
\end{aligned}$$

where the UV singularities

$$\begin{aligned}
D_7^{\text{UV}}(0, M_2, M_3; r_{ij}) &\stackrel{\text{NLL}}{=} \frac{M_2^2}{M_3^2} \left[ -2\epsilon^{-3} + L^2\epsilon^{-1} + \frac{2}{3}L^3 \right], \\
D_7^{\text{UV}}(M_1, M_2, 0; r_{ij}) &\stackrel{\text{NLL}}{=} \frac{M_2^2}{M_1^2} \left[ -2\epsilon^{-3} + L^2\epsilon^{-1} + \frac{2}{3}L^3 \right] \tag{5.25}
\end{aligned}$$

have been subtracted.

Diagram 8

$$\begin{aligned}
\tilde{\mathcal{M}}_2^{8,ij} &= \text{Diagram 8} = -e^2 v^2 \mathcal{M}_0 \sum_{V_1, V_3, V_4=A, Z, W^\pm} I_i^{\bar{V}_1} I_j^{\bar{V}_4} \sum_{\Phi_{i_2}=H, \chi, \phi^\pm} \{I^{V_1}, I^{\bar{V}_3}\}_{H\Phi_{i_2}} \\
&\times \{I^{V_3}, I^{V_4}\}_{\Phi_{i_2}H} D_8(M_{V_1}, M_{\Phi_{i_2}}, M_{V_3}, M_{V_4}; r_{ij}), \tag{5.26}
\end{aligned}$$

where the curly brackets denote anticommutators and  $v$  is the vacuum expectation value. The loop integral  $D_8$  is defined in (A.6) and yields

$$\begin{aligned}
M_W^2 D_8(M_W, M_W, M_W, M_W; r_{ij}) &\stackrel{\text{NLL}}{=} 0, \\
M_W^2 \Delta D_8(M_1, M_2, M_3, M_4; r_{ij}) &\stackrel{\text{NLL}}{=} 0, \\
\Delta D_8(0, M_2, M_3, M_4; r_{ij}) &\stackrel{\text{NLL}}{=} \frac{1}{M_4^2} \left[ -2L\epsilon^{-2} - L^2\epsilon^{-1} + \frac{2}{3}L^3 \right],
\end{aligned}$$

$$\begin{aligned}
M_W^2 \Delta D_8(M_1, M_2, 0, M_4; r_{ij}) &\stackrel{\text{NLL}}{=} 0, \\
\Delta D_8(M_1, M_2, M_3, 0; r_{ij}) &\stackrel{\text{NLL}}{=} \frac{1}{M_1^2} \left[ -2L\epsilon^{-2} - L^2\epsilon^{-1} + \frac{2}{3}L^3 \right], \\
M_W^2 \Delta D_8(0, M_2, M_3, 0; r_{ij}) &\stackrel{\text{NLL}}{=} 0.
\end{aligned} \tag{5.27}$$

Here the UV singularities

$$\begin{aligned}
D_8^{\text{UV}}(0, M_2, M_3, M_4; r_{ij}) &\stackrel{\text{NLL}}{=} \frac{1}{M_4^2} \left[ -2\epsilon^{-3} + L^2\epsilon^{-1} + \frac{2}{3}L^3 \right], \\
D_8^{\text{UV}}(M_1, M_2, M_3, 0; r_{ij}) &\stackrel{\text{NLL}}{=} \frac{1}{M_1^2} \left[ -2\epsilon^{-3} + L^2\epsilon^{-1} + \frac{2}{3}L^3 \right]
\end{aligned} \tag{5.28}$$

have been subtracted. The above diagram represents the only contribution involving couplings proportional to  $v$ , which originate from spontaneous symmetry breaking.

*Diagram 9*

$$\begin{aligned}
\tilde{\mathcal{M}}_2^{9,ij} &= \text{Diagram} = -\frac{1}{2} \mathcal{M}_0 \sum_{V_1, V_4=A, Z, W^\pm} I_i^{\bar{V}_1} I_j^{\bar{V}_4} \sum_{\Phi_{i_2}, \Phi_{i_3}=H, \chi, \phi^\pm} I_{\Phi_{i_3}\Phi_{i_2}}^{V_1} I_{\Phi_{i_2}\Phi_{i_3}}^{V_4} \\
&\times D_9(M_{V_1}, M_{\Phi_{i_2}}, M_{\Phi_{i_3}}, M_{V_4}; r_{ij}),
\end{aligned} \tag{5.29}$$

where the loop integral  $D_9$  is defined in (A.6) and yields

$$\begin{aligned}
D_9(M_W, M_W, M_W, M_W; r_{ij}) &\stackrel{\text{NLL}}{=} \frac{2}{9}L^3, \\
\Delta D_9(M_1, M_2, M_3, M_4; r_{ij}) &\stackrel{\text{NLL}}{=} 0, \\
\Delta D_9(0, M_2, M_3, M_4; r_{ij}) &\stackrel{\text{NLL}}{=} \frac{M_2^2 + M_3^2}{2M_4^2} \left[ 4L\epsilon^{-2} + 2L^2\epsilon^{-1} - \frac{4}{3}L^3 \right], \\
\Delta D_9(M_1, M_2, M_3, 0; r_{ij}) &\stackrel{\text{NLL}}{=} \frac{M_2^2 + M_3^2}{2M_1^2} \left[ 4L\epsilon^{-2} + 2L^2\epsilon^{-1} - \frac{4}{3}L^3 \right], \\
\Delta D_9(0, M_2, M_3, 0; r_{ij}) &\stackrel{\text{NLL}}{=} \frac{2}{3}L\epsilon^{-2} + \frac{1}{3}L^2\epsilon^{-1} - \frac{2}{9}L^3.
\end{aligned} \tag{5.30}$$

Here the UV singularities

$$\begin{aligned}
D_9^{\text{UV}}(M_1, M_2, M_3, M_4; r_{ij}) &\stackrel{\text{NLL}}{=} \frac{1}{3}L^2\epsilon^{-1} + \frac{2}{9}L^3, \\
D_9^{\text{UV}}(0, M_2, M_3, M_4; r_{ij}) &\stackrel{\text{NLL}}{=} \frac{1}{3}L^2\epsilon^{-1} + \frac{2}{9}L^3 + \frac{M_2^2 + M_3^2}{2M_4^2} \left[ 4\epsilon^{-3} - 2L^2\epsilon^{-1} - \frac{4}{3}L^3 \right], \\
D_9^{\text{UV}}(M_1, M_2, M_3, 0; r_{ij}) &\stackrel{\text{NLL}}{=} \frac{1}{3}L^2\epsilon^{-1} + \frac{2}{9}L^3 + \frac{M_2^2 + M_3^2}{2M_1^2} \left[ 4\epsilon^{-3} - 2L^2\epsilon^{-1} - \frac{4}{3}L^3 \right], \\
D_9^{\text{UV}}(0, M_2, M_3, 0; r_{ij}) &\stackrel{\text{NLL}}{=} \frac{2}{3}\epsilon^{-3}
\end{aligned} \tag{5.31}$$

have been subtracted.

Diagram 10

$$\begin{aligned}
\tilde{\mathcal{M}}_2^{10,ij} &= \text{Diagram} = -\frac{1}{2} \mathcal{M}_0 \sum_{V_1, V_3=A, Z, W^\pm} I_i^{\bar{V}_1} I_j^{\bar{V}_3} \sum_{\Phi_{i_2}=H, \chi, \phi^\pm} \{I^{V_1}, I^{V_3}\}_{\Phi_{i_2} \Phi_{i_2}} \\
&\times D_{10}(M_{V_1}, M_{\Phi_{i_2}}, M_{V_3}; r_{ij}), \tag{5.32}
\end{aligned}$$

where

$$D_{10} \equiv D_7. \tag{5.33}$$

Also this diagram, which yields NLL contributions only through  $A$ - $Z$  mixing-energy sub-diagrams, gives rise to a correction proportional to  $M_W^2/M_Z^2$  originating from  $\Delta D_7(0, M_{\phi^\pm}, M_Z; r_{ij})$ . This correction cancels the contribution proportional to  $M_W^2/M_Z^2$  that originates from diagram 9.

Diagram 11

For the diagrams involving fermionic self-energy subdiagrams we consider the contributions of a generic fermionic doublet  $\Psi$  with components  $\Psi_i = u, d$ . The sum over the three generations of leptons and quarks is denoted by  $\sum_\Psi$ , and colour factors are implicitly understood. Assuming that all down-type fermions are massless,  $m_d = 0$ , and that the masses of up-type fermions are  $m_u = 0$  or  $m_t$ , we have

$$\begin{aligned}
\tilde{\mathcal{M}}_2^{11,ij} &= \text{Diagram} = -\frac{1}{2} \mathcal{M}_0 \sum_{V_1, V_4=A, Z, W^\pm} I_i^{\bar{V}_1} I_j^{\bar{V}_4} \\
&\times \sum_\Psi \left\{ \sum_{\Psi_{i_2}, \Psi_{i_3}=u, d} \sum_{\kappa=R, L} I_{\Psi_{i_3}^\kappa}^{V_1} I_{\Psi_{i_2}^\kappa}^{V_4} D_{11,0}(M_{V_1}, m_{i_2}, m_{i_3}, M_{V_4}; r_{ij}) \right. \\
&\left. - \left( I_{u^R u^R}^{V_1} I_{u^L u^L}^{V_4} + I_{u^L u^L}^{V_1} I_{u^R u^R}^{V_4} \right) m_u^2 D_{11,m}(M_{V_1}, m_u, m_u, M_{V_4}; r_{ij}) \right\}, \tag{5.34}
\end{aligned}$$

where  $D_{11,m} \equiv -4D_8$  represents the contribution associated to the  $m_u$ -terms in the numerator of the up-type fermion propagators, whereas the integral  $D_{11,0}$ , which is defined in (A.6), accounts for the remaining contributions. This latter integral yields

$$\begin{aligned}
D_{11,0}(M_W, M_W, M_W, M_W; r_{ij}) &\stackrel{\text{NLL}}{=} \frac{8}{9} L^3, \\
\Delta D_{11,0}(M_1, m_2, m_3, M_4; r_{ij}) &\stackrel{\text{NLL}}{=} 0, \\
\Delta D_{11,0}(0, m_2, m_3, M_4; r_{ij}) &\stackrel{\text{NLL}}{=} \frac{m_2^2 + m_3^2}{2M_4^2} \left[ 8L\epsilon^{-2} + 4L^2\epsilon^{-1} - \frac{8}{3}L^3 \right], \\
\Delta D_{11,0}(M_1, m_2, m_3, 0; r_{ij}) &\stackrel{\text{NLL}}{=} \frac{m_2^2 + m_3^2}{2M_1^2} \left[ 8L\epsilon^{-2} + 4L^2\epsilon^{-1} - \frac{8}{3}L^3 \right],
\end{aligned}$$

$$\begin{aligned}
\Delta D_{11,0}(0, M_2, M_3, 0; r_{ij}) &\stackrel{\text{NLL}}{=} \frac{8}{3}L\epsilon^{-2} + \frac{4}{3}L^2\epsilon^{-1} - \frac{8}{9}L^3, \\
\Delta D_{11,0}(0, 0, 0, 0; r_{ij}) &\stackrel{\text{NLL}}{=} -2\epsilon^{-3} - \frac{8}{9}L^3,
\end{aligned} \tag{5.35}$$

where the UV singularities

$$\begin{aligned}
D_{11,0}^{\text{UV}}(M_1, m_2, m_3, M_4; r_{ij}) &\stackrel{\text{NLL}}{=} \frac{4}{3}L^2\epsilon^{-1} + \frac{8}{9}L^3, \\
D_{11,0}^{\text{UV}}(0, m_2, m_3, M_4; r_{ij}) &\stackrel{\text{NLL}}{=} \frac{4}{3}L^2\epsilon^{-1} + \frac{8}{9}L^3 + \frac{m_2^2 + m_3^2}{2M_4^2} \left[ 8\epsilon^{-3} - 4L^2\epsilon^{-1} - \frac{8}{3}L^3 \right], \\
D_{11,0}^{\text{UV}}(M_1, m_2, m_3, 0; r_{ij}) &\stackrel{\text{NLL}}{=} \frac{4}{3}L^2\epsilon^{-1} + \frac{8}{9}L^3 + \frac{m_2^2 + m_3^2}{2M_1^2} \left[ 8\epsilon^{-3} - 4L^2\epsilon^{-1} - \frac{8}{3}L^3 \right], \\
D_{11,0}^{\text{UV}}(0, m_2, m_3, 0; r_{ij}) &\stackrel{\text{NLL}}{=} \frac{8}{3}\epsilon^{-3}
\end{aligned} \tag{5.36}$$

have been subtracted. As a consequence of

$$\begin{aligned}
\Delta D_{11,0}(0, m_2, m_3, M_4; r_{ij}) &= \frac{m_2^2 + m_3^2}{2} \Delta D_{11,m}(0, m_2, m_3, M_4; r_{ij}), \\
\Delta D_{11,0}(M_1, m_2, m_3, 0; r_{ij}) &= \frac{m_2^2 + m_3^2}{2} \Delta D_{11,m}(M_1, m_2, m_3, 0; r_{ij}),
\end{aligned} \tag{5.37}$$

all terms proportional to the fermion masses in  $\tilde{\mathcal{M}}_2^{11,ij}$  cancel.

*Diagram 12*

$$\tilde{\mathcal{M}}_2^{12,ijk} = \text{Diagram} = \mathcal{M}_0 \sum_{V_1, V_2=A, Z, W^\pm} I_i^{\bar{V}_2} I_i^{\bar{V}_1} I_j^{V_1} I_k^{V_2} D_{12}(M_{V_1}, M_{V_2}; r_{ik}), \tag{5.38}$$

where the loop integral  $D_{12}$  is defined in (A.6) and yields

$$\begin{aligned}
D_{12}(M_W, M_W; r_{ik}) &\stackrel{\text{NLL}}{=} \frac{1}{2}L^4 - 2(2 - l_{ik})L^3, \\
\Delta D_{12}(M_1, M_2; r_{ik}) &\stackrel{\text{NLL}}{=} -\frac{2}{3}(2l_1 + l_2)L^3, \\
\Delta D_{12}(0, M_2; r_{ik}) &\stackrel{\text{NLL}}{=} 2L^2\epsilon^{-2} + 2L^3\epsilon^{-1} + \frac{2}{3}L^4 - (2 - l_{ik}) \left( 4L\epsilon^{-2} + 2L^2\epsilon^{-1} - \frac{4}{3}L^3 \right) \\
&\quad - l_2 \left( 4L\epsilon^{-2} + 6L^2\epsilon^{-1} + \frac{14}{3}L^3 \right), \\
\Delta D_{12}(M_1, 0; r_{ik}) &\stackrel{\text{NLL}}{=} -\frac{2}{3}L^3\epsilon^{-1} - \frac{7}{6}L^4 + (2 - l_{ik}) \left( 2L^2\epsilon^{-1} + \frac{10}{3}L^3 \right) \\
&\quad + l_1 \left( 2L^2\epsilon^{-1} + \frac{8}{3}L^3 \right), \\
\Delta D_{12}(0, 0; r_{ik}) &\stackrel{\text{NLL}}{=} 2\epsilon^{-4} - \frac{1}{2}L^4 + (2 - l_{ik}) \left( 4\epsilon^{-3} + 2L^3 \right).
\end{aligned} \tag{5.39}$$



Here the UV singularities

$$\begin{aligned}
D_{12}^{\text{UV}}(M_1, m_2; r_{ik}) &\stackrel{\text{NLL}}{=} -4L^2\epsilon^{-1} - \frac{8}{3}L^3, \\
D_{12}^{\text{UV}}(0, m_2; r_{ik}) &\stackrel{\text{NLL}}{=} -8\epsilon^{-3}
\end{aligned} \tag{5.40}$$

have been subtracted. Note that, to NLL accuracy, the above diagram does not depend on  $r_{ij}$  and  $r_{jk}$ .

*Diagram 13*

$$\begin{aligned}
\tilde{\mathcal{M}}_2^{13,ijk} &= \text{Diagram} = \\
&= -i\frac{g_2}{e}\mathcal{M}_0 \sum_{V_1, V_2, V_3=A, Z, W^\pm} \varepsilon^{V_1 V_2 V_3} I_i^{\bar{V}_1} I_j^{\bar{V}_2} I_k^{\bar{V}_3} D_{13}(M_{V_1}, M_{V_2}, M_{V_3}; r_{ij}, r_{ik}, r_{jk}),
\end{aligned} \tag{5.41}$$

where the loop integral  $D_{13}$  is defined in (A.6). This integral is free of UV singularities and yields

$$\begin{aligned}
D_{13}(M_W, M_W, M_W; r_{ij}, r_{ik}, r_{jk}) &\stackrel{\text{NLL}}{=} 0, \\
\Delta D_{13}(M_1, M_2, M_3; r_{ij}, r_{ik}, r_{jk}) &\stackrel{\text{NLL}}{=} 0, \\
\Delta D_{13}(0, M_2, M_3; r_{ij}, r_{ik}, r_{jk}) &\stackrel{\text{NLL}}{=} (l_{ij} - l_{ik}) \left( L^2\epsilon^{-1} + \frac{5}{3}L^3 \right), \\
\Delta D_{13}(M_1, 0, M_3; r_{ij}, r_{ik}, r_{jk}) &\stackrel{\text{NLL}}{=} (l_{jk} - l_{ij}) \left( L^2\epsilon^{-1} + \frac{5}{3}L^3 \right), \\
\Delta D_{13}(M_1, M_2, 0; r_{ij}, r_{ik}, r_{jk}) &\stackrel{\text{NLL}}{=} (l_{ik} - l_{jk}) \left( L^2\epsilon^{-1} + \frac{5}{3}L^3 \right).
\end{aligned} \tag{5.42}$$

*Diagram 14*

$$\tilde{\mathcal{M}}_2^{14,ijkl} = \text{Diagram} = \mathcal{M}_0 \sum_{V_1, V_2=A, Z, W^\pm} I_i^{\bar{V}_1} I_j^{V_1} I_k^{\bar{V}_2} I_l^{V_2} D_{14}(M_{V_1}, M_{V_2}; r_{ij}, r_{kl}), \tag{5.43}$$

where the loop integral  $D_{14}$  is simply given by the product of one-loop integrals (5.2),

$$D_{14}(M_{V_1}, M_{V_2}; r_{ij}, r_{kl}) = D_0(M_{V_1}; r_{ij}) D_0(M_{V_2}; r_{kl}). \tag{5.44}$$

## 6 Renormalization

In this section we discuss the NLL counterterm contributions that result from the renormalization of the gauge-boson masses,<sup>13</sup>

$$M_{V,0} = M_V + \sum_{l=1}^{\infty} \left( \frac{\alpha_\epsilon}{4\pi} \right)^l \delta M_V^{(l)}, \quad (6.1)$$

and the electroweak couplings,

$$g_{0,i} = g_i + \sum_{l=1}^{\infty} \left( \frac{\alpha_\epsilon}{4\pi} \right)^l \delta g_i^{(l)}, \quad e_0 = e + \sum_{l=1}^{\infty} \left( \frac{\alpha_\epsilon}{4\pi} \right)^l \delta e^{(l)}, \quad (6.2)$$

as well as from the renormalization constants associated with the wave functions of the external fermions  $k = 1, \dots, n$ ,

$$Z_k = 1 + \sum_{l=1}^{\infty} \left( \frac{\alpha_\epsilon}{4\pi} \right)^l \delta Z_k^{(l)}. \quad (6.3)$$

The renormalized one- and two-loop amplitudes are presented in Sect. 7.

### 6.1 One-loop contributions

At one loop, the mass counterterms  $\delta M_V^{(1)}$  can be neglected, since the gauge-boson mass terms in the Born amplitude give only contributions of order  $M_V^2/Q^2$ , which are suppressed in the high-energy limit, and the same holds for the contributions resulting from their renormalization.

The electroweak couplings are renormalized in the  $\overline{\text{MS}}$  scheme with an additional subtraction of the UV singularities as explained in Sect. 3.3. Assuming that the renormalization scale<sup>14</sup>  $\mu_R$  is of the order of or larger than  $M_W$ , this yields the counterterms

$$\delta g_i^{(1)} \stackrel{\text{NLL}}{=} -\frac{g_i}{2} \frac{1}{\epsilon} b_i^{(1)} \left[ \left( \frac{Q^2}{\mu_R^2} \right)^\epsilon - 1 \right], \quad \delta e^{(1)} \stackrel{\text{NLL}}{=} -\frac{e}{2} \frac{1}{\epsilon} b_e^{(1)} \left[ \left( \frac{Q^2}{\mu_R^2} \right)^\epsilon - 1 \right], \quad (6.4)$$

and the one-loop  $\beta$ -function coefficients  $b_1^{(1)}$ ,  $b_2^{(1)}$ , and  $b_e^{(1)}$  are defined in App. C. The dependence of the counterterms (6.4) on the factor  $(Q^2/\mu_R)^epsilon$  is due to the normalization of the expansion parameter  $\alpha_\epsilon$  in (6.2). As explained in Sect. 3.3, the expressions (6.4) are obtained by subtracting the UV poles from the usual  $\overline{\text{MS}}$  counterterms. Since the same subtraction is performed in the bare loop diagrams, the resulting renormalized amplitudes correspond to the usual  $\overline{\text{MS}}$  renormalized amplitudes. The renormalization of the mixing parameters  $c_W$  and  $s_W$  can be determined from the renormalization of the coupling constants via (2.22). In NLL approximation, this prescription is equivalent to using the on-shell renormalization condition, i.e. relation (2.21), for the weak mixing angle.

Here and in the following we assume that the Born amplitude  $\mathcal{M}_0$  is expressed in terms of coupling constants renormalized at the scale  $\mu_R = Q$ . As a consequence, the contribution of the counterterms (6.4) to the one-loop amplitude  $\mathcal{M}_1$  vanishes.

<sup>13</sup>Note that in (6.1)–(6.3) we use the expansion parameter  $\alpha_\epsilon$  defined in (2.7).

<sup>14</sup>We do not identify the renormalization scale  $\mu_R$  and the scale of dimensional regularization  $\mu_D$ .

The only one-loop counterterm contribution arises from the on-shell wave-function renormalization constants  $\delta Z_k^{(1)}$  for the massless fermionic external legs. These receive contributions only from massive weak bosons, whereas the photonic contribution vanishes owing to a cancellation between UV and mass singularities within dimensional regularization. After subtraction of the UV poles we find

$$\delta Z_k^{(1)} \stackrel{\text{NLL}}{=} -\frac{1}{\epsilon} \left\{ \sum_{V=Z,W^\pm} I_k^{\bar{V}} I_k^V \left[ \left( \frac{Q^2}{M_V^2} \right)^\epsilon - 1 \right] - I_k^A I_k^A \right\}. \quad (6.5)$$

Finally, the one-loop counterterm for a process with  $n$  external massless fermions in NLL approximation is obtained as

$$\tilde{\mathcal{M}}_1^{\text{WF}} = \mathcal{M}_0 \sum_{k=1}^n \frac{1}{2} \delta Z_k^{(1)}. \quad (6.6)$$

## 6.2 Two-loop contributions

At two loops, the mass renormalization leads to non-suppressed logarithmic terms only through the insertion of the one-loop counterterms  $\delta M_V^{(1)}$  in the one-loop logarithmic corrections. However, these contributions are of NNLL order and can thus be neglected in NLL approximation [28]. In this approximation also the purely two-loop counterterms that are associated with the renormalization of the external-fermion wave functions and the couplings, i.e.  $\delta Z_k^{(2)}$ ,  $\delta g_i^{(2)}$  and  $\delta e^{(2)}$ , do not contribute.

The only NLL two-loop counterterm contributions are those that result from the combination of the one-loop amplitude with the one-loop counterterms  $\delta Z_k^{(1)}$ ,  $\delta g_i^{(1)}$  and  $\delta e^{(1)}$ . The wave-function counterterms yield

$$\tilde{\mathcal{M}}_2^{\text{WF}} = \tilde{\mathcal{M}}_1^{\text{F}} \sum_{k=1}^n \frac{1}{2} \delta Z_k^{(1)}. \quad (6.7)$$

The wave-function renormalization constants  $\delta Z_k^{(1)}$  and the unrenormalized one-loop amplitude  $\tilde{\mathcal{M}}_1^{\text{F}}$  are given in (6.5) and in (D.1), respectively. In NLL approximation the one-loop counterterms  $\tilde{\mathcal{M}}_1^{\text{WF}}$  do not contribute, and only the LL part of the one-loop amplitude  $\tilde{\mathcal{M}}_1^{\text{F}}$  is relevant for (6.7). This is easily obtained from (D.1) by neglecting the NLL terms depending on  $r_{ij}$  and  $l_Z$ , and using global gauge invariance (2.30) as

$$e^2 \tilde{\mathcal{M}}_1^{\text{F}} \stackrel{\text{LL}}{=} \frac{1}{2} \mathcal{M}_0 \sum_{i=1}^n \left\{ \sum_{V=A,Z,W^\pm} e^2 I_i^{\bar{V}} I_i^V D_0(M_W; -Q^2) + e^2 I_i^A I_i^A \Delta D_0(0; -Q^2) \right\} \quad (6.8)$$

$$\stackrel{\text{LL}}{=} \frac{1}{2} \mathcal{M}_0 \sum_{i=1}^n \left\{ \left[ g_1^2 \left( \frac{Y_i}{2} \right)^2 + g_2^2 C_i \right] D_0(M_W; -Q^2) + e^2 Q_i^2 \Delta D_0(0; -Q^2) \right\}. \quad (6.9)$$

In the second line we used the identity (2.16). Note that only the LL contributions of  $D_0$  and  $\Delta D_0$  contribute in (6.8) and (6.9).

The remaining NLL two-loop counterterms result from the insertion of the one-loop coupling-constant counterterms (6.4) in the LL one-loop amplitude (6.9) and read

$$e^2 \tilde{\mathcal{M}}_2^{\text{PR}} \stackrel{\text{NLL}}{=} -\frac{1}{2\epsilon} \left[ \left( \frac{Q^2}{\mu_R^2} \right)^\epsilon - 1 \right] \mathcal{M}_0 \sum_{i=1}^n \left\{ \left[ g_1^2 b_1^{(1)} \left( \frac{Y_i}{2} \right)^2 + g_2^2 b_2^{(1)} C_i \right] D_0(M_W; -Q^2) \right.$$

$$+ e^2 b_e^{(1)} Q_i^2 \Delta D_0(0; -Q^2) \Big\}. \quad (6.10)$$

The various one-loop  $\beta$ -function coefficients in (6.10),  $b_1^{(1)}$ ,  $b_2^{(1)}$ , and  $b_e^{(1)}$ , are defined in App. C.

## 7 Complete one- and two-loop results

In this section we combine the unrenormalized and the counterterm contributions presented in Sects. 5 and 6 and provide explicit NLL results for the renormalized one- and two-loop  $n$ -fermion amplitudes. As we have seen in Sects. 5 and 6, the NLL corrections factorize, i.e. they can be expressed through correction factors that multiply the Born amplitude. Moreover, we find that the two-loop correction factors can be entirely expressed in terms of one-loop quantities. In this section we concentrate on the results. Details on the combination of the various contributions can be found in Apps. D and E.

### 7.1 Renormalized one-loop amplitude

The renormalized one-loop matrix element for a process with  $n$  external massless fermions is given by

$$\tilde{\mathcal{M}}_1 = \tilde{\mathcal{M}}_1^{\text{F}} + \tilde{\mathcal{M}}_1^{\text{WF}}, \quad (7.1)$$

where

$$\tilde{\mathcal{M}}_1^{\text{F}} = \frac{1}{2} \sum_{i=1}^n \sum_{\substack{j=1 \\ j \neq i}}^n \tilde{\mathcal{M}}_1^{ij} \quad (7.2)$$

represents the bare one-loop contribution, which is given by the factorizable part (3.5), and  $\tilde{\mathcal{M}}_1^{\text{WF}}$  is the wave-function-renormalization counterterm (6.6). Using the explicit results presented in Sect. 5.1 we can write (more details can be found in App. D)

$$\tilde{\mathcal{M}}_1 \stackrel{\text{NLL}}{=} \mathcal{M}_0 \left[ F_1^{\text{sew}} + \Delta F_1^{\text{em}} + \Delta F_1^{\text{Z}} \right]. \quad (7.3)$$

Here the corrections are split into a symmetric-electroweak (sew) part,

$$F_1^{\text{sew}} = -\frac{1}{2} \sum_{i=1}^n \sum_{\substack{j=1 \\ j \neq i}}^n \sum_{V=A,Z,W^\pm} I_i^{\bar{V}} I_j^V I(\epsilon, M_W; -r_{ij}), \quad (7.4)$$

which is obtained by setting the masses of all gauge bosons,  $A, Z$  and  $W^\pm$ , equal to  $M_W$  in the loop diagrams, an electromagnetic (em) part

$$\Delta F_1^{\text{em}} = -\frac{1}{2} \sum_{i=1}^n \sum_{\substack{j=1 \\ j \neq i}}^n I_i^A I_j^A \Delta I(\epsilon, 0; -r_{ij}), \quad (7.5)$$

resulting from the mass gap between the  $W$  boson and the massless photon, and an  $M_Z$ -dependent part

$$\Delta F_1^{\text{Z}} = -\frac{1}{2} \sum_{i=1}^n \sum_{\substack{j=1 \\ j \neq i}}^n I_i^Z I_j^Z \Delta I(\epsilon, M_Z; -r_{ij}), \quad (7.6)$$

describing the effect that results from the difference between  $M_W$  and  $M_Z$ . For the functions  $I$ , including contributions up to the order  $\epsilon^2$ , we obtain

$$\begin{aligned} I(\epsilon, M_W; -r_{ij}) &\stackrel{\text{NLL}}{=} -L^2 - \frac{2}{3}L^3\epsilon - \frac{1}{4}L^4\epsilon^2 + (3 - 2l_{ij}) \left( L + \frac{1}{2}L^2\epsilon + \frac{1}{6}L^3\epsilon^2 \right) + \mathcal{O}(\epsilon^3), \\ I(\epsilon, M_Z; -r_{ij}) &\stackrel{\text{NLL}}{=} I(\epsilon, M_W; -r_{ij}) + l_Z \left( 2L + 2L^2\epsilon + L^3\epsilon^2 \right) + \mathcal{O}(\epsilon^3), \\ I(\epsilon, 0; -r_{ij}) &\stackrel{\text{NLL}}{=} -2\epsilon^{-2} - (3 - 2l_{ij})\epsilon^{-1}, \end{aligned} \quad (7.7)$$

and the subtracted functions  $\Delta I$  are defined as

$$\Delta I(\epsilon, m; -r_{ij}) = I(\epsilon, m; -r_{ij}) - I(\epsilon, M_W; -r_{ij}). \quad (7.8)$$

In LL approximation we have

$$I(\epsilon, m; -r_{ij}) \stackrel{\text{LL}}{=} D_0(m; r_{ij}), \quad (7.9)$$

such that we can replace  $D_0$  and  $\Delta D_0$  by  $I$  and  $\Delta I$ , respectively, in (6.8), (6.9), and (6.10).

## 7.2 Renormalized two-loop amplitude

The renormalized two-loop matrix element reads

$$\tilde{\mathcal{M}}_2 = \tilde{\mathcal{M}}_2^{\text{F}} + \tilde{\mathcal{M}}_2^{\text{WF}} + \tilde{\mathcal{M}}_2^{\text{PR}}, \quad (7.10)$$

where

$$\begin{aligned} \tilde{\mathcal{M}}_2^{\text{F}} &= \sum_{i=1}^n \sum_{\substack{j=1 \\ j \neq i}}^n \left[ \frac{1}{2} \left( \tilde{\mathcal{M}}_2^{1,ij} + \tilde{\mathcal{M}}_2^{2,ij} \right) + \tilde{\mathcal{M}}_2^{3,ij} + \tilde{\mathcal{M}}_2^{4,ij} + \tilde{\mathcal{M}}_2^{5,ij} \right. \\ &\quad \left. + \frac{1}{2} \sum_{m=6}^{11} \tilde{\mathcal{M}}_2^{m,ij} + \sum_{\substack{k=1 \\ k \neq i,j}}^n \left( \tilde{\mathcal{M}}_2^{12,ijk} + \frac{1}{6} \tilde{\mathcal{M}}_2^{13,ijk} + \frac{1}{8} \sum_{\substack{l=1 \\ l \neq i,j,k}}^n \tilde{\mathcal{M}}_2^{14,ijkl} \right) \right] \end{aligned} \quad (7.11)$$

represents the bare two-loop contribution, which is given by the factorizable terms (3.8), and  $\tilde{\mathcal{M}}_2^{\text{WF}}$  and  $\tilde{\mathcal{M}}_2^{\text{PR}}$  are the wave-function- and parameter-renormalization counterterms given in (6.7) and (6.10), respectively. As shown in App. E, the two-loop amplitude (7.10) can be expressed in terms of the Born matrix element  $\mathcal{M}_0$  and the one-loop correction factors (7.4)–(7.6) as

$$\begin{aligned} \tilde{\mathcal{M}}_2 &\stackrel{\text{NLL}}{=} \mathcal{M}_0 \left\{ \frac{1}{2} [F_1^{\text{sew}}]^2 + F_1^{\text{sew}} \Delta F_1^{\text{em}} + \frac{1}{2} [\Delta F_1^{\text{em}}]^2 + F_1^{\text{sew}} \Delta F_1^Z + \Delta F_1^Z \Delta F_1^{\text{em}} \right. \\ &\quad \left. + G_2^{\text{sew}} + \Delta G_2^{\text{em}} \right\}, \end{aligned} \quad (7.12)$$

where the additional terms

$$\begin{aligned} e^2 G_2^{\text{sew}} &= \frac{1}{2} \sum_{i=1}^n \left[ b_1^{(1)} g_1^2 \left( \frac{Y_i}{2} \right)^2 + b_2^{(1)} g_2^2 C_i \right] J(\epsilon, M_W, \mu_{\text{R}}^2), \\ \Delta G_2^{\text{em}} &= \frac{1}{2} \sum_{i=1}^n Q_i^2 \left\{ b_e^{(1)} \left[ \Delta J(\epsilon, 0, \mu_{\text{R}}^2) - \Delta J(\epsilon, 0, M_W^2) \right] + b_{\text{QED}}^{(1)} \Delta J(\epsilon, 0, M_W^2) \right\} \end{aligned} \quad (7.13)$$

contain one-loop  $\beta$ -function coefficients, defined in App. C, and the combinations

$$\begin{aligned} J(\epsilon, m, \mu_{\text{R}}^2) &= \frac{1}{\epsilon} \left[ I(2\epsilon, m, Q^2) - \left( \frac{Q^2}{\mu_{\text{R}}^2} \right)^\epsilon I(\epsilon, m, Q^2) \right], \\ \Delta J(\epsilon, m, \mu_{\text{R}}^2) &= J(\epsilon, m, \mu_{\text{R}}^2) - J(\epsilon, M_{\text{W}}, \mu_{\text{R}}^2) \end{aligned} \quad (7.14)$$

of one-loop  $I$ -functions (7.7) and (7.8) for  $m = M_{\text{W}}, M_{\text{Z}}, 0$ . The relevant  $J$ -functions read explicitly

$$\begin{aligned} J(\epsilon, M_{\text{W}}, \mu_{\text{R}}^2) &\stackrel{\text{NLL}}{=} \frac{1}{3} L^3 - l_{\mu_{\text{R}}} L^2 + \mathcal{O}(\epsilon), \\ \Delta J(\epsilon, 0, M_{\text{W}}^2) &\stackrel{\text{NLL}}{=} \frac{3}{2} \epsilon^{-3} + 2L\epsilon^{-2} + L^2\epsilon^{-1} + \mathcal{O}(\epsilon), \\ \Delta J(\epsilon, 0, \mu_{\text{R}}^2) - \Delta J(\epsilon, 0, M_{\text{W}}^2) &\stackrel{\text{NLL}}{=} l_{\mu_{\text{R}}} \left( -2\epsilon^{-2} + \epsilon^{-1}(l_{\mu_{\text{R}}} - 2L) + l_{\mu_{\text{R}}} L - \frac{1}{3} l_{\mu_{\text{R}}}^2 \right) + \mathcal{O}(\epsilon), \end{aligned} \quad (7.15)$$

where

$$l_{\mu_{\text{R}}} = \ln \left( \frac{\mu_{\text{R}}^2}{M_{\text{W}}^2} \right). \quad (7.16)$$

In order to be able to express (7.12) in terms of the one-loop operators (7.4)–(7.6) it is crucial that terms up to order  $\epsilon^2$  are included in the latter.

The coefficients  $b_e^{(1)}$  and  $b_{\text{QED}}^{(1)}$  describe the running of the electromagnetic coupling above and below the electroweak scale, respectively. The former receives contributions from all charged fermions and bosons, whereas the latter receives contributions only from light fermions, i.e. all charged leptons and quarks apart from the top quark.

The couplings that enter the one- and two-loop correction factors<sup>15</sup> are renormalized at the scale  $\mu_{\text{R}}$ . Instead, as discussed in Sect. 6.1, the coupling constants in the Born matrix element  $\mathcal{M}_0$  in (7.3) and (7.12) are renormalized at the scale  $Q$ , i.e.

$$\mathcal{M}_0 \equiv \mathcal{M}_0 \Big|_{\substack{g_i = g_i(Q^2) \\ e = e(Q^2)}} \quad (7.17)$$

with

$$\begin{aligned} g_i^2(Q^2) &\stackrel{\text{NLL}}{=} g_i^2(\mu_{\text{R}}^2) \left[ 1 - \frac{\alpha_\epsilon}{4\pi} b_i^{(1)} \frac{1}{\epsilon} \left[ \left( \frac{Q^2}{\mu_{\text{R}}^2} \right)^\epsilon - 1 \right] \right], \\ e^2(Q^2) &\stackrel{\text{NLL}}{=} e^2(\mu_{\text{R}}^2) \left[ 1 - \frac{\alpha_\epsilon}{4\pi} b_e^{(1)} \frac{1}{\epsilon} \left[ \left( \frac{Q^2}{\mu_{\text{R}}^2} \right)^\epsilon - 1 \right] \right]. \end{aligned} \quad (7.18)$$

Thus, by definition, the Born amplitude  $\mathcal{M}_0$  is independent of the renormalization scale  $\mu_{\text{R}}$ , and the dependence of the one- and two-loop amplitudes on  $\mu_{\text{R}}$  is described by the terms (7.13).

---

<sup>15</sup> These are the coupling  $\alpha$  in the perturbative expansion (2.5)–(2.7) and the couplings  $g_1, g_2$  and  $e$  that appear in (7.12)–(7.14) and enter also (7.4)–(7.6) through the dependence of the generators (2.13) on the couplings and the mixing parameters  $c_{\text{W}}$  and  $s_{\text{W}}$ .

The contributions (7.13) originate from combinations of UV and mass singularities. We observe that the term proportional to  $b_e^{(1)}$  vanishes for  $\mu_R = M_W$ . Instead, the terms proportional to  $b_1^{(1)}$ ,  $b_2^{(1)}$ , and  $b_{\text{QED}}^{(1)}$  cannot be eliminated through an appropriate choice of the renormalization scale. This indicates that such two-loop terms do not originate exclusively from the running of the couplings in the one-loop amplitude.

Combining the Born amplitude with the one- and two-loop NLL corrections we can write

$$\mathcal{M} \stackrel{\text{NLL}}{=} \mathcal{M}_0 F^{\text{sew}} F^Z F^{\text{em}}, \quad (7.19)$$

where we observe a factorization of the symmetric-electroweak contributions,

$$F^{\text{sew}} \stackrel{\text{NLL}}{=} 1 + \frac{\alpha_\epsilon}{4\pi} F_1^{\text{sew}} + \left(\frac{\alpha_\epsilon}{4\pi}\right)^2 \left[ \frac{1}{2} (F_1^{\text{sew}})^2 + G_2^{\text{sew}} \right], \quad (7.20)$$

the terms resulting from the difference between  $M_W$  and  $M_Z$ ,

$$F^Z \stackrel{\text{NLL}}{=} 1 + \frac{\alpha_\epsilon}{4\pi} \Delta F_1^Z, \quad (7.21)$$

and the electromagnetic terms resulting from the mass gap between the photon and the W boson,

$$F^{\text{em}} \stackrel{\text{NLL}}{=} 1 + \frac{\alpha_\epsilon}{4\pi} \Delta F_1^{\text{em}} + \left(\frac{\alpha_\epsilon}{4\pi}\right)^2 \left[ \frac{1}{2} (\Delta F_1^{\text{em}})^2 + \Delta G_2^{\text{em}} \right]. \quad (7.22)$$

We also observe that the symmetric-electroweak and electromagnetic terms are consistent with the exponentiated expressions

$$\begin{aligned} F^{\text{sew}} &\stackrel{\text{NLL}}{=} \exp \left[ \frac{\alpha_\epsilon}{4\pi} F_1^{\text{sew}} + \left(\frac{\alpha_\epsilon}{4\pi}\right)^2 G_2^{\text{sew}} \right], \\ F^{\text{em}} &\stackrel{\text{NLL}}{=} \exp \left[ \frac{\alpha_\epsilon}{4\pi} \Delta F_1^{\text{em}} + \left(\frac{\alpha_\epsilon}{4\pi}\right)^2 \Delta G_2^{\text{em}} \right]. \end{aligned} \quad (7.23)$$

In particular, these two contributions exponentiate separately. This double-exponentiating structure is indicated by the ordering of the one-loop operators  $F_1^{\text{sew}}$  and  $\Delta F_1^{\text{em}}$  in the interference term  $F_1^{\text{sew}} \Delta F_1^{\text{em}}$  in our result (7.12). It is important to realize that the commutator of these two operators yields a non-vanishing NLL two-loop contribution. This means that the double-exponentiated structure of the result is not equivalent to a simple exponentiation, i.e.

$$F^{\text{sew}} F^{\text{em}} \neq \exp \left[ \frac{\alpha_\epsilon}{4\pi} (F_1^{\text{sew}} + \Delta F_1^{\text{em}}) + \left(\frac{\alpha_\epsilon}{4\pi}\right)^2 (G_2^{\text{sew}} + \Delta G_2^{\text{em}}) \right]. \quad (7.24)$$

Instead we observe that in NLL approximation the commutator of  $\Delta F_1^Z$  with all operators in (7.19)–(7.22) vanishes, and also  $[\Delta F_1^Z]^2$  does not contribute. Thus, we have

$$F^{\text{sew}} F^Z F^{\text{em}} \stackrel{\text{NLL}}{=} F^Z F^{\text{sew}} F^{\text{em}} \stackrel{\text{NLL}}{=} F^{\text{sew}} F^{\text{em}} F^Z, \quad (7.25)$$

and, in principle,  $F^Z$  can be written in exponentiated form,

$$F^Z \stackrel{\text{NLL}}{=} \exp\left(\frac{\alpha_\epsilon}{4\pi} \Delta F_1^Z\right), \quad (7.26)$$

or absorbed in one of the other exponentials,

$$\begin{aligned} F^{\text{sew}} F^Z \stackrel{\text{NLL}}{=} \exp\left[\frac{\alpha_\epsilon}{4\pi} (F_1^{\text{sew}} + \Delta F_1^Z) + \left(\frac{\alpha_\epsilon}{4\pi}\right)^2 G_2^{\text{sew}}\right], \\ F^Z F^{\text{em}} \stackrel{\text{NLL}}{=} \exp\left[\frac{\alpha_\epsilon}{4\pi} (\Delta F_1^{\text{em}} + \Delta F_1^Z) + \left(\frac{\alpha_\epsilon}{4\pi}\right)^2 \Delta G_2^{\text{em}}\right]. \end{aligned} \quad (7.27)$$

The one- and two-loop corrections (7.3)–(7.6) and (7.12)–(7.13) contain various combinations of matrices  $I_i^V$ , which are in general non-commuting and non-diagonal. These matrices have to be applied to the Born amplitude  $\mathcal{M}_0$  according to the definition (2.28). In order to express the results in a form which is more easily applicable to a specific process, it is useful to split the integrals  $I(\epsilon, M_V; -r_{ij})$  and  $\Delta I(\epsilon, M_V; -r_{ij})$  in (7.4)–(7.6) into an angular-independent part  $I(\epsilon, M_V; Q^2)$  and  $\Delta I(\epsilon, M_V; Q^2)$ , which only involves  $\epsilon$  and  $L$ , and an angular-dependent part, which additionally depends on logarithms of  $r_{ij}$ . This permits to eliminate the sum over  $j$  for the angular-independent parts of (7.4)–(7.6) using the charge-conservation relation (2.30),

$$\mathcal{M}_0 \sum_{i=1}^n \sum_{\substack{j=1 \\ j \neq i}}^n I_i^{\bar{V}} I_j^V I(\epsilon, M_V; Q^2) = -\mathcal{M}_0 \sum_{i=1}^n I_i^V I_i^{\bar{V}} I(\epsilon, M_V; Q^2). \quad (7.28)$$

Moreover, one can easily see that the angular-independent part of (7.4) leads to the Casimir operator (2.16). After these simplifications, all operators that are associated with the angular-independent parts can be replaced by the corresponding eigenvalues, and the one- and two-loop results can be written as

$$\tilde{\mathcal{M}}_1 \stackrel{\text{NLL}}{=} \mathcal{M}_0 [f_1^{\text{sew}} + \Delta f_1^{\text{em}} + \Delta f_1^Z], \quad (7.29)$$

and

$$\begin{aligned} \tilde{\mathcal{M}}_2 \stackrel{\text{NLL}}{=} \mathcal{M}_0 \left\{ \frac{1}{2} [f_1^{\text{sew}}]^2 + f_1^{\text{sew}} \Delta f_1^{\text{em}} + \frac{1}{2} [\Delta f_1^{\text{em}}]^2 + f_1^{\text{sew}} \Delta f_1^Z + \Delta f_1^Z \Delta f_1^{\text{em}} \right. \\ \left. + g_2^{\text{sew}} + \Delta g_2^{\text{em}} \right\}, \end{aligned} \quad (7.30)$$

with

$$\begin{aligned} f_1^{\text{sew}} \stackrel{\text{NLL}}{=} -\frac{1}{2} \left( L^2 + \frac{2}{3} L^3 \epsilon + \frac{1}{4} L^4 \epsilon^2 - 3L - \frac{3}{2} L^2 \epsilon - \frac{1}{2} L^3 \epsilon^2 \right) \sum_{i=1}^n \left[ \frac{g_1^2}{e^2} \left( \frac{y_i}{2} \right)^2 + \frac{g_2^2}{e^2} c_i \right] \\ + \left( L + \frac{1}{2} L^2 \epsilon + \frac{1}{6} L^3 \epsilon^2 \right) \mathcal{K}_1^{\text{ad}} + \mathcal{O}(\epsilon^3), \\ \Delta f_1^{\text{em}} \stackrel{\text{NLL}}{=} -\frac{1}{2} \left( 2\epsilon^{-2} + 3\epsilon^{-1} - L^2 - \frac{2}{3} L^3 \epsilon - \frac{1}{4} L^4 \epsilon^2 + 3L + \frac{3}{2} L^2 \epsilon + \frac{1}{2} L^3 \epsilon^2 \right) \sum_{i=1}^n q_i^2 \end{aligned}$$



$$\begin{aligned}
& - \left( \epsilon^{-1} + L + \frac{1}{2}L^2\epsilon + \frac{1}{6}L^3\epsilon^2 \right) \sum_{i=1}^n \sum_{\substack{j=1 \\ j \neq i}}^n l_{ij} q_i q_j + \mathcal{O}(\epsilon^3), \\
\Delta f_1^Z \stackrel{\text{NLL}}{=} & \left( L + L^2\epsilon + \frac{1}{2}L^3\epsilon^2 \right) l_Z \sum_{i=1}^n \left( \frac{g_2}{e} c_{\text{W}t_i^3} - \frac{g_1}{e} s_{\text{W}} \frac{y_i}{2} \right)^2 + \mathcal{O}(\epsilon^3), \\
g_2^{\text{sew}} \stackrel{\text{NLL}}{=} & \left( \frac{1}{6}L^3 - \frac{1}{2}l_{\mu_{\text{R}}} L^2 \right) \sum_{i=1}^n \left[ \frac{g_1^2}{e^2} b_1^{(1)} \left( \frac{y_i}{2} \right)^2 + \frac{g_2^2}{e^2} b_2^{(1)} c_i \right] + \mathcal{O}(\epsilon), \\
\Delta g_2^{\text{em}} \stackrel{\text{NLL}}{=} & \left\{ -l_{\mu_{\text{R}}} \left[ \epsilon^{-2} + \left( L - \frac{1}{2}l_{\mu_{\text{R}}} \right) \epsilon^{-1} - l_{\mu_{\text{R}}} \left( \frac{1}{2}L - \frac{1}{6}l_{\mu_{\text{R}}} \right) \right] b_e^{(1)} \right. \\
& \left. + \left( \frac{3}{4}\epsilon^{-3} + L\epsilon^{-2} + \frac{1}{2}L^2\epsilon^{-1} \right) b_{\text{QED}}^{(1)} \right\} \sum_{i=1}^n q_i^2 + \mathcal{O}(\epsilon), \tag{7.31}
\end{aligned}$$

where  $l_{\mu_{\text{R}}} = \ln(\mu_{\text{R}}^2/M_{\text{W}}^2)$ , and  $c_i$ ,  $t_i^3$ ,  $y_i$ ,  $q_i$ , represent the eigenvalues of the operators  $C_i$ ,  $T_i^3$ ,  $Y_i$ , and  $Q_i$ , respectively. The only matrix-valued expression in (7.31) is the angular-dependent part of the symmetric-electroweak contribution  $f_1^{\text{sew}}$ ,

$$\mathcal{K}_1^{\text{ad}} = \sum_{i=1}^n \sum_{\substack{j=1 \\ j \neq i}}^n l_{ij} \sum_{V=A,Z,W^\pm} I_i^{\bar{V}} I_j^V. \tag{7.32}$$

The two-loop corrections (7.30) involve terms proportional to  $\mathcal{K}_1^{\text{ad}}$  and  $[\mathcal{K}_1^{\text{ad}}]^2$ . However, the latter are of NNLL order and thus negligible in NLL approximation. The combination of the matrix (7.32) with the Born amplitude,

$$\begin{aligned}
\mathcal{M}_0 \mathcal{K}_1^{\text{ad}} &= \sum_{i=1}^n \sum_{\substack{j=1 \\ j \neq i}}^n l_{ij} \sum_{V=A,Z,W^\pm} \mathcal{M}_0^{\varphi_1 \dots \varphi'_i \dots \varphi'_j \dots \varphi_n} I_{\varphi'_i \varphi_i}^{\bar{V}} I_{\varphi'_j \varphi_j}^V \\
&= \sum_{i=1}^n \sum_{\substack{j=1 \\ j \neq i}}^n l_{ij} \left\{ \mathcal{M}_0^{\varphi_1 \dots \varphi_i \dots \varphi_j \dots \varphi_n} \left[ \frac{g_1^2}{e^2} \frac{y_i y_j}{4} + \frac{g_2^2}{e^2} t_i^3 t_j^3 \right] \right. \\
&\quad \left. + \sum_{V=W^\pm} \mathcal{M}_0^{\varphi_1 \dots \varphi'_i \dots \varphi'_j \dots \varphi_n} I_{\varphi'_i \varphi_i}^{\bar{V}} I_{\varphi'_j \varphi_j}^V \right\}, \tag{7.33}
\end{aligned}$$

requires the evaluation of matrix elements involving SU(2)-transformed external fermions  $\varphi'_i, \varphi'_j$ , i.e. isospin partners of the fermions  $\varphi_i, \varphi_j$ .

## 8 Discussion

In this section we compare our results presented in Sect. 7 to existing results from the literature and apply them to specific processes.

### 8.1 Extension of previous results

In Ref. [27] the one- and two-loop LL and angular-dependent NLL contributions have been calculated for arbitrary non-mass-suppressed Standard Model processes, using a photon mass and fermion masses for the regularization of soft and collinear singularities, respectively. The purely symmetric-electroweak parts of our results, made up of  $F_1^{\text{sew}}$  or

$f_1^{\text{sew}}$  and its square, confirm the corresponding terms involving  $\delta_{\text{sew}}$  in Ref. [27], which can be seen e.g. by comparing (7.29), (7.30) and (7.31) from our paper with (4.9), (4.10) and (4.24) from Ref. [27]. In addition to the existing results we have added all the remaining (non-angular-dependent) NLL contributions, including those proportional to  $\ln(M_Z^2/M_W^2)$  and the terms involving  $\beta$ -function coefficients, as well as higher orders in  $\epsilon$  in the one-loop results. We cannot compare the electromagnetic parts contained in  $\Delta F_1^{\text{em}}$  or  $\Delta f_1^{\text{em}}$  and  $\delta_{\text{sem}}$  because of the different regularization schemes for the photonic singularities, i.e. for the soft and collinear divergences resulting from massless photons.

In Ref. [28] the complete one- and two-loop LL and NLL contributions for the electroweak singlet form factors have been derived. We can easily reproduce these form factor contributions as a special case of our results, as for only two external fermions no angular-dependent logarithms appear and the summation over external legs, using (7.28), is trivial. The functions  $I$ ,  $\Delta I$ ,  $J$ , and  $\Delta J$  appearing in (4.69), (4.70), and (4.73) of Ref. [28] correspond to the equally named functions from this paper for  $r_{ij} = -Q^2 = s$ . In the form factor case, due to the absence of the angular-dependent term  $\mathcal{K}_1^{\text{ad}}$  in (7.31), the one-loop operators  $F_1^{\text{sew}}$  and  $\Delta F_1^{\text{em}}$  commute, so that the two-loop result can be written as a single exponential and we have  $\tilde{\mathcal{M}}_2 \stackrel{\text{NLL}}{=} \mathcal{M}_0 \{ \frac{1}{2} [F_1^{\text{sew}} + \Delta F_1^{\text{em}} + \Delta F_1^Z]^2 + G_2^{\text{sew}} + \Delta G_2^{\text{em}} \}$ , corresponding to the form in Ref. [28]. Note that we have renormalized all couplings of the loop corrections at the unique scale  $\mu_w = \mu_e = \mu_R$ , where the last two lines of (4.73) in Ref. [28] vanish.

## 8.2 Comparison to Catani's formula in QCD

The structure of our results for electroweak logarithmic corrections is similar to the singular structure of scattering amplitudes in QCD. In Ref. [35] the singular part of a QCD one-loop amplitude, i.e. the pole part with terms  $\epsilon^{-2}$  and  $\epsilon^{-1}$ , is obtained from the Born amplitude by applying an operator  $\mathbf{I}^{(1)}(\epsilon, \mu^2; \{p\})$  which, for only fermions and antifermions as external particles, can be expressed through Eqs. (12)–(15) of Ref. [35] as

$$\frac{\alpha_S(\mu_R^2)}{2\pi} \mathbf{I}^{(1)}(\epsilon, \mu_R^2; \{p\}) \stackrel{\text{NLL}}{=} \frac{\alpha_{S,\epsilon}}{4\pi} \left( -\frac{1}{2} \right) \sum_i \sum_{j \neq i} \mathbf{T}_i \cdot \mathbf{T}_j I(\epsilon, 0; -r_{ij}), \quad (8.1)$$

where  $I(\epsilon, 0; -r_{ij})$  is the function defined in (7.7), and  $\alpha_{S,\epsilon}$  represents the strong coupling renormalized at  $\mu_R^2$  and rescaled as in (2.7). The product  $\mathbf{T}_i \cdot \mathbf{T}_j$  of the colour charge operators corresponds to  $\sum_{V=A,Z,W^\pm} I_i^V I_j^V$  for electroweak interactions, so that (8.1) has exactly the form of  $F_1^{\text{sew}}$  (7.4) for  $M_W = 0$ , including the angular-dependent logarithms. Note that the factor  $(Q^2/\mu_R^2)^\epsilon$  from the difference in the definitions of  $\alpha_S$  [35] and  $\alpha_\epsilon$  (2.7),

$$\alpha_S(\mu_R^2) = \alpha_{S,\epsilon} \left( \frac{Q^2}{\mu_R^2} \right)^\epsilon, \quad (8.2)$$

is multiplied by a factor  $(-\mu_R^2/r_{ij})^\epsilon$  from  $\mathbf{I}^{(1)}(\epsilon, \mu_R^2; \{p\})$ , producing the correct angular-dependent logarithms  $l_{ij} = \ln(-r_{ij}/Q^2)$  contained in  $I(\epsilon, 0; -r_{ij})$ . The  $\epsilon$ -dependent prefactor in the definition of  $\mathbf{I}^{(1)}(\epsilon, \mu_R^2; \{p\})$ ,  $e^{-\epsilon\psi(1)}/\Gamma(1-\epsilon) = 1 + \mathcal{O}(\epsilon^2)$ , is irrelevant in NLL accuracy, and the same holds for the corresponding factors in the two-loop result.

In two loops, the operator acting on the Born amplitude is given by Catani's formula, Eqs. (18)–(21) of Ref. [35], in NLL accuracy as

$$\left(\frac{\alpha_S(\mu_R^2)}{2\pi}\right)^2 \left\{ \frac{1}{2} [\mathbf{I}^{(1)}(\epsilon, \mu_R^2; \{p\})]^2 + \frac{2\pi\beta_0}{\epsilon} [\mathbf{I}^{(1)}(2\epsilon, \mu_R^2; \{p\}) - \mathbf{I}^{(1)}(\epsilon, \mu_R^2; \{p\})] \right\}. \quad (8.3)$$

The first term in the curly brackets originates from the combination of  $\mathbf{I}^{(1)}(\epsilon, \mu_R^2; \{p\})$  applied to the one-loop amplitude and  $-\frac{1}{2}[\mathbf{I}^{(1)}(\epsilon, \mu_R^2; \{p\})]^2$  acting on the Born amplitude in Ref. [35]. It can be identified with the term  $\frac{1}{2}[F_1^{\text{sew}}]^2$  from our two-loop result (7.12). Using colour conservation, the second term gives

$$\begin{aligned} & \left(\frac{\alpha_S(\mu_R^2)}{2\pi}\right)^2 \frac{2\pi\beta_0}{\epsilon} [\mathbf{I}^{(1)}(2\epsilon, \mu_R^2; \{p\}) - \mathbf{I}^{(1)}(\epsilon, \mu_R^2; \{p\})] \\ & \stackrel{\text{NLL}}{=} \left(\frac{\alpha_{S,\epsilon}}{4\pi}\right)^2 4\pi\beta_0 \cdot \frac{1}{2} \sum_i \mathbf{T}_i^2 J(\epsilon, 0, \mu_R^2), \end{aligned} \quad (8.4)$$

where  $J(\epsilon, 0, \mu_R^2)$  is the function defined in (7.14). In the electroweak model, the expression  $4\pi\beta_0 \mathbf{T}_i^2$  in (8.4) corresponds directly to the term  $[b_1^{(1)} g_1^2 (Y_i/2)^2 + b_2^{(1)} g_2^2 C_i]/e^2$  in (7.13). Therefore (8.4) can be identified with the contribution of  $G_2^{\text{sew}}$  for  $M_W = 0$ .

The symmetric-electroweak part of our results can thus be obtained from Catani's formula by an obvious replacement of gauge-group quantities together with a simple substitution of massless one-loop integrals by massive ones. The remaining parts of our results, which are due to the differences between the masses of the photon, Z boson, and W boson and which cannot be inferred from Catani's formula, can be expressed as simple combinations of the same one-loop integrals.

### 8.3 Comparison to electroweak resummation results

In Refs. [18–21] a resummation of electroweak one-loop results has been proposed, including all LL and NLL corrections apart from the  $\ln(M_Z^2/M_W^2)$  terms.

The non-angular-dependent  $\mathcal{O}(\epsilon^0)$ -terms of  $f_1^{\text{sew}}$  are found in Ref. [18] in the sum  $\sum_{k=1}^{n_f}$  of Eq. (48) [Eq. (49) in the hep-ph version] for the contribution of external fermionic lines above the weak scale. These expressions are extended in Eq. (48) of Ref. [20] in order to include the  $\beta$ -function terms of  $g_2^{\text{sew}}$ . Here care must be taken to use the *resummed* one-loop running of the couplings, i.e.  $\alpha(s) = \alpha(M^2)/(1 + c \ln s/M^2)$  with  $c = \alpha(M^2)\beta_0/\pi$ , in order to correctly arrive at

$$\frac{1}{c} \ln \frac{s}{M^2} \left( \ln \frac{\alpha(M^2)}{\alpha(s)} - 1 \right) + \frac{1}{c^2} \ln \frac{\alpha(M^2)}{\alpha(s)} = \frac{1}{2} \ln^2 \frac{s}{M^2} - \frac{c}{6} \ln^3 \frac{s}{M^2} + \mathcal{O}(c^2), \quad (8.5)$$

and equivalently for  $\alpha \rightarrow \alpha'$ ,  $c \rightarrow c'$ , reproducing the coefficient of the  $\beta$ -function terms in  $g_2^{\text{sew}}$  (7.31) for  $\mu_R = M_W$ .

The angular-dependent NLL corrections are treated in Ref. [21]. The last line of Eq. (13) there [Eq. (11) in the hep-ph version] matches the  $\mathcal{K}_1^{\text{ad}}$ -term of (7.31) and (7.32) in  $\mathcal{O}(\epsilon^0)$  if one takes all gauge-boson masses to be  $m_{V_a} = M_W$ . The symmetric-electroweak parts of the one- and two-loop amplitudes in Ref. [21] are thus in agreement with our results.

To summarize, our explicit one- and two-loop results (7.29), (7.30) and (7.31) confirm the symmetric-electroweak parts of the resummed ansatz. The electromagnetic contributions, i.e. the contributions from below the weak scale, cannot be compared due to the different regularization schemes for the photonic singularities. However, the factorization of the electromagnetic contributions from the symmetric-electroweak ones and the fact that the former can be expressed in terms of one-loop QED corrections are in agreement with the approach proposed in Refs. [18–21].

## 8.4 Four-fermion scattering processes

We now apply our results to massless four-fermion processes

$$\varphi_1(p_1) \varphi_2(p_2) \rightarrow \varphi_3(-p_3) \varphi_4(-p_4), \quad (8.6)$$

where each of the  $\varphi_i$  may be a massless fermion,  $\varphi_i = f_{\sigma_i}^{\kappa_i}$ , or antifermion,  $\varphi_i = \bar{f}_{\sigma_i}^{\kappa_i}$ , with the notations from Sect. 2, provided that the number of fermions and antifermions in the initial and final state is equal. The scattering amplitudes for the processes (8.6) follow directly from our results for the generic  $n \rightarrow 0$  process (2.1) by crossing symmetry. The Mandelstam invariants are given by  $s = r_{12} = r_{34}$ ,  $t = r_{13} = r_{24}$ , and  $u = r_{14} = r_{23}$  with  $r_{ij} = (p_i + p_j)^2$ .

The following discussion focuses on  $s$ -channel processes of the form

$$f_{\sigma}^{\kappa} \bar{f}_{\rho}^{\kappa} \rightarrow f_{\sigma'}^{\kappa'} \bar{f}_{\rho'}^{\kappa'} \quad (8.7)$$

with one fermion and one antifermion in the initial as well as in the final state, where  $f_{\sigma}^{\kappa}$  and  $f_{\sigma'}^{\kappa'}$  are neither identical nor isospin partners of each other, and the same holds for  $\bar{f}_{\rho}^{\kappa}$  and  $\bar{f}_{\rho'}^{\kappa'}$ . Therefore the external fermion lines are always connected between  $f_{\sigma}^{\kappa}$  and  $\bar{f}_{\rho}^{\kappa}$  in the initial state and between  $f_{\sigma'}^{\kappa'}$  and  $\bar{f}_{\rho'}^{\kappa'}$  in the final state. The number of independent chiralities  $\kappa_i$  is thus restricted to two,  $\kappa$  and  $\kappa'$ , and the particle pairs in the initial and final state must either be antiparticles of each other or antiparticles of the mutual isospin partners. The first case corresponds to neutral-current four-fermion scattering, which is treated in Sect. 8.4.1. The second case refers to charged-current four-fermion scattering and is treated in Sect. 8.4.2.

The scattering amplitudes of all other processes (8.6) can be obtained from (8.7) by crossing symmetry and additive combinations of amplitudes. For instance, the full four-quark amplitude for  $u\bar{u} \rightarrow d\bar{d}$  is given by the sum of the  $s$ -channel neutral-current amplitude and the  $t$ -channel charged-current amplitude, where the latter follows from the result of the  $s$ -channel charged-current amplitude for  $u\bar{d} \rightarrow u\bar{d}$  by exchanging  $p_2$  and  $p_3$ , and thus  $s$  and  $t$ . The neutral- and charged-current results in Sects. 8.4.1 and 8.4.2 together are thus sufficient to construct the scattering amplitudes for all massless four-fermion processes (8.6).

### 8.4.1 Neutral-current four-fermion scattering

This section deals with the  $s$ -channel neutral-current four-fermion processes

$$f_{\sigma}^{\kappa} \bar{f}_{\sigma}^{\kappa} \rightarrow f_{\sigma'}^{\kappa'} \bar{f}_{\sigma'}^{\kappa'}, \quad (8.8)$$

where a fermion–antifermion pair annihilates and produces another fermion–antifermion pair. The electromagnetic charge quantum numbers of the external particles are given by  $q_f = q_{f_\sigma^\kappa} = -q_{\bar{f}_\sigma^\kappa}$  and  $q_{f'} = q_{f_{\sigma'}^{\kappa'}} = -q_{\bar{f}_{\sigma'}^{\kappa'}}$ , the hypercharges by  $y_f = y_{f_\sigma^\kappa} = -y_{\bar{f}_\sigma^\kappa}$  and  $y_{f'} = y_{f_{\sigma'}^{\kappa'}} = -y_{\bar{f}_{\sigma'}^{\kappa'}}$ , the isospin components by  $t_f^3 = t_{f_\sigma^\kappa}^3 = -t_{\bar{f}_\sigma^\kappa}^3$  and  $t_{f'}^3 = t_{f_{\sigma'}^{\kappa'}}^3 = -t_{\bar{f}_{\sigma'}^{\kappa'}}^3$ , and the isospin by  $t_f = |t_f^3|$ ,  $t_{f'} = |t_{f'}^3|$ . These electroweak quantum numbers depend on the flavour and the chirality of the fermions.

The Born amplitude reads

$$\mathcal{M}_{0,\text{NC}} = \frac{1}{s} \mathcal{A}_{\text{NC}} C_{0,\text{NC}} \quad (8.9)$$

in the high-energy limit, where

$$\mathcal{A}_{\text{NC}} = \bar{v}(p_2, \kappa) \gamma^\mu u(p_1, \kappa) \bar{u}(-p_3, \kappa') \gamma_\mu v(-p_4, \kappa') \quad (8.10)$$

represents the spinor structure of the incoming and outgoing massless fermions with chiralities  $\kappa$  and  $\kappa'$ , and

$$C_{0,\text{NC}} = g_1^2(Q^2) \frac{y_f y_{f'}}{4} + g_2^2(Q^2) t_f^3 t_{f'}^3. \quad (8.11)$$

As indicated, the couplings  $g_i(Q^2)$  in the Born amplitude are renormalized at the scale  $Q$ , whereas the additional couplings and mixing angles in the loop corrections below are renormalized at the scale  $\mu_R$ .

We write the neutral-current amplitude in the form

$$\mathcal{M}_{\text{NC}} \stackrel{\text{NLL}}{=} \mathcal{M}_{0,\text{NC}} F_{\text{NC}}^{\text{sew}} F_{\text{NC}}^Z F_{\text{NC}}^{\text{em}} \quad (8.12)$$

according to (7.19). Applying the non-diagonal operator  $F^{\text{sew}}$  (7.20) to the Born amplitude, we find

$$\begin{aligned} \mathcal{M}_{0,\text{NC}} F_{\text{NC}}^{\text{sew}} \stackrel{\text{NLL}}{=} \frac{1}{s} \mathcal{A}_{\text{NC}} \left\{ C_{0,\text{NC}} + \frac{\alpha_\epsilon}{4\pi} \left[ - \left( L^2 + \frac{2}{3} L^3 \epsilon + \frac{1}{4} L^4 \epsilon^2 - 3L - \frac{3}{2} L^2 \epsilon - \frac{1}{2} L^3 \epsilon^2 \right) \right. \right. \\ \left. \left. \times C_{0,\text{NC}} C_{1,\text{NC}}^{\text{sew}} + \left( L + \frac{1}{2} L^2 \epsilon + \frac{1}{6} L^3 \epsilon^2 \right) C_{1,\text{NC}}^{\text{ad}} + \mathcal{O}(\epsilon^3) \right] \right. \\ \left. + \left( \frac{\alpha_\epsilon}{4\pi} \right)^2 \left[ \left( \frac{1}{2} L^4 - 3L^3 \right) C_{0,\text{NC}} \left( C_{1,\text{NC}}^{\text{sew}} \right)^2 - L^3 C_{1,\text{NC}}^{\text{ad}} C_{1,\text{NC}}^{\text{sew}} + C_{0,\text{NC}} g_{2,\text{NC}}^{\text{sew}} + \mathcal{O}(\epsilon) \right] \right\}, \quad (8.13) \end{aligned}$$

where

$$C_{1,\text{NC}}^{\text{sew}} = \frac{g_1^2}{e^2} \frac{y_f^2}{4} + \frac{g_2^2}{e^2} t_f(t_f + 1) + (f \leftrightarrow f') \quad (8.14)$$

results from the non-angular-dependent contributions to  $f_1^{\text{sew}}$  in (7.31), whereas the application of the angular-dependent operator  $\mathcal{K}_1^{\text{ad}}$  on the Born amplitude yields

$$\begin{aligned} C_{1,\text{NC}}^{\text{ad}} = C_{0,\text{NC}} \left[ 4 \ln \left( \frac{u}{t} \right) \left( \frac{g_1^2}{e^2} \frac{y_f y_{f'}}{4} + \frac{g_2^2}{e^2} t_f^3 t_{f'}^3 \right) - 2 \ln \left( \frac{-s}{Q^2} \right) C_{1,\text{NC}}^{\text{sew}} \right] \\ + 2 g_2^2(Q^2) \frac{g_2^2}{e^2} \left[ \ln \left( \frac{u}{t} \right) t_f t_{f'} - \left( \ln \left( \frac{t}{s} \right) + \ln \left( \frac{u}{s} \right) \right) t_f^3 t_{f'}^3 \right]. \quad (8.15) \end{aligned}$$

The last missing part in (8.13),

$$g_{2,\text{NC}}^{\text{sew}} \stackrel{\text{NLL}}{=} \left( \frac{1}{3} L^3 - l_{\mu_R} L^2 \right) \left[ \frac{g_1^2}{e^2} b_1^{(1)} \frac{y_f^2}{4} + \frac{g_2^2}{e^2} b_2^{(1)} t_f (t_f + 1) + (f \leftrightarrow f') \right] + \mathcal{O}(\epsilon), \quad (8.16)$$

results directly from (7.31), where the values for the  $\beta$ -function coefficients  $b_1^{(1)}$  and  $b_2^{(1)}$  in the electroweak Standard Model are given in (C.7).

The symmetric-electroweak result (8.13) is multiplied with the diagonal factors

$$F_{\text{NC}}^Z \stackrel{\text{NLL}}{=} 1 + \frac{\alpha_\epsilon}{4\pi} \Delta f_{1,\text{NC}}^Z \quad (8.17)$$

and

$$F_{\text{NC}}^{\text{em}} \stackrel{\text{NLL}}{=} 1 + \frac{\alpha_\epsilon}{4\pi} \Delta f_{1,\text{NC}}^{\text{em}} + \left( \frac{\alpha_\epsilon}{4\pi} \right)^2 \left[ \frac{1}{2} (\Delta f_{1,\text{NC}}^{\text{em}})^2 + \Delta g_{2,\text{NC}}^{\text{em}} \right]. \quad (8.18)$$

The factors  $F_{\text{NC}}^Z$  and  $F_{\text{NC}}^{\text{em}}$  follow from (7.31),

$$\Delta f_{1,\text{NC}}^Z \stackrel{\text{NLL}}{=} 2 \left( L + L^2 \epsilon + \frac{1}{2} L^3 \epsilon^2 \right) l_Z \left[ \left( \frac{g_2}{e} c_w t_f^3 - \frac{g_1}{e} s_w \frac{y_f}{2} \right)^2 + (f \leftrightarrow f') \right] + \mathcal{O}(\epsilon^3), \quad (8.19)$$

$$\begin{aligned} \Delta f_{1,\text{NC}}^{\text{em}} \stackrel{\text{NLL}}{=} & - \left( 2\epsilon^{-2} + 3\epsilon^{-1} - L^2 - \frac{2}{3} L^3 \epsilon - \frac{1}{4} L^4 \epsilon^2 + 3L + \frac{3}{2} L^2 \epsilon + \frac{1}{2} L^3 \epsilon^2 \right) (q_f^2 + q_{f'}^2) \\ & - \left( \epsilon^{-1} + L + \frac{1}{2} L^2 \epsilon + \frac{1}{6} L^3 \epsilon^2 \right) \left[ 4 \ln \left( \frac{u}{t} \right) q_f q_{f'} - 2 \ln \left( \frac{-s}{Q^2} \right) (q_f^2 + q_{f'}^2) \right] \\ & + \mathcal{O}(\epsilon^3), \end{aligned} \quad (8.20)$$

$$\begin{aligned} \Delta g_{2,\text{NC}}^{\text{em}} \stackrel{\text{NLL}}{=} & \left\{ -l_{\mu_R} \left[ 2\epsilon^{-2} + (2L - l_{\mu_R}) \epsilon^{-1} - l_{\mu_R} \left( L - \frac{1}{3} l_{\mu_R} \right) \right] b_e^{(1)} \right. \\ & \left. + \left( \frac{3}{2} \epsilon^{-3} + 2L\epsilon^{-2} + L^2 \epsilon^{-1} \right) b_{\text{QED}}^{(1)} \right\} (q_f^2 + q_{f'}^2) + \mathcal{O}(\epsilon), \end{aligned} \quad (8.21)$$

where the values for the  $\beta$ -function coefficients  $b_e^{(1)}$  and  $b_{\text{QED}}^{(1)}$  in the electroweak Standard Model are given in (C.7) and (C.8).

Our result can be compared to Refs. [22, 23, 31], where the logarithmic two-loop contributions to neutral-current four-fermion scattering have been determined by resummation techniques. These papers use the renormalization scale  $\mu_R = M_W$  for the couplings in the loop corrections, so that we have to set  $l_{\mu_R} = \ln(\mu_R^2/M_W^2) = 0$  in (8.16) and (8.21). The large electroweak logarithms in Refs. [22, 23, 31] are defined with the choice  $Q^2 = -s$ , such that  $\ln(-s/Q^2) = 0$  in (8.15) and (8.20).

In Refs. [22, 23, 31] the photonic singularities are regularized with a finite photon mass. Therefore we cannot directly compare their electromagnetic corrections with our dimensionally regularized result. But Refs. [22, 23, 31] define a finite scattering amplitude by factorizing the complete QED corrections,

$$\mathcal{M}_{\text{NC}}^{\text{fin}} = \frac{\mathcal{M}_{\text{NC}}}{U_{\text{QED}}}. \quad (8.22)$$

The factor  $U_{\text{NC}}^{\text{QED}}$  represents the full QED corrections from photons coupling exclusively to fermions, with the photonic singularities regularized in the same way as in the amplitude  $\mathcal{M}_{\text{NC}}$ . The soft and collinear divergences resulting from massless photons cancel in the ratio (8.22), and  $\mathcal{M}_{\text{NC}}^{\text{fin}}$  is independent of the regularization scheme for the photonic singularities. Using our dimensional regularization scheme and  $\mu_{\text{R}} = M_{\text{W}}$ ,  $Q^2 = -s$  as above,  $U_{\text{NC}}^{\text{QED}}$  is given by

$$U_{\text{NC}}^{\text{QED}} \stackrel{\text{NLL}}{=} 1 + \frac{\alpha_{\epsilon}}{4\pi} f_{1,\text{NC}}^{\text{QED}} + \left(\frac{\alpha_{\epsilon}}{4\pi}\right)^2 \left[ \frac{1}{2} \left(f_{1,\text{NC}}^{\text{QED}}\right)^2 + g_{2,\text{NC}}^{\text{QED}} \right], \quad (8.23)$$

with

$$f_{1,\text{NC}}^{\text{QED}} \stackrel{\text{NLL}}{=} - \left(2\epsilon^{-2} + 3\epsilon^{-1}\right) \left(q_f^2 + q_{f'}^2\right) - 4\epsilon^{-1} \ln\left(\frac{u}{t}\right) q_f q_{f'}, \quad (8.24)$$

$$g_{2,\text{NC}}^{\text{QED}} \stackrel{\text{NLL}}{=} \left[ \left(\frac{3}{2}\epsilon^{-3} + 2L\epsilon^{-2} + L^2\epsilon^{-1} + \frac{1}{3}L^3\right) b_{\text{QED}}^{(1)} + \frac{1}{3}L^3 b_{\text{top}}^{(1)} \right] \left(q_f^2 + q_{f'}^2\right) + \mathcal{O}(\epsilon). \quad (8.25)$$

In contrast to  $F_{\text{NC}}^{\text{em}}$  (8.18),  $U_{\text{NC}}^{\text{QED}}$ , according to its definition in Refs. [22, 23, 31], contains the complete photon contribution without the subtractions at a photon mass equal to  $M_{\text{W}}$ . This is why (8.24) and (8.25) differ from (8.20) and (8.21) by finite logarithmic terms. The expressions  $f_{1,\text{NC}}^{\text{QED}}$  and  $g_{2,\text{NC}}^{\text{QED}}$  can be obtained from  $\Delta F_1^{\text{em}}$  (7.5) and  $\Delta G_2^{\text{em}}$  (7.13) by replacing  $\Delta I \rightarrow I$  and  $\Delta J \rightarrow J$  and adding the term proportional to  $b_{\text{top}}^{(1)}$  in (8.25), where  $b_{\text{top}}^{(1)}$  is defined in (C.9) and corresponds to the top-quark contribution to the electromagnetic  $\beta$ -function. In our result, this latter term is implicitly contained in  $g_{2,\text{NC}}^{\text{sew}}$  (8.16) and, by construction, cancels in the subtracted expression  $\Delta g_{2,\text{NC}}^{\text{em}}$  (8.21). The factor  $U_{\text{NC}}^{\text{QED}}$  in (8.23) is valid for  $m_t \sim M_{\text{W}}$ , whereas the corresponding factor in Refs. [23, 31] is only valid for a massless top quark. However, the finite amplitude  $\mathcal{M}_{\text{NC}}^{\text{fin}}$  is independent of the top-quark mass in NLL approximation.

The one- and two-loop contributions to  $\mathcal{M}_{\text{NC}}^{\text{fin}}$  (8.22) can be expressed as follows:

$$\begin{aligned} \tilde{\mathcal{M}}_{1,\text{NC}}^{\text{fin}} \stackrel{\text{NLL}}{=} \frac{1}{s} \mathcal{A}_{\text{NC}} \left\{ -C_{0,\text{NC}} \left[ \left(L^2 - 3L\right) C_{1,\text{NC}}^{\text{sew}} - \Delta f_{1,\text{NC}}^{\text{em}} + f_{1,\text{NC}}^{\text{QED}} \right] \right. \\ \left. + L C_{1,\text{NC}}^{\text{ad}} + C_{0,\text{NC}} \Delta f_{1,\text{NC}}^{\text{Z}} \right\} + \mathcal{O}(\epsilon), \\ \tilde{\mathcal{M}}_{2,\text{NC}}^{\text{fin}} \stackrel{\text{NLL}}{=} \frac{1}{s} \mathcal{A}_{\text{NC}} \left\{ \frac{1}{2} C_{0,\text{NC}} \left[ \left(L^2 - 3L\right) C_{1,\text{NC}}^{\text{sew}} - \Delta f_{1,\text{NC}}^{\text{em}} + f_{1,\text{NC}}^{\text{QED}} \right]^2 \right. \\ \left. - \left( L C_{1,\text{NC}}^{\text{ad}} + C_{0,\text{NC}} \Delta f_{1,\text{NC}}^{\text{Z}} \right) \left( L^2 C_{1,\text{NC}}^{\text{sew}} - \Delta f_{1,\text{NC}}^{\text{em}} + f_{1,\text{NC}}^{\text{QED}} \right) \right. \\ \left. + C_{0,\text{NC}} \left( g_{2,\text{NC}}^{\text{sew}} + \Delta g_{2,\text{NC}}^{\text{em}} - g_{2,\text{NC}}^{\text{QED}} \right) \right\} + \mathcal{O}(\epsilon). \quad (8.26) \end{aligned}$$

The one-loop result reproduces Eq. (50) from Ref. [22], and the two-loop result agrees with Eqs. (51), (52) of Ref. [22] and Eqs. (51), (52), (54) of Ref. [23] for  $N_g = 3$  families of leptons and quarks. Note that in these papers  $(\alpha/4\pi)(g_2^2/e^2)$  is used as the parameter of the perturbative expansion. The corrections proportional to  $\Delta f_{1,\text{NC}}^{\text{Z}}$ , which account for the mass difference of the heavy electroweak gauge bosons,  $M_Z \neq M_{\text{W}}$ , have to be compared to Eq. (62) of Ref. [31], where the first order of an expansion in the parameter  $\delta_M = s_{\text{W}}^2 = 1 - M_{\text{W}}^2/M_Z^2$  is presented. Using  $l_Z = \ln(M_Z^2/M_{\text{W}}^2) = s_{\text{W}}^2 + \mathcal{O}(s_{\text{W}}^4)$ , Ref. [31] gives indeed the first order in  $s_{\text{W}}^2$  of our result, provided that we set  $s_{\text{W}} = 0$  and  $c_{\text{W}} = 1$  in  $\Delta f_{1,\text{NC}}^{\text{Z}}$  (8.19), thus neglecting higher orders in  $s_{\text{W}}^2$ .

### 8.4.2 Charged-current four-fermion scattering

In order to complete our predictions for massless four-fermion scattering, we apply our results to the  $s$ -channel charged-current processes

$$f_\sigma^L \bar{f}_\rho^L \rightarrow f_{\sigma'}^L \bar{f}_{\rho'}^L, \quad (8.27)$$

where the fermions  $f_\sigma^L$  and  $f_{\sigma'}^L$  are the isospin partners of  $f_\rho^L$  and  $f_{\rho'}^L$ , respectively. The hypercharge quantum numbers of the external particles are given by  $y_f = y_{f_\sigma^L} = -y_{\bar{f}_\rho^L}$  and  $y_{f'} = y_{f_{\sigma'}^L} = -y_{\bar{f}_{\rho'}^L}$  and the isospin components by  $t^3 = t_{f_\sigma^L}^3 = t_{\bar{f}_\rho^L}^3 = t_{f_{\sigma'}^L}^3 = t_{\bar{f}_{\rho'}^L}^3$ . All external fermions have to be left-handed, so  $t = |t^3| = 1/2$ .

In the high-energy approximation, the Born amplitude reads

$$\mathcal{M}_{0,\text{CC}} = \frac{1}{s} \mathcal{A}_{\text{CC}} \frac{g_2^2(Q^2)}{2} \quad (8.28)$$

with the spinor structure

$$\mathcal{A}_{\text{CC}} = \bar{v}(p_2, L) \gamma^\mu u(p_1, L) \bar{u}(-p_3, L) \gamma_\mu v(-p_4, L). \quad (8.29)$$

As in the previous section, the amplitude is written in the form

$$\mathcal{M}_{\text{CC}} \stackrel{\text{NLL}}{=} \mathcal{M}_{0,\text{CC}} F_{\text{CC}}^{\text{sew}} F_{\text{CC}}^Z F_{\text{CC}}^{\text{em}}. \quad (8.30)$$

Applying the non-diagonal operator  $F^{\text{sew}}$  (7.20) to the Born amplitude, we find

$$\begin{aligned} \mathcal{M}_{0,\text{CC}} F_{\text{CC}}^{\text{sew}} \stackrel{\text{NLL}}{=} & \frac{1}{s} \mathcal{A}_{\text{CC}} \left\{ \frac{g_2^2(Q^2)}{2} + \frac{\alpha_\epsilon}{4\pi} \left[ - \left( L^2 + \frac{2}{3} L^3 \epsilon + \frac{1}{4} L^4 \epsilon^2 - 3L - \frac{3}{2} L^2 \epsilon - \frac{1}{2} L^3 \epsilon^2 \right) \right. \right. \\ & \times \left. \frac{g_2^2(Q^2)}{2} C_{1,\text{CC}}^{\text{sew}} + \left( L + \frac{1}{2} L^2 \epsilon + \frac{1}{6} L^3 \epsilon^2 \right) C_{1,\text{CC}}^{\text{rad}} + \mathcal{O}(\epsilon^3) \right] \\ & \left. + \left( \frac{\alpha_\epsilon}{4\pi} \right)^2 \left[ \left( \frac{1}{2} L^4 - 3L^3 \right) \frac{g_2^2(Q^2)}{2} \left( C_{1,\text{CC}}^{\text{sew}} \right)^2 - L^3 C_{1,\text{CC}}^{\text{rad}} C_{1,\text{CC}}^{\text{sew}} + \frac{g_2^2(Q^2)}{2} g_{2,\text{CC}}^{\text{sew}} + \mathcal{O}(\epsilon) \right] \right\}, \end{aligned} \quad (8.31)$$

with

$$\begin{aligned} C_{1,\text{CC}}^{\text{sew}} &= \frac{g_1^2}{e^2} \frac{y_f^2 + y_{f'}^2}{4} + \frac{3}{2} \frac{g_2^2}{e^2}, \\ C_{1,\text{CC}}^{\text{rad}} &= \frac{g_2^2(Q^2)}{2} \left[ 4 \ln \left( \frac{u}{t} \right) \frac{g_1^2}{e^2} \frac{y_f y_{f'}}{4} - 2 \left( \ln \left( \frac{t}{s} \right) + \ln \left( \frac{u}{s} \right) \right) \frac{g_2^2}{e^2} - 2 \ln \left( \frac{-s}{Q^2} \right) C_{1,\text{CC}}^{\text{sew}} \right] \\ & \quad + 2 \ln \left( \frac{u}{t} \right) g_1^2(Q^2) \frac{y_f y_{f'}}{4} \frac{g_2^2}{e^2}, \\ g_{2,\text{NC}}^{\text{sew}} \stackrel{\text{NLL}}{=} & \left( \frac{1}{3} L^3 - l_{\mu\text{R}} L^2 \right) \left( \frac{g_1^2}{e^2} b_1^{(1)} \frac{y_f^2 + y_{f'}^2}{4} + \frac{3}{2} \frac{g_2^2}{e^2} b_2^{(1)} \right). \end{aligned} \quad (8.32)$$

The diagonal factors

$$F_{\text{CC}}^Z \stackrel{\text{NLL}}{=} 1 + \frac{\alpha_\epsilon}{4\pi} \Delta f_{1,\text{CC}}^Z \quad (8.33)$$



and

$$F_{\text{CC}}^{\text{em}} \stackrel{\text{NLL}}{=} 1 + \frac{\alpha_\epsilon}{4\pi} \Delta f_{1,\text{CC}}^{\text{em}} + \left(\frac{\alpha_\epsilon}{4\pi}\right)^2 \left[ \frac{1}{2} (\Delta f_{1,\text{CC}}^{\text{em}})^2 + \Delta g_{2,\text{CC}}^{\text{em}} \right] \quad (8.34)$$

are expressed through

$$\begin{aligned} \Delta f_{1,\text{CC}}^{\text{Z}} &\stackrel{\text{NLL}}{=} \left( L + L^2 \epsilon + \frac{1}{2} L^3 \epsilon^2 \right) l_{\text{Z}} \left( \frac{g_2^2}{e^2} c_{\text{W}}^2 + 2 \frac{g_1^2}{e^2} s_{\text{W}}^2 \frac{y_f^2 + y_{f'}}{4} \right) + \mathcal{O}(\epsilon^3), \\ \Delta f_{1,\text{CC}}^{\text{em}} &\stackrel{\text{NLL}}{=} - \left( 2\epsilon^{-2} + 3\epsilon^{-1} - L^2 - \frac{2}{3} L^3 \epsilon - \frac{1}{4} L^4 \epsilon^2 + 3L + \frac{3}{2} L^2 \epsilon + \frac{1}{2} L^3 \epsilon^2 \right) C_{1,\text{CC}}^{\text{em}} \\ &\quad - \left( \epsilon^{-1} + L + \frac{1}{2} L^2 \epsilon + \frac{1}{6} L^3 \epsilon^2 \right) C_{1,\text{CC}}^{\text{ad,em}} + \mathcal{O}(\epsilon^3), \\ \Delta g_{2,\text{CC}}^{\text{em}} &\stackrel{\text{NLL}}{=} \left\{ -l_{\mu_{\text{R}}} \left[ 2\epsilon^{-2} + (2L - l_{\mu_{\text{R}}}) \epsilon^{-1} - l_{\mu_{\text{R}}} \left( L - \frac{1}{3} l_{\mu_{\text{R}}} \right) \right] b_e^{(1)} \right. \\ &\quad \left. + \left( \frac{3}{2} \epsilon^{-3} + 2L\epsilon^{-2} + L^2 \epsilon^{-1} \right) b_{\text{QED}}^{(1)} \right\} C_{1,\text{CC}}^{\text{em}} + \mathcal{O}(\epsilon), \end{aligned} \quad (8.35)$$

with

$$\begin{aligned} C_{1,\text{CC}}^{\text{em}} &= \frac{1}{2} \left( q_{f_\sigma}^2 + q_{f_{\rho'}}^2 + q_{f_{\sigma'}}^2 + q_{f_{\rho}}^2 \right) = \frac{g_1^2}{e^2} c_{\text{W}}^2 \frac{y_f^2 + y_{f'}}{4} + \frac{1}{2} \frac{g_2^2}{e^2} s_{\text{W}}^2, \\ C_{1,\text{CC}}^{\text{ad,em}} &= 2 \left[ \ln \left( \frac{-s}{Q^2} \right) \left( q_{f_\sigma} q_{f_{\rho'}} + q_{f_{\sigma'}} q_{f_\rho} \right) - \ln \left( \frac{-t}{Q^2} \right) \left( q_{f_\sigma} q_{f_{\sigma'}} + q_{f_{\rho'}} q_{f_{\rho}} \right) \right. \\ &\quad \left. - \ln \left( \frac{-u}{Q^2} \right) \left( q_{f_\sigma} q_{f_{\rho}} + q_{f_{\sigma'}} q_{f_{\rho'}} \right) \right] \\ &= 4 \ln \left( \frac{u}{t} \right) \frac{g_1^2}{e^2} c_{\text{W}}^2 \frac{y_f y_{f'}}{4} - \left( \ln \left( \frac{t}{s} \right) + \ln \left( \frac{u}{s} \right) \right) \frac{g_2^2}{e^2} s_{\text{W}}^2 - 2 \ln \left( \frac{-s}{Q^2} \right) C_{1,\text{CC}}^{\text{em}}. \end{aligned} \quad (8.36)$$

## 9 Conclusion

We have studied the one- and two-loop virtual electroweak corrections to arbitrary processes with external massless fermions in the Standard Model. In the high-energy region, where all kinematical invariants are at an energy scale  $Q$  that is large compared to the electroweak gauge-boson masses, we have calculated mass singularities in  $D = 4 - 2\epsilon$  dimensions taking into account all leading logarithmic (LL) and next-to-leading logarithmic (NLL) contributions. This approximation includes all combinations  $\alpha^l \epsilon^{-k} \ln^{j-k}(Q^2/M_{\text{W}}^2)$  of mass-singular logarithms and  $1/\epsilon$  poles with  $j = 2l, 2l-1$  and  $2l-4 \leq k \leq j$ . All masses of the heavy particles have been assumed to be of the same order  $M_{\text{W}} \sim M_{\text{Z}} \sim M_{\text{H}} \sim m_t$  but not equal, and all light fermions have been assumed to be massless.

The calculation has been performed in the complete spontaneously-broken electroweak Standard Model using the 't Hooft–Feynman gauge. All contributions have been split into those that factorize the lowest-order matrix element and non-factorizable parts. The non-factorizable parts have been shown to vanish in NLL approximation owing to collinear Ward identities. All factorizable contributions have been evaluated using a suitable soft–collinear approximation and minimal subtraction of the ultraviolet singularities. Explicit

results have been given for all contributing factorizable Feynman diagrams. The two-loop integrals have been solved by two independent methods in NLL approximation. One makes use of sector decomposition to isolate the mass singularities, the other uses the strategy of regions. The fermionic wave functions are renormalized on shell, and coupling-constant renormalization is performed in the  $\overline{\text{MS}}$  scheme, but can be generalized easily.

In order to isolate the effects resulting from the mass gaps between the photon, the W boson, and the Z boson, all contributions have been split into parts corresponding to  $M_A = M_Z = M_W$  and remaining subtracted parts associated with the massless photon and the Z boson. By combining the results of all diagrams we found that the electroweak mass singularities assume a form that is analogous to the singular structure of scattering amplitudes in massless QCD. The sum of the two-loop leading and next-to-leading logarithms is composed of terms that can be written as the second-order terms of exponentials of the one-loop contribution plus additional NLL contributions that are proportional to the one-loop  $\beta$ -function coefficients. All terms can be cast into a product of three exponentials. The first inner exponential contains the part of the corrections corresponding to  $M_A = M_Z = M_W$ , i.e. the  $\text{SU}(2) \times \text{U}(1)$  symmetric part. The second exponential contains the part originating from the mass gap between the Z boson and the W boson and contains only terms involving  $\ln(M_Z^2/M_W^2)$ . The third outer exponential summarizes the contributions that originate from the mass gap between the photon and the W boson and corresponds to the QED corrections subtracted by the corresponding corrections with  $M_A = M_W$ . While the second exponential commutes with the other two and does in fact get no second-order contribution in NLL approximation, the first and the last exponential do not commute.

If one neglects the NLL contributions proportional to  $\ln(M_Z^2/M_W^2)$ , our result confirms the resummation prescriptions that have been proposed in the literature. These prescriptions are based on the assumption that, in the high-energy limit, the electroweak theory can be described by a symmetric, unmixed  $\text{SU}(2) \times \text{U}(1)$  theory, where all electroweak gauge bosons have mass  $M_W$ , matched with QED at the electroweak scale. Indeed, apart from the terms involving  $\ln(M_Z^2/M_W^2)$ , in the final result we observe a cancellation of all effects associated with symmetry breaking, i.e. gauge-boson mixing, the gap between  $M_Z$  and  $M_W$ , and couplings proportional to the vacuum expectation value. This simple behaviour of the two-loop NLL corrections is ensured by subtle cancellations of mass singularities from different diagrams, where the details of spontaneous symmetry breaking cannot be neglected but have to be taken into account properly.

In massless fermionic processes, the symmetry-breaking effects are restricted to a small subset of diagrams, since the Higgs sector is coupled to massless fermions only via one-loop insertions in the gauge-boson self-energies. Using the techniques developed in this paper, which are to a large extent process independent, we plan to extend our study of two-loop NLL mass singularities to processes involving heavy external particles that are directly coupled to the Higgs sector.

As an application of our results for general  $n$ -fermion processes we have presented explicit expressions for the case of neutral-current and charged-current 4-fermion reactions. In the former case we found agreement with existing predictions obtained with the help of resummations prescriptions.

Our results are also applicable to reactions that involve massless fermions and (hard) gluons, such as 2-jet production at hadron colliders, since gluons do not couple to electroweak gauge bosons.

## A Loop integrals

In this appendix, we list the explicit expressions for the Feynman integrals that contribute to the one- and two-loop diagrams discussed in Sects. 5.1 and 5.2. In order to keep our expressions as compact as possible we define the momenta

$$\begin{aligned} k_1 &= p_i + l_1, & k_2 &= p_i + l_2, & k_3 &= p_i + l_1 + l_2, \\ q_1 &= p_j - l_1, & q_2 &= p_j - l_2, & q_3 &= p_j - l_1 - l_2, & l_3 &= -l_1 - l_2, \\ r_1 &= p_k - l_1, & r_2 &= p_k - l_2, & r_3 &= p_k - l_1 + l_2, & l_4 &= l_1 - l_2. \end{aligned} \quad (\text{A.1})$$

For massive and massless propagators we use the notation

$$P(q, m) = q^2 - m^2 + i0, \quad P(q) = q^2 + i0, \quad (\text{A.2})$$

and for triple gauge-boson couplings we write

$$\Gamma^{\mu_1\mu_2\mu_3}(l_1, l_2, l_3) = g^{\mu_1\mu_2}(l_1 - l_2)^{\mu_3} + g^{\mu_2\mu_3}(l_2 - l_3)^{\mu_1} + g^{\mu_3\mu_1}(l_3 - l_1)^{\mu_2}. \quad (\text{A.3})$$

The normalization factors occurring in (2.7) are absorbed into the integration measure

$$d\tilde{l}_i = (4\pi)^2 \left( \frac{4\pi\mu_D^2}{e^{\gamma_E} Q^2} \right)^{D/2-2} \mu_D^{4-D} \frac{d^D l_i}{(2\pi)^D} = \frac{1}{\pi^2} \left( e^{\gamma_E} Q^2 \pi \right)^{2-D/2} d^D l_i, \quad (\text{A.4})$$

and for the projection introduced in (3.24) we use the shorthand

$$\Pi_{ij}(\Gamma) = \frac{1}{r_{ij}} \text{Tr}(\Gamma \omega_{\kappa_i} \not{l}_i \not{l}_j) = \frac{1}{2r_{ij}} \text{Tr}(\Gamma \not{l}_i \not{l}_j), \quad (\text{A.5})$$

where the second equality holds if  $\Gamma$  does not involve  $\gamma_5$  or  $\omega_{R,L}$ , as it is the case in the following equations. With this notation we have

$$\begin{aligned} D_0(m_1; r_{ij}) &= \int d\tilde{l}_1 \frac{4i k_1 q_1}{P(l_1, m_1) P(k_1) P(q_1)}, \\ D_1(m_1, m_2; r_{ij}) &= \int d\tilde{l}_1 d\tilde{l}_2 \frac{-16(k_1 q_1)(k_3 q_3)}{P(l_1, m_1) P(l_2, m_2) P(k_1) P(k_3) P(q_1) P(q_3)}, \\ D_2(m_1, m_2; r_{ij}) &= \int d\tilde{l}_1 d\tilde{l}_2 \frac{-16(k_1 q_3)(k_3 q_2)}{P(l_1, m_1) P(l_2, m_2) P(k_1) P(k_3) P(q_2) P(q_3)}, \\ D_3(m_1, m_2, m_3; r_{ij}) &= \int d\tilde{l}_1 d\tilde{l}_2 \frac{-2\Pi_{ij}(\not{k}_3 \gamma^{\mu_2} \not{k}_1 \gamma^{\mu_1}) q_3^{\mu_3} \Gamma_{\mu_1\mu_2\mu_3}(l_1, l_2, l_3)}{P(l_1, m_1) P(l_2, m_2) P(l_3, m_3) P(k_1) P(k_3) P(q_3)}, \\ D_4(m_1, m_2; r_{ij}) &= \int d\tilde{l}_1 d\tilde{l}_2 \frac{2\Pi_{ij}(\not{k}_1 \gamma^{\mu_2} \not{k}_3 \gamma_{\mu_2} \not{k}_1 \not{q}_1)}{P(l_1, m_1) P(l_2, m_2) [P(k_1)]^2 P(k_3) P(q_1)}, \\ D_5(m_1, m_2; r_{ij}) &= \int d\tilde{l}_1 d\tilde{l}_2 \frac{2\Pi_{ij}(\not{k}_1 \gamma^{\mu_2} \not{k}_3 \not{q}_1 \not{k}_2 \gamma_{\mu_2})}{P(l_1, m_1) P(l_2, m_2) P(k_1) P(k_3) P(k_2) P(q_1)}, \end{aligned}$$

$$\begin{aligned}
D_6(m_1, m_2, m_3, m_4; r_{ij}) &= \int d\tilde{l}_1 d\tilde{l}_2 \frac{-4k_1^{\mu_1} q_{1\mu_4}}{P(l_1, m_1)P(l_2, m_2)P(l_3, m_3)P(l_1, m_4)P(k_1)P(q_1)} \\
&\quad \times [\Gamma_{\mu_1\mu_2\mu_3}(l_1, l_2, l_3)\Gamma^{\mu_4\mu_2\mu_3}(l_1, l_2, l_3) + 2l_{2\mu_1}l_3^{\mu_4}], \\
D_7(m_1, m_2, m_3; r_{ij}) &= \int d\tilde{l}_1 d\tilde{l}_2 \frac{-4k_1 q_1}{P(l_1, m_1)P(l_2, m_2)P(l_1, m_3)P(k_1)P(q_1)}, \\
D_8(m_1, m_2, m_3, m_4; r_{ij}) &= \int d\tilde{l}_1 d\tilde{l}_2 \frac{-4k_1 q_1}{P(l_1, m_1)P(l_2, m_2)P(l_3, m_3)P(l_1, m_4)P(k_1)P(q_1)}, \\
D_9(m_1, m_2, m_3, m_4; r_{ij}) &= \int d\tilde{l}_1 d\tilde{l}_2 \frac{4k_1^{\mu_1} q_1^{\mu_4} (l_2 - l_3)_{\mu_1} (l_2 - l_3)_{\mu_4}}{P(l_1, m_1)P(l_2, m_2)P(l_3, m_3)P(l_1, m_4)P(k_1)P(q_1)}, \\
D_{10}(m_1, m_2, m_3; r_{ij}) &= D_7(m_1, m_2, m_3; r_{ij}), \\
D_{11,0}(m_1, m_2, m_3, m_4; r_{ij}) &= \int d\tilde{l}_1 d\tilde{l}_2 \frac{4k_1^{\mu_1} q_1^{\mu_4} \text{Tr}(\gamma_{\mu_1} \not{l}_2 \gamma_{\mu_4} \not{l}_3)}{P(l_1, m_1)P(l_2, m_2)P(l_3, m_3)P(l_1, m_4)P(k_1)P(q_1)}, \\
D_{11,m}(m_1, m_2, m_3, m_4; r_{ij}) &= -4D_8(m_1, m_2, m_3, m_4; r_{ij}), \\
D_{12}(m_1, m_2; r_{ik}) &= \int d\tilde{l}_1 d\tilde{l}_2 \frac{-16(k_1 q_1)(k_3 r_2)}{P(l_1, m_1)P(l_2, m_2)P(k_1)P(k_3)P(q_1)P(r_2)}, \\
D_{13}(m_1, m_2, m_3; r_{ij}, r_{ik}, r_{jk}) &= \int d\tilde{l}_1 d\tilde{l}_2 \frac{8k_1^{\mu_1} q_2^{\mu_2} r_3^{\mu_3} \Gamma_{\mu_1\mu_2\mu_3}(-l_1, l_2, l_4)}{P(l_1, m_1)P(l_2, m_2)P(l_4, m_3)P(k_1)P(q_2)P(r_3)}, \\
D_{14}(m_1, m_2; r_{ij}, r_{kl}) &= D_0(m_1; r_{ij})D_0(m_2; r_{kl}). \tag{A.6}
\end{aligned}$$

## B Relations between loop integrals in NLL approximation

In the following we list relations between one- and two-loop integrals defined in App. A. These relations are valid after subtraction of the UV singularities and in NLL approximation. They have been obtained from the explicit results listed in Sects. 5.1 and 5.2 and are employed in App. E in order to simplify the sum over all NLL two-loop contributions.

As in Sect. 5.2, also in the following the symbols  $m_i$  are used to denote generic mass parameters, which can assume the values  $m_i = M_W, M_Z, m_t, M_H$  or  $m_i = 0$ , and the symbols  $M_i$  are used to denote non-zero masses, i.e.  $M_i = M_W, M_Z, m_t, M_H$ .

Combinations of the 2-leg ladder integrals in (5.5) and (5.8) can be expressed as products of one-loop integrals using

$$\begin{aligned}
&D_1(m_1, m_2; r_{ij}) + D_2(m_1, m_2; r_{ij}) + D_1(m_2, m_1; r_{ij}) + D_2(m_2, m_1; r_{ij}) \\
&\stackrel{\text{NLL}}{=} D_0(m_1; r_{ij})D_0(m_2; r_{ij}) \\
&\stackrel{\text{NLL}}{=} D_0(M_W; r_{ij})D_0(M_W; r_{ij}) + \Delta D_0(m_1; r_{ij})D_0(M_W; r_{ij}) \\
&\quad + D_0(M_W; r_{ij})\Delta D_0(m_2; r_{ij}) + \Delta D_0(m_1; r_{ij})\Delta D_0(m_2; r_{ij}), \tag{B.1}
\end{aligned}$$

where the subtracted functions  $\Delta D_h$  have been defined in (5.4). For the relations in (B.1) it is crucial that the results for  $D_0(m_k; r_{ij})$  including terms up to order  $\epsilon^2$  are used. Moreover,  $D_1$  and  $D_2$  fulfil the relations

$$\begin{aligned}
D_1(M_1, m_2; r_{ij}) &\stackrel{\text{NLL}}{=} D_1(M_1, M_W; r_{ij}), \\
D_2(m_1, m_2; r_{ij}) &= D_2(m_2, m_1; r_{ij}). \tag{B.2}
\end{aligned}$$

The loop integrals corresponding to the non-abelian diagrams involving two external legs (5.10) can be replaced as

$$\begin{aligned}
D_3(M_1, m_2, m_3; r_{ij}) &\stackrel{\text{NLL}}{=} \frac{1}{2}D_2(m_3, M_1; r_{ij}) - D_4(m_3, M_1; r_{ij}) \\
&\quad - 6D_9(m_3, M_1, M_1, m_3; r_{ij}), \\
\Delta D_3(M_W, M_W, m_1; r_{ij}) &\stackrel{\text{NLL}}{=} \frac{1}{2}\Delta D_{12}(M_W, m_1; r_{ij}) - \Delta D_4(m_1, M_W; r_{ij}) \\
&\quad - 6\Delta D_9(m_1, M_W, M_W, m_1; r_{ij}), \\
\Delta D_3(m_1, M_W, M_W; r_{ij}) &\stackrel{\text{NLL}}{=} \Delta D_3(M_W, m_1, M_W; r_{ij}) + \Delta D_1(M_W, m_1; r_{ij}) \\
&\quad + \Delta D_2(M_W, m_1; r_{ij}) + \Delta D_4(M_W, m_1; r_{ij}) \\
&\quad - \frac{1}{2}\Delta D_{12}(M_W, m_1; r_{ij}), \\
\Delta D_3(M_W, m_1, M_W; r_{ij}) &\stackrel{\text{NLL}}{=} -\frac{1}{2}\Delta D_1(M_W, m_1; r_{ij}) - \Delta D_4(M_W, m_1; r_{ij}). \tag{B.3}
\end{aligned}$$

The first of these relations has been verified and is needed only if at most one of the masses  $m_2$  and  $m_3$  is zero.

The loop functions for the diagrams (5.13) and (5.16) are equal up to a minus sign

$$D_5(m_1, m_2; r_{ij}) \stackrel{\text{NLL}}{=} -D_4(m_1, m_2; r_{ij}). \tag{B.4}$$

Next we give relations for the loop integrals appearing in the diagrams with self-energy insertions in the gauge-boson line, (5.19), (5.23), (5.26), (5.29), (5.32), and (5.34). The loop integrals  $D_6$ ,  $D_7$ ,  $D_8$ , and  $D_{11}$  can be related to  $D_9$  as

$$\begin{aligned}
D_6(M_1, M_2, M_3, M_4; r_{ij}) &\stackrel{\text{NLL}}{=} 10D_9(M_1, M_2, M_3, M_4; r_{ij}), \\
D_{11,0}(M_1, M_2, M_3, M_4; r_{ij}) &\stackrel{\text{NLL}}{=} 4D_9(M_1, M_2, M_3, M_4; r_{ij}), \\
\Delta D_6(0, M_W, M_W, 0; r_{ij}) &\stackrel{\text{NLL}}{=} 10\Delta D_9(0, M_W, M_W, 0; r_{ij}), \\
\Delta D_{11,0}(0, M_W, M_W, 0; r_{ij}) &\stackrel{\text{NLL}}{=} 4\Delta D_9(0, M_W, M_W, 0; r_{ij}), \\
\Delta D_6(0, M_2, M_3, M_4; r_{ij}) &\stackrel{\text{NLL}}{=} \Delta D_6(M_4, M_2, M_3, 0; r_{ij}) \\
&\stackrel{\text{NLL}}{=} -12 \frac{M_2^2 + M_3^2}{M_4^2} \Delta D_9(0, M_W, M_W, 0; r_{ij}), \\
\Delta D_7(0, M_2, M_3; r_{ij}) &\stackrel{\text{NLL}}{=} \Delta D_7(M_3, M_2, 0; r_{ij}) \\
&\stackrel{\text{NLL}}{=} -3 \frac{M_2^2}{M_3^2} \Delta D_9(0, M_W, M_W, 0; r_{ij}), \\
\Delta D_8(0, M_2, M_3, M_4; r_{ij}) &\stackrel{\text{NLL}}{=} \Delta D_8(M_4, M_2, M_3, 0; r_{ij}) \\
&\stackrel{\text{NLL}}{=} -\frac{3}{M_4^2} \Delta D_9(0, M_W, M_W, 0; r_{ij}), \\
\Delta D_9(0, M_2, M_3, M_4; r_{ij}) &\stackrel{\text{NLL}}{=} \Delta D_9(M_4, M_2, M_3, 0; r_{ij}) \\
&\stackrel{\text{NLL}}{=} 3 \frac{M_2^2 + M_3^2}{M_4^2} \Delta D_9(0, M_W, M_W, 0; r_{ij}), \\
\Delta D_{11,0}(0, M_2, M_3, M_4; r_{ij}) &\stackrel{\text{NLL}}{=} \Delta D_{11,0}(M_4, M_2, M_3, 0; r_{ij})
\end{aligned}$$

$$\stackrel{\text{NLL}}{=} 6 \frac{M_2^2 + M_3^2}{M_4^2} \Delta D_9(0, M_W, M_W, 0; r_{ij}). \quad (\text{B.5})$$

The loop integral  $D_9$  can be expressed as

$$\begin{aligned} 3D_9(M_W, M_W, M_W, M_W; r_{ij}) &\stackrel{\text{NLL}}{=} -J(\epsilon, M_W, Q^2), \\ 3\Delta D_9(0, M_W, M_W, 0; r_{ij}) &\stackrel{\text{NLL}}{=} -\left[\Delta J(\epsilon, 0, Q^2) - \Delta J(\epsilon, 0, M_W^2)\right], \end{aligned} \quad (\text{B.6})$$

and the loop integral  $D_{11}$  as

$$3[\Delta D_{11,0}(0, 0, 0, 0; r_{ij}) - \Delta D_{11,0}(0, M_W, M_W, 0; r_{ij})] \stackrel{\text{NLL}}{=} -4\Delta J(\epsilon, 0, M_W^2) \quad (\text{B.7})$$

in terms of the functions  $J$  and  $\Delta J$  defined in (7.14).

Combinations of 3-leg ladder integrals in (5.38) can be expressed as products of one-loop integrals

$$\begin{aligned} D_{12}(m_1, m_2; r_{ij}) + D_{12}(m_2, m_1; r_{ik}) &\stackrel{\text{NLL}}{=} D_0(m_2; r_{ij})D_0(m_1; r_{ik}) \\ &\stackrel{\text{NLL}}{=} D_0(M_W; r_{ij})D_0(M_W; r_{ik}) + \Delta D_0(m_2; r_{ij})D_0(M_W; r_{ik}) \\ &\quad + D_0(M_W; r_{ij})\Delta D_0(m_1; r_{ik}) + \Delta D_0(m_2; r_{ij})\Delta D_0(m_1; r_{ik}). \end{aligned} \quad (\text{B.8})$$

For these relations again the terms of  $\mathcal{O}(\epsilon^2)$  in  $D_0(m_k; r_{ij})$  are crucial. Furthermore

$$\sum_{\pi(i,j,k)} \text{sgn}(\pi(i, j, k)) D_{12}(M_W, M_W; r_{ik}) \stackrel{\text{NLL}}{=} 0, \quad (\text{B.9})$$

where the sum runs over all permutations  $\pi(i, j, k)$  of  $i, j, k$ , with sign  $\text{sgn}(\pi(i, j, k))$ . This identity simply follows from the fact that  $D_{12}$  is symmetric under the interchange of  $i$  and  $k$  and does not depend on  $r_{ij}$  and  $r_{jk}$ .

The loop functions appearing in the non-abelian diagrams involving three external legs (5.41) can be replaced as

$$\begin{aligned} D_{13}(M_1, M_2, M_3; r_{ij}) &\stackrel{\text{NLL}}{=} 0, \\ 2\Delta D_{13}(M_1, M_2, m_3; r_{ij}, r_{ik}, r_{jk}) &\stackrel{\text{NLL}}{=} 2\Delta D_{13}(m_1, M_2, M_3; r_{ik}, r_{jk}, r_{ij}) \\ &\stackrel{\text{NLL}}{=} 2\Delta D_{13}(M_1, m_2, M_3; r_{jk}, r_{ij}, r_{ik}) \\ &\stackrel{\text{NLL}}{=} \Delta D_{12}(M_W, m_3; r_{jk}) - \Delta D_{12}(M_W, m_3; r_{ik}). \end{aligned} \quad (\text{B.10})$$

## C $\beta$ -function coefficients

In this appendix we give relations and explicit expressions for the one-loop  $\beta$ -function coefficients  $b_{V_1 V_2}^{(1)}$ ,  $b_1^{(1)}$ ,  $b_2^{(1)}$ ,  $b_e^{(1)}$ ,  $b_{\text{QED}}^{(1)}$ , and  $b_{\text{top}}^{(1)}$  that have been used in the calculation. For more details we refer to Refs. [8, 28].

The matrix of  $\beta$ -function coefficients is defined as

$$b_{V_1 V_2}^{(1)} = \frac{11}{3} \text{Tr}_V(I^{\bar{V}_1} I^{V_2}) - \frac{1}{6} \text{Tr}_\Phi(I^{\bar{V}_1} I^{V_2}) - \frac{2}{3} \sum_\Psi \sum_{\kappa=R,L} \text{Tr}_{\Psi^\kappa}(I^{\bar{V}_1} I^{V_2}), \quad (\text{C.1})$$

where  $I^{V_i}$  are the generators defined in (2.13) and  $\text{Tr}_V$ ,  $\text{Tr}_\Phi$ , and  $\text{Tr}_\Psi$  denote the traces in the representations for the gauge bosons, scalars, and fermionic doublets, respectively. The sum  $\sum_\Psi$  runs over all doublets of leptons and quarks including different colours. The traces read more explicitly<sup>16</sup>

$$e^2 \text{Tr}_V(I^{\bar{V}_1} I^{V_2}) = g_2^2 \sum_{V_3, V_4=A, Z, W^\pm} \varepsilon^{\bar{V}_1 \bar{V}_3 \bar{V}_4} \varepsilon^{V_2 V_3 V_4}, \quad (\text{C.2})$$

$$e^2 \text{Tr}_\Phi(I^{\bar{V}_1} I^{V_2}) = e^2 \sum_{\Phi_i, \Phi_j=H, \chi, \phi^\pm} I_{\Phi_i \Phi_j}^{\bar{V}_1} I_{\Phi_j \Phi_i}^{V_2}, \quad (\text{C.3})$$

$$e^2 \text{Tr}_{\Psi^\kappa}(I^{\bar{V}_1} I^{V_2}) = e^2 \sum_{\Psi_i, \Psi_j=u, d} I_{\Psi_i^\kappa \Psi_j^\kappa}^{\bar{V}_1} I_{\Psi_j^\kappa \Psi_i^\kappa}^{V_2}. \quad (\text{C.4})$$

Multiplying  $b_{V_1 V_2}^{(1)}$  with generators and summing over all gauge bosons yields

$$e^2 \sum_{V_1, V_2=A, Z, W^\pm} b_{V_1 V_2}^{(1)} I_i^{V_1} I_i^{\bar{V}_2} = g_1^2 b_1^{(1)} \left( \frac{Y_i}{2} \right)^2 + g_2^2 b_2^{(1)} C_i, \quad (\text{C.5})$$

from which the coefficients corresponding to the weak couplings  $g_1$  and  $g_2$  can be read off. The coefficient corresponding to the electric-charge renormalization is given by

$$b_e^{(1)} \equiv b_{AA}^{(1)} = c_w^2 b_1^{(1)} + s_w^2 b_2^{(1)}. \quad (\text{C.6})$$

The explicit values in the electroweak Standard Model are ( $Y_\Phi = 1$ )

$$b_1^{(1)} = -\frac{41}{6c_w^2}, \quad b_2^{(1)} = \frac{19}{6s_w^2}, \quad b_e^{(1)} = -\frac{11}{3}. \quad (\text{C.7})$$

The QED  $\beta$ -function coefficient is determined by the light-fermion contributions only, i.e.

$$b_{\text{QED}}^{(1)} = -\frac{4}{3} \sum_{f \neq t} N_c^f Q_f^2 = -\frac{80}{9}, \quad (\text{C.8})$$

where  $N_c^f$  represents the colour factor, i.e.  $N_c^f = 1$  for leptons and  $N_c^f = 3$  for quarks.

The top-quark contribution to the electromagnetic  $\beta$ -function coefficient reads

$$b_{\text{top}}^{(1)} = -\frac{16}{9}. \quad (\text{C.9})$$

## D Summing up the one-loop contributions

In NLL approximation, the contribution of all bare one-loop diagrams to the matrix element for a process with  $n$  external massless fermions is given by (7.2), which results from the factorizable diagrams (3.5). Using the explicit results presented in Sect. 5.1 we can write

$$\tilde{\mathcal{M}}_1^{\text{F}} \stackrel{\text{NLL}}{=} \mathcal{M}_0 \left[ F_1^{\text{F, sew}} + \Delta F_1^{\text{F, em}} + \Delta F_1^{\text{F, Z}} \right] \quad (\text{D.1})$$

---

<sup>16</sup>Note that our normalization for the trace of the scalar fields differs from the one used in Refs. [8, 28].

with

$$\begin{aligned}
F_1^{\text{F,sew}} &= -\frac{1}{2} \sum_{i=1}^n \sum_{\substack{j=1 \\ j \neq i}}^n \sum_{V=A,Z,W^\pm} I_i^{\bar{V}} I_j^V D_0(M_W; r_{ij}), \\
\Delta F_1^{\text{F,em}} &= -\frac{1}{2} \sum_{i=1}^n \sum_{\substack{j=1 \\ j \neq i}}^n I_i^A I_j^A \Delta D_0(0; r_{ij}), \\
\Delta F_1^{\text{F,Z}} &= -\frac{1}{2} \sum_{i=1}^n \sum_{\substack{j=1 \\ j \neq i}}^n I_i^Z I_j^Z \Delta D_0(M_Z; r_{ij}).
\end{aligned} \tag{D.2}$$

Using the charge-conservation identity (2.30), the counterterms (6.6) can be cast into the form

$$\tilde{\mathcal{M}}_1^{\text{WF}} \stackrel{\text{NLL}}{=} \frac{1}{2} \mathcal{M}_0 \sum_{i=1}^n \sum_{\substack{j=1 \\ j \neq i}}^n \left\{ \sum_{V=A,Z,W^\pm} I_i^{\bar{V}} I_j^V C(M_W; Q^2) + I_i^A I_j^A \Delta C(0; Q^2) \right\} \tag{D.3}$$

with

$$\begin{aligned}
C(M_W; Q^2) &\stackrel{\text{NLL}}{=} L + \frac{1}{2} L^2 \epsilon + \frac{1}{6} L^3 \epsilon^2 + \mathcal{O}(\epsilon^3), \\
\Delta C(0; Q^2) &\stackrel{\text{NLL}}{=} -\frac{1}{\epsilon} - L - \frac{1}{2} L^2 \epsilon - \frac{1}{6} L^3 \epsilon^2 + \mathcal{O}(\epsilon^3).
\end{aligned} \tag{D.4}$$

When adding (D.1) and (D.3) we find (7.3)–(7.7) with

$$\begin{aligned}
I(\epsilon, M_W; -r_{ij}) &\stackrel{\text{NLL}}{=} D_0(M_W; r_{ij}) - C(M_W; Q^2), \\
\Delta I(\epsilon, M_Z; -r_{ij}) &\stackrel{\text{NLL}}{=} \Delta D_0(M_Z; r_{ij}), \\
\Delta I(\epsilon, 0; -r_{ij}) &\stackrel{\text{NLL}}{=} \Delta D_0(0; r_{ij}) - \Delta C(0; Q^2).
\end{aligned} \tag{D.5}$$

## E Summing up the two-loop contributions

In this appendix, the two-loop results listed in Sect. 5.2 are summed and decomposed into reducible contributions, which involve products of the one-loop integrals  $D_0$  (5.2), plus remaining irreducible parts. To this end, we split the integrals according to (5.4) and use the relations given in App. B as well as the commutation relations (2.29) and, in particular, the fact that  $I_i^A$ ,  $I_j^Z$ , and  $\sum_{V=A,Z,W^\pm} I_k^{\bar{V}} I_k^V$  commute with each other. As we show, all irreducible contributions cancel apart from those that can be expressed in terms of the one-loop functions  $J$  (7.14) and  $\beta$ -function coefficients. To start with, we consider four separate subsets and combine these in a later stage.

### Terms related to two external lines not involving gauge-boson self-energies

We begin by considering the contributions that result from the diagrams where the soft-collinear gauge bosons couple to two on-shell external lines and that do not involve self-energy contributions to the soft-collinear gauge bosons, i.e. from the diagrams 1, 2, 3, 4, and 5 of Sect. 5.2,

$$\tilde{\mathcal{M}}_{2,\text{no-se}}^{ij} = \tilde{\mathcal{M}}_2^{1,ij} + \tilde{\mathcal{M}}_2^{2,ij} + \left[ \tilde{\mathcal{M}}_2^{3,ij} + \tilde{\mathcal{M}}_2^{4,ij} + \tilde{\mathcal{M}}_2^{5,ij} + (i \leftrightarrow j) \right]. \tag{E.1}$$



These can be summarized as

$$\begin{aligned}
\tilde{\mathcal{M}}_{2,\text{no-se}}^{ij} &= \mathcal{M}_0 \sum_{V_1, V_2=A, Z, W^\pm} \left\{ I_i^{\bar{V}_2} I_i^{\bar{V}_1} I_j^{V_2} I_j^{V_1} D_1(M_{V_1}, M_{V_2}; r_{ij}) \right. \\
&\quad + I_i^{\bar{V}_2} I_i^{\bar{V}_1} I_j^{V_1} I_j^{V_2} D_2(M_{V_1}, M_{V_2}; r_{ij}) \\
&\quad - \left[ i \frac{g_2}{e} \sum_{V_3=A, Z, W^\pm} \varepsilon^{V_1 V_2 V_3} I_i^{\bar{V}_2} I_i^{\bar{V}_1} I_j^{\bar{V}_3} D_3(M_{V_1}, M_{V_2}, M_{V_3}; r_{ij}) \right. \\
&\quad + I_i^{V_2} I_i^{\bar{V}_2} I_j^{V_1} I_j^{\bar{V}_1} D_4(M_{V_1}, M_{V_2}; r_{ij}) \\
&\quad \left. \left. + I_i^{V_2} I_i^{V_1} I_j^{\bar{V}_2} I_j^{\bar{V}_1} D_5(M_{V_1}, M_{V_2}; r_{ij}) + (i \leftrightarrow j) \right] \right\} \\
&\stackrel{\text{NLL}}{=} \mathcal{M}_0 \left\{ \frac{1}{2} \sum_{V_1, V_2=A, Z, W^\pm} I_i^{\bar{V}_2} I_i^{\bar{V}_1} I_j^{V_2} I_j^{V_1} D_0(M_W; r_{ij}) D_0(M_W; r_{ij}) \right. \\
&\quad + \sum_{V=A, Z, W^\pm} I_i^{\bar{V}} I_i^A I_j^V I_j^A D_0(M_W; r_{ij}) \Delta D_0(0; r_{ij}) \\
&\quad + \sum_{V=A, Z, W^\pm} I_i^{\bar{V}} I_i^Z I_j^V I_j^Z D_0(M_W; r_{ij}) \Delta D_0(M_Z; r_{ij}) \\
&\quad + \frac{1}{2} I_i^A I_i^A I_j^A I_j^A \Delta D_0(0; r_{ij}) \Delta D_0(0; r_{ij}) \\
&\quad + I_i^Z I_i^A I_j^Z I_j^A \Delta D_0(M_Z; r_{ij}) \Delta D_0(0; r_{ij}) \\
&\quad + \left[ \sum_{V_1, V_2=A, Z, W^\pm} i \frac{g_2}{e} \frac{1}{2} \varepsilon^{AV_1 V_2} \left( I_i^{\bar{V}_1} I_i^A I_j^{\bar{V}_2} + I_i^A I_j^{\bar{V}_1} I_j^{\bar{V}_2} \right) \Delta D_{12}(M_W, 0; r_{ij}) \right. \\
&\quad + \sum_{V_1, V_2=A, Z, W^\pm} i \frac{g_2}{e} \frac{1}{2} \varepsilon^{ZV_1 V_2} \left( I_i^{\bar{V}_1} I_i^Z I_j^{\bar{V}_2} + I_i^Z I_j^{\bar{V}_1} I_j^{\bar{V}_2} \right) \Delta D_{12}(M_W, M_Z; r_{ij}) \\
&\quad \left. + (i \leftrightarrow j) \right] \\
&\quad + 6 \sum_{V_1, V_2=A, Z, W^\pm} I_i^{\bar{V}_1} I_j^{\bar{V}_2} \text{Tr}_V(I^{V_1} I^{V_2}) D_9(M_W, M_W, M_W, M_W; r_{ij}) \\
&\quad \left. + 3 \sum_{V_1=A, Z, W^\pm} \left( I_i^A I_j^{\bar{V}_1} + I_i^{\bar{V}_1} I_j^A \right) \text{Tr}_V(I^A I^{V_1}) \Delta D_9(0, M_W, M_W, 0; r_{ij}) \right\}, \quad (\text{E.2})
\end{aligned}$$

where we have made use of the identities (B.1), (B.2), (B.3), (B.4), and (C.2).

### Terms involving gauge-boson self-energy contributions

The contributions where a soft-collinear gauge boson connects two external lines and involves self-energy corrections result from diagrams 6–11 in Sect. 5.2 and read

$$\tilde{\mathcal{M}}_{2,\text{se}}^{ij} = \sum_{m=6}^{11} \tilde{\mathcal{M}}_2^{m,ij}. \quad (\text{E.3})$$

They can be summarized as

$$\tilde{\mathcal{M}}_{2,\text{se}}^{ij} = \mathcal{M}_0 \left\{ \frac{1}{2} \frac{g_2^2}{e^2} \sum_{V_1, V_2, V_3, V_4=A, Z, W^\pm} I_i^{\bar{V}_1} I_j^{\bar{V}_4} \varepsilon^{V_1 \bar{V}_2 \bar{V}_3} \varepsilon^{V_4 V_2 V_3} D_6(M_{V_1}, M_{V_2}, M_{V_3}, M_{V_4}; r_{ij}) \right.$$

$$\begin{aligned}
& -\frac{g_2^2}{e^2} \sum_{V_1, V_2, V_3, V_4=A, Z, W^\pm} I_i^{\bar{V}_1} I_j^{\bar{V}_4} \varepsilon^{V_1 \bar{V}_2 \bar{V}_3} \varepsilon^{V_4 V_2 V_3} (D-1) D_7(M_{V_1}, M_{V_2}, M_{V_4}; r_{ij}) \\
& - e^2 v^2 \sum_{V_1, V_3, V_4=A, Z, W^\pm} I_i^{\bar{V}_1} I_j^{\bar{V}_4} \sum_{\Phi_{i_2}=H, \chi, \phi^\pm} \left\{ I^{V_1}, I^{\bar{V}_3} \right\}_{H\Phi_{i_2}} \left\{ I^{V_3}, I^{V_4} \right\}_{\Phi_{i_2} H} \\
& \quad \times D_8(M_{V_1}, M_{\Phi_2}, M_{V_3}, M_{V_4}; r_{ij}) \\
& - \frac{1}{2} \sum_{V_1, V_4=A, Z, W^\pm} I_i^{\bar{V}_1} I_j^{\bar{V}_4} \sum_{\Phi_{i_2}, \Phi_{i_3}=H, \chi, \phi^\pm} I_{\Phi_{i_3} \Phi_{i_2}}^{V_1} I_{\Phi_{i_2} \Phi_{i_3}}^{V_4} \\
& \quad \times D_9(M_{V_1}, M_{\Phi_{i_2}}, M_{\Phi_{i_3}}, M_{V_4}; r_{ij}) \\
& - \frac{1}{2} \sum_{V_1, V_4=A, Z, W^\pm} I_i^{\bar{V}_1} I_j^{\bar{V}_4} \sum_{\Phi_{i_2}=H, \chi, \phi^\pm} \left\{ I^{V_1}, I^{V_4} \right\}_{\Phi_{i_2} \Phi_{i_2}} \\
& \quad \times D_{10}(M_{V_1}, M_{\Phi_{i_2}}, M_{V_4}; r_{ij}) \\
& - \frac{1}{2} \sum_{V_1, V_4=A, Z, W^\pm} I_i^{\bar{V}_1} I_j^{\bar{V}_4} \\
& \quad \times \sum_{\Psi} \left\{ \sum_{\Psi_{i_2}, \Psi_{i_3}=u, d} \sum_{\kappa=R, L} I_{\Psi_{i_3} \Psi_{i_2}}^{V_1} I_{\Psi_{i_2} \Psi_{i_3}}^{V_4} D_{11,0}(M_{V_1}, m_{i_2}, m_{i_3}, M_{V_4}; r_{ij}) \right. \\
& \quad \left. - \left( I_{u^R u^R}^{V_1} I_{u^L u^L}^{V_4} + I_{u^L u^L}^{V_1} I_{u^R u^R}^{V_4} \right) m_u^2 D_{11,m}(M_{V_1}, m_u, m_u, M_{V_4}; r_{ij}) \right\} \\
\stackrel{\text{NLL}}{=} & -\mathcal{M}_0 \left\{ \sum_{V_1, V_2=A, Z, W^\pm} I_i^{V_1} I_j^{\bar{V}_2} b_{V_1 V_2}^{(1)} J(\epsilon, M_W, Q^2) \right. \\
& + I_i^A I_j^A b_{AA}^{(1)} \left[ \Delta J(\epsilon, 0, Q^2) - \Delta J(\epsilon, 0, M_W^2) \right] \\
& + I_i^A I_j^A b_{\text{QED}}^{(1)} \Delta J(\epsilon, 0, M_W^2) \\
& + \sum_{V_1, V_2=A, Z, W^\pm} 6 I_i^{\bar{V}_1} I_j^{\bar{V}_2} \text{Tr}_V(I^{V_1} I^{V_2}) D_9(M_W, M_W, M_W, M_W; r_{ij}) \\
& + 6 I_i^A I_j^A \text{Tr}_V(I^A I^A) \Delta D_9(0, M_W, M_W, 0; r_{ij}) \\
& \left. + 3(I_i^A I_j^Z + I_i^Z I_j^A) \text{Tr}_V(I^A I^Z) \Delta D_9(0, M_W, M_W, 0; r_{ij}) \right\}, \tag{E.4}
\end{aligned}$$

where we used the relations (B.5), (B.6), (B.7), (C.1), (C.2), (C.3), (C.4), and (C.8). For the simplification of the diagram (5.26) in addition (2.19) was employed. We note that in this calculation terms of the form  $\sum_{V_2, V_3=A, Z, W^\pm} I_i^A I_j^Z \varepsilon^{A \bar{V}_2 \bar{V}_3} \varepsilon^{Z V_2 V_3} M_{V_2}^2$  cancel, where  $M_{V_2}^2$  results either from the loop integrals or from (2.19).

### Terms related to three external lines

The terms where the soft-collinear gauge bosons couple to three of the  $n$  on-shell external lines result from diagrams 12 and 13 in Sect. 5.2 and can be written as

$$\tilde{\mathcal{M}}_2^{ijk} = \left( \sum_{\pi(i,j,k)} \tilde{\mathcal{M}}_2^{12,ijk} \right) + \tilde{\mathcal{M}}_2^{13,ijk}, \tag{E.5}$$

where the sum runs over all six permutations  $\pi(i, j, k)$  of external lines  $i, j, k$ . These contributions yield

$$\begin{aligned}
\tilde{\mathcal{M}}_2^{ijk} &= \mathcal{M}_0 \left\{ \sum_{\pi(i,j,k)} \sum_{V_1, V_2=A, Z, W^\pm} I_i^{\bar{V}_2} I_i^{\bar{V}_1} I_j^{V_1} I_k^{V_2} D_{12}(M_{V_1}, M_{V_2}; r_{ik}) \right. \\
&\quad \left. - i \frac{g_2}{e} \sum_{V_1, V_2, V_3=A, Z, W^\pm} \varepsilon^{V_1 V_2 V_3} I_i^{\bar{V}_1} I_j^{\bar{V}_2} I_k^{\bar{V}_3} D_{13}(M_{V_1}, M_{V_2}, M_{V_3}; r_{ij}, r_{ik}, r_{jk}) \right\} \\
&\stackrel{\text{NLL}}{=} \mathcal{M}_0 \sum_{\pi(i,j,k)} \left\{ \frac{1}{2} \sum_{V_1, V_2=A, Z, W^\pm} I_i^{\bar{V}_2} I_i^{\bar{V}_1} I_j^{V_2} I_k^{V_1} D_0(M_W; r_{ij}) D_0(M_W; r_{ik}) \right. \\
&\quad + \sum_{V=A, Z, W^\pm} I_i^{\bar{V}} I_i^A I_j^V I_k^A D_0(M_W; r_{ij}) \Delta D_0(0; r_{ik}) \\
&\quad + \sum_{V=A, Z, W^\pm} I_i^{\bar{V}} I_i^Z I_j^V I_k^Z D_0(M_W; r_{ij}) \Delta D_0(M_Z; r_{ik}) \\
&\quad + \frac{1}{2} I_i^A I_i^A I_j^A I_k^A \Delta D_0(0; r_{ij}) \Delta D_0(0; r_{ik}) + I_i^Z I_i^A I_j^Z I_k^A \Delta D_0(M_Z; r_{ij}) \Delta D_0(0; r_{ik}) \\
&\quad + \sum_{V_1, V_2=A, Z, W^\pm} i \frac{g_2}{e} \frac{1}{2} \varepsilon^{AV_1 V_2} I_i^A I_j^{\bar{V}_2} I_k^{\bar{V}_1} \Delta D_{12}(M_W, 0; r_{ij}) \\
&\quad \left. + \sum_{V_1, V_2=A, Z, W^\pm} i \frac{g_2}{e} \frac{1}{2} \varepsilon^{ZV_1 V_2} I_i^Z I_j^{\bar{V}_2} I_k^{\bar{V}_1} \Delta D_{12}(M_W, M_Z; r_{ij}) \right\}, \tag{E.6}
\end{aligned}$$

where we used (B.8), (B.9), and (B.10).

### Terms from four external lines

Finally, we have the contributions where the soft-collinear gauge bosons couple to four of the  $n$  on-shell external lines, i.e. diagram 14 in Sect. 5.2:

$$\tilde{\mathcal{M}}_2^{ijkl} = \tilde{\mathcal{M}}_2^{14,ijkl}. \tag{E.7}$$

These reduce according to (5.44) directly to products of one-loop integrals

$$\begin{aligned}
\tilde{\mathcal{M}}_2^{ijkl} &= \mathcal{M}_0 \sum_{V_1, V_2=A, Z, W^\pm} I_i^{\bar{V}_1} I_j^{V_1} I_k^{\bar{V}_2} I_l^{V_2} D_{14}(M_{V_1}, M_{V_2}; r_{ij}, r_{kl}) \\
&\stackrel{\text{NLL}}{=} \mathcal{M}_0 \sum_{V_1, V_2=A, Z, W^\pm} I_i^{\bar{V}_1} I_j^{V_1} I_k^{\bar{V}_2} I_l^{V_2} D_0(M_{V_1}; r_{ij}) D_0(M_{V_2}; r_{kl}). \tag{E.8}
\end{aligned}$$

### Complete two-loop correction

The contributions from the above subsets of diagrams can be combined for an arbitrary process involving  $n$  on-shell external massless fermions according to (3.8) or (7.11) as

$$\tilde{\mathcal{M}}_2^{\text{F}} = \sum_{i=1}^n \sum_{\substack{j=1 \\ j \neq i}}^n \left[ \frac{1}{2} (\tilde{\mathcal{M}}_{2, \text{no-se}}^{ij} + \tilde{\mathcal{M}}_{2, \text{se}}^{ij}) + \sum_{\substack{k=1 \\ k \neq i, j}}^n \left( \frac{1}{6} \tilde{\mathcal{M}}_2^{ijk} + \sum_{\substack{l=1 \\ l \neq i, j, k}}^n \frac{1}{8} \tilde{\mathcal{M}}_2^{ijkl} \right) \right]. \tag{E.9}$$

As a first step, we show that all terms that cannot be expressed by the one-loop functions  $D_0$  and  $J$  cancel. The terms involving explicit factors  $\text{Tr}_V(I^{V_1}I^{V_2})$  or  $\text{Tr}_V(I^{V_1}I^A)$ , i.e. the last two lines in (E.2) and the last three lines in (E.4) cancel directly if we use the fact that the latter trace is only non-vanishing for  $V_1 = A, Z$ . The irreducible terms involving explicit  $\varepsilon^{V_1V_2V_3}$  tensors appearing in (E.2) and (E.6) yield

$$\begin{aligned}
\mathcal{M}_0 \sum_{i=1}^n \sum_{\substack{j=1 \\ j \neq i}}^n \left\{ \sum_{V_1, V_2=A, Z, W^\pm} i \frac{g_2}{e} \frac{1}{2} \varepsilon^{AV_1V_2} (I_i^{\bar{V}_1} I_i^A I_j^{\bar{V}_2} + I_i^A I_j^{\bar{V}_1} I_j^{\bar{V}_2}) \Delta D_{12}(M_W, 0; r_{ij}) \right. \\
+ \sum_{V_1, V_2=A, Z, W^\pm} i \frac{g_2}{e} \frac{1}{2} \varepsilon^{ZV_1V_2} (I_i^{\bar{V}_1} I_i^Z I_j^{\bar{V}_2} + I_i^Z I_j^{\bar{V}_1} I_j^{\bar{V}_2}) \Delta D_{12}(M_W, M_Z; r_{ij}) \\
+ \sum_{\substack{k=1 \\ k \neq i, j}}^n \left[ \sum_{V_1, V_2=A, Z, W^\pm} i \frac{g_2}{e} \frac{1}{2} \varepsilon^{AV_1V_2} I_i^A I_j^{\bar{V}_2} I_k^{\bar{V}_1} \Delta D_{12}(M_W, 0; r_{ij}) \right. \\
\left. \left. + \sum_{V_1, V_2=A, Z, W^\pm} i \frac{g_2}{e} \frac{1}{2} \varepsilon^{ZV_1V_2} I_i^Z I_j^{\bar{V}_2} I_k^{\bar{V}_1} \Delta D_{12}(M_W, M_Z; r_{ij}) \right] \right\}. \quad (\text{E.10})
\end{aligned}$$

These terms vanish upon using global gauge invariance (2.30).

The complete two-loop correction is thus given by the contributions to (E.2), (E.6), and (E.8) involving products of  $D_0$ -functions and the terms involving  $\beta$ -function coefficients and  $J$ -functions in (E.4). These can be summarized straightforwardly as

$$\begin{aligned}
\tilde{\mathcal{M}}_2^{\text{F, NLL}} \stackrel{\text{NLL}}{=} \frac{1}{4} \mathcal{M}_0 \sum_{i=1}^n \sum_{\substack{j=1 \\ j \neq i}}^n \sum_{k=1}^n \sum_{\substack{l=1 \\ l \neq k}}^n \left\{ \frac{1}{2} \sum_{V_1, V_2=A, Z, W^\pm} I_i^{\bar{V}_2} I_j^{V_2} I_k^{\bar{V}_1} I_l^{V_1} D_0(M_W; r_{ij}) D_0(M_W; r_{kl}) \right. \\
+ \sum_{V=A, Z, W^\pm} I_i^{\bar{V}} I_j^V I_k^A I_l^A D_0(M_W; r_{ij}) \Delta D_0(0; r_{kl}) \\
+ \sum_{V=A, Z, W^\pm} I_i^{\bar{V}} I_j^V I_k^Z I_l^Z D_0(M_W; r_{ij}) \Delta D_0(M_Z; r_{kl}) \\
+ \frac{1}{2} I_i^A I_j^A I_k^A I_l^A \Delta D_0(0; r_{ij}) \Delta D_0(0; r_{kl}) + I_i^Z I_j^Z I_k^A I_l^A \Delta D_0(M_Z; r_{ij}) \Delta D_0(0; r_{kl}) \left. \right\} \\
- \frac{1}{2} \mathcal{M}_0 \sum_{i=1}^n \sum_{\substack{j=1 \\ j \neq i}}^n \left\{ \sum_{V_1, V_2=A, Z, W^\pm} I_i^{V_1} I_j^{\bar{V}_2} b_{V_1V_2}^{(1)} J(\epsilon, M_W, Q^2) \right. \\
\left. + I_i^A I_j^A b_{AA}^{(1)} [\Delta J(\epsilon, 0, Q^2) - \Delta J(\epsilon, 0, M_W^2)] + I_i^A I_j^A b_{\text{QED}}^{(1)} \Delta J(\epsilon, 0, M_W^2) \right\}. \quad (\text{E.11})
\end{aligned}$$

In NLL accuracy, this result can be expressed in terms of the lowest-order matrix element  $\mathcal{M}_0$  and the one-loop correction factors (D.2) as

$$\begin{aligned}
\tilde{\mathcal{M}}_2^{\text{F, NLL}} \stackrel{\text{NLL}}{=} \mathcal{M}_0 \left\{ \frac{1}{2} [F_1^{\text{F, sew}}]^2 + F_1^{\text{F, sew}} \Delta F_1^{\text{F, em}} + F_1^{\text{F, sew}} \Delta F_1^{\text{F, Z}} \right. \\
\left. + \frac{1}{2} [\Delta F_1^{\text{F, em}}]^2 + \Delta F_1^{\text{F, Z}} \Delta F_1^{\text{F, em}} + G_2^{\text{F, sew}} + \Delta G_2^{\text{F, em}} \right\}. \quad (\text{E.12})
\end{aligned}$$

Note that in NLL approximation  $F_1^{\text{F,sew}}$  and  $\Delta F_1^{\text{F,em}}$  do not commute, while  $\Delta F_1^{\text{F,Z}}$  commutes with the other terms. Using (2.30), (C.5), and (C.6), the terms resulting from the last two lines of (E.11) can be written as

$$\begin{aligned}
e^2 G_2^{\text{F,sew}} &= \frac{1}{2} \sum_{i=1}^n \left[ b_1^{(1)} g_1^2 \left( \frac{Y_i}{2} \right)^2 + b_2^{(1)} g_2^2 C_i \right] J(\epsilon, M_W, Q^2), \\
\Delta G_2^{\text{F,em}} &= \frac{1}{2} \sum_{i=1}^n Q_i^2 \left\{ b_e^{(1)} \left[ \Delta J(\epsilon, 0, Q^2) - \Delta J(\epsilon, 0, M_W^2) \right] + b_{\text{QED}}^{(1)} \Delta J(\epsilon, 0, M_W^2) \right\}.
\end{aligned}
\tag{E.13}$$

Adding the term (6.10) resulting from parameter renormalization with  $D_0$  replaced by  $I$  and using the definition of  $J$ , (7.14), the functions  $G_2^{\text{F,sew}}$  and  $\Delta G_2^{\text{F,em}}$  in (E.12) get replaced by the functions  $G_2^{\text{sew}}$  and  $\Delta G_2^{\text{em}}$  as defined in (7.13).

Finally, when combining the wave-function counterterm (6.7) with the parts of (E.12) involving products of the functions  $F_1^{\text{F}}$  these terms can be written in the form given in (7.12). In order to arrive at this result we write  $\tilde{\mathcal{M}}_1^{\text{F}}$  in the form (6.8) and  $\delta Z_k^{(1)}$  in the form (6.5). After arranging the Casimir operators in an appropriate order, we can use global gauge invariance (2.30) to transform the wave-function counterterm contributions to the form needed.

## References

- [1] M. Kuroda, G. Moultaka and D. Schildknecht, *Nucl. Phys. B* **350** (1991) 25;  
G. Degrossi and A. Sirlin, *Phys. Rev. D* **46** (1992) 3104;  
W. Beenakker *et al.*, *Nucl. Phys. B* **410** (1993) 245; *Phys. Lett. B* **317** (1993) 622;  
A. Denner, S. Dittmaier and R. Schuster, *Nucl. Phys. B* **452** (1995) 80;  
A. Denner, S. Dittmaier and T. Hahn, *Phys. Rev. D* **56** (1997) 117;  
A. Denner and T. Hahn, *Nucl. Phys. B* **525** (1998) 27;  
M. Beccaria *et al.*, *Phys. Rev. D* **58** (1998) 093014 [hep-ph/9805250];  
P. Ciafaloni and D. Comelli, *Phys. Lett. B* **446** (1999) 278 [hep-ph/9809321].
- [2] S. Haywood, P. R. Hobson, W. Hollik, Z. Kunszt *et al.*, hep-ph/0003275, in *Standard Model Physics (and more) at the LHC*, eds. G. Altarelli and M. L. Mangano, (CERN-2000-004, Genève, 2000) p. 117.
- [3] J. A. Aguilar-Saavedra *et al.*, TESLA Technical Design Report Part III: Physics at an  $e^+e^-$  Linear Collider, hep-ph/0106315.
- [4] T. Abe *et al.* [American Linear Collider Working Group Collaboration], in *Proc. of the APS/DPF/DPB Summer Study on the Future of Particle Physics (Snowmass 2001)*, ed. N. Graf, SLAC-R-570, *Resource book for Snowmass 2001* [hep-ex/0106055, hep-ex/0106056, hep-ex/0106057, hep-ex/0106058].
- [5] K. Abe *et al.* [ACFA Linear Collider Working Group Collaboration], ACFA Linear Collider Working Group report [hep-ph/0109166].
- [6] V. V. Sudakov, *Sov. Phys. JETP* **3** (1956) 65 [*Zh. Eksp. Teor. Fiz.* **30** (1956) 87].

- [7] A. Denner and S. Pozzorini, *Eur. Phys. J. C* **18** (2001) 461 [hep-ph/0010201]; *Eur. Phys. J. C* **21** (2001) 63 [hep-ph/0104127].
- [8] S. Pozzorini, *doctoral thesis, Universität Zürich, 2001*, hep-ph/0201077.
- [9] M. Beccaria *et al.*, *Phys. Rev. D* **61** (2000) 073005 [hep-ph/9906319]; *Phys. Rev. D* **61** (2000) 011301 [hep-ph/9907389];  
M. Beccaria, F. M. Renard and C. Verzegnassi, *Phys. Rev. D* **63** (2001) 053013 [hep-ph/0010205]; *Phys. Rev. D* **64** (2001) 073008 [hep-ph/0103335]; *Nucl. Phys. B* **663** (2003) 394 [hep-ph/0304175].
- [10] J. Layssac and F. M. Renard, *Phys. Rev. D* **64** (2001) 053018 [hep-ph/0104205];  
G. J. Gounaris, J. Layssac and F. M. Renard, *Phys. Rev. D* **67** (2003) 013012 [hep-ph/0211327].
- [11] E. Accomando, A. Denner and S. Pozzorini, *Phys. Rev. D* **65** (2002) 073003 [hep-ph/0110114];  
W. Hollik and C. Meier, *Phys. Lett. B* **590** (2004) 69 [hep-ph/0402281];  
E. Accomando, A. Denner and A. Kaiser, *Nucl. Phys. B* **706** (2005) 325 [hep-ph/0409247];  
E. Accomando and A. Kaiser, *Phys. Rev. D* **73** (2006) 093006 [hep-ph/0511088].
- [12] E. Accomando, A. Denner and C. Meier, *Eur. Phys. J. C* **47** (2006) 125 [hep-ph/0509234].
- [13] E. Maina, S. Moretti, M. R. Nolten and D. A. Ross, *Phys. Lett. B* **570** (2003) 205 [hep-ph/0307021];  
E. Maina, S. Moretti and D. A. Ross, *Phys. Lett. B* **593** (2004) 143 [Erratum-ibid. *B* **614** (2005) 216] [hep-ph/0403050];  
S. Moretti, M. R. Nolten and D. A. Ross, *Phys. Lett. B* **639** (2006) 513 [hep-ph/0603083]; hep-ph/0606201.
- [14] J. H. Kühn, A. Kulesza, S. Pozzorini and M. Schulze, *Phys. Lett. B* **609** (2005) 277 [hep-ph/0408308]; *Nucl. Phys. B* **727** (2005) 368 [hep-ph/0507178]; *JHEP* **0603** (2006) 059 [hep-ph/0508253].
- [15] M. Beccaria and E. Mirabella, *Phys. Rev. D* **72** (2005) 055004 [hep-ph/0507070];  
M. Beccaria, G. Macorini, F. M. Renard and C. Verzegnassi, *Phys. Rev. D* **74** (2006) 013008 [hep-ph/0605108].
- [16] G. Passarino and S. Uccirati, *Nucl. Phys. B* **747** (2006) 113 [hep-ph/0603121].
- [17] V. S. Fadin, L. N. Lipatov, A. D. Martin and M. Melles, *Phys. Rev. D* **61** (2000) 094002 [hep-ph/9910338].
- [18] M. Melles, *Phys. Rev. D* **63** (2001) 034003 [hep-ph/0004056].
- [19] M. Melles, *Phys. Rev. D* **64** (2001) 014011 [hep-ph/0012157]; *Phys. Rept.* **375** (2003) 219 [hep-ph/0104232].

- [20] M. Melles, *Phys. Rev. D* **64** (2001) 054003 [hep-ph/0102097].
- [21] M. Melles, *Eur. Phys. J. C* **24** (2002) 193 [hep-ph/0108221].
- [22] J. H. Kühn, A. A. Penin and V. A. Smirnov, *Eur. Phys. J. C* **17** (2000) 97 [hep-ph/9912503].
- [23] J. H. Kühn, S. Moch, A. A. Penin and V. A. Smirnov, *Nucl. Phys. B* **616** (2001) 286 [Erratum-ibid. *B* **648** (2003) 455] [hep-ph/0106298].
- [24] M. Melles, *Phys. Lett. B* **495** (2000) 81 [hep-ph/0006077].
- [25] M. Hori, H. Kawamura and J. Kodaira, *Phys. Lett. B* **491** (2000) 275 [hep-ph/0007329].
- [26] W. Beenakker and A. Werthenbach, *Phys. Lett. B* **489** (2000) 148 [hep-ph/0005316]; *Nucl. Phys. B* **630** (2002) 3 [hep-ph/0112030].
- [27] A. Denner, M. Melles and S. Pozzorini, *Nucl. Phys. B* **662** (2003) 299 [hep-ph/0301241].
- [28] S. Pozzorini, *Nucl. Phys. B* **692** (2004) 135 [hep-ph/0401087].
- [29] B. Feucht, J. H. Kühn and S. Moch, *Phys. Lett. B* **561** (2003) 111 [hep-ph/0303016]; B. Feucht, J. H. Kühn, A. A. Penin and V. A. Smirnov, *Phys. Rev. Lett.* **93** (2004) 101802 [hep-ph/0404082].
- [30] B. Jantzen, J. H. Kühn, A. A. Penin and V. A. Smirnov, *Phys. Rev. D* **72** (2005) 051301 [Erratum-ibid. *D* **74** (2006) 019901] [hep-ph/0504111].
- [31] B. Jantzen, J. H. Kühn, A. A. Penin and V. A. Smirnov, *Nucl. Phys. B* **731** (2005) 188 [Erratum-ibid. *B* **752** (2006) 327] [hep-ph/0509157].
- [32] M. Ciafaloni, P. Ciafaloni and D. Comelli, *Phys. Rev. Lett.* **84** (2000) 4810 [hep-ph/0001142]; *Nucl. Phys. B* **589** (2000) 359 [hep-ph/0004071]; *Phys. Lett. B* **501** (2001) 216 [hep-ph/0007096]; *Phys. Rev. Lett.* **87** (2001) 211802 [hep-ph/0103315]; *Nucl. Phys. B* **613** (2001) 382 [hep-ph/0103316]; *Phys. Rev. Lett.* **88** (2002) 102001 [hep-ph/0111109]; P. Ciafaloni and D. Comelli, *JHEP* **0511** (2005) 022 [hep-ph/0505047].
- [33] A. Denner and S. Pozzorini, *Nucl. Phys. B* **717** (2005) 48 [hep-ph/0408068].
- [34] B. Jantzen and V. A. Smirnov, *Eur. Phys. J. C* **47** (2006) 671 [hep-ph/0603133].
- [35] S. Catani, *Phys. Lett. B* **427** (1998) 161 [hep-ph/9802439].